UNIVERSITY *of the*
WESTERN CAPE

Synthesis and evaluation of fluorescently linked polycyclic cage derivatives for application in neurodegenerative disorders.

BY

LOCARNO LAWRENCE FOURIE

B.Pharm (UWC)

Thesis submitted in fulfilment of the requirements for the degree of Masters in Pharmaceutical Science

SCHOOL OF PHARMACY, UNIVERSITY OF THE WESTERN CAPE,

BELLVILLE,

SOUTH AFRICA

Supervisor: Prof. J. Joubert

Co-supervisor: Prof. S. F. Malan

October 2020

DECLARATION

I declare that my research work titled “Synthesis and evaluation of fluorescently linked polycyclic cage derivatives for application in neurodegenerative disorders.” is my own work, and that it has not been submitted before for any degree or examination in any other university, and that all the sources I have used or quoted have been indicated and acknowledged by means of complete references.

Locarno L Fourie October 2020

……

Signature

Dedicated to my parents Leon and Carlene Fourie,

My Fiancé Priya Pillay

And

My brother Raynier Fourie

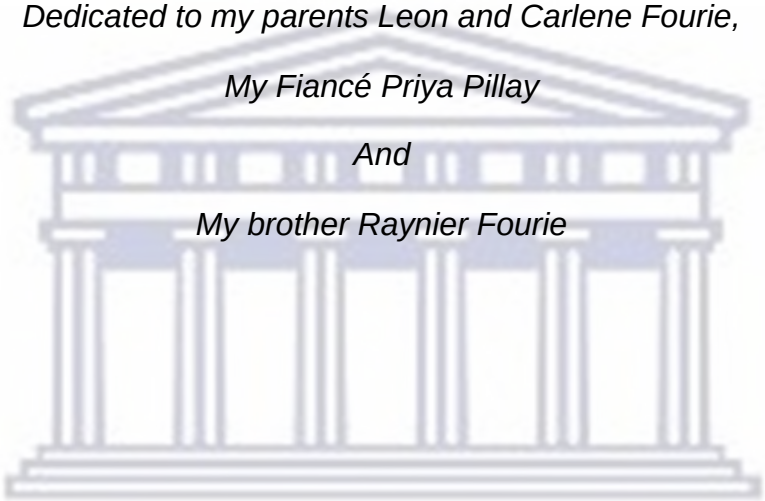

Acknowledgements

I would like to acknowledge and express my deepest gratitude and appreciation to the following people and institutions for their guidance, support, motivation and assistance towards the completion of this thesis. Without you this would not have been possible.

To my supervisors, Prof Jacques Joubert and Prof Sarel Malan, I am forever grateful for your time and effort in this work, and this amazing opportunity.

Dr Rajan Sharma, Dr Frank Zindo, Dr Ayodeji Egunlusi, Dr Sylvester Omoruyi and Ms Audrey Ramplin, your assistance was crucial to the success and completetion of this thesis.

To my parents, Leon and Carlene Fourie, and you always believed in me, motivated me and pushed me. Your hard work helped give me the opportunity to study and strive for my dreams. My brother Raynier Fourie, you are the person that made me believe I can achieve anything, and you always supported me.

My Fiancé, Priya Pillay, who has been so understanding, loving and supportive. Being there when I worked late nights and early mornings, losing sleep with me and through a difficult time you were always by my side, you motivated me like no one else, and stuck with me when I wasn't the easiest person. I will always be grateful for your love and support during this time.

Lastly my great friends Ireen, Adeyemi and Yvette. You were with me from the first day to the last of this. Thank you so much for your friendship, guidance, laughs and support.

The Ada and Bertie Levenstein Scholorship and University of the Western Cape (UWC) for funding. UWC, School of Pharmacy and Pharmaceutical Chemisitry.

Synthesis and evaluation of fluorescently linked polycyclic cage derivatives for application in neurodegenerative disorders.

Locarno Lawrence Fourie

Keywords

Neurodegeneration

Alzheimer's disease

Parkinson's Disease

Fluorescence

Pentacycloundecane

Polycyclic cage

N-Methyl-D-Aspartate receptor

Voltage gated calcium channel

Blood brain barrier

Oxidative stress

Excitotoxicity

Apoptosis

Abbreviations

Aβ: Amyloid- Beta

Abs: Absorption

AD: Alzheimer's Disease

AChE: Acetylcholinesterase

ALS: Amyotropic lateral sclerosis

AMPA: α-amino-3-hydroxy-5-methyl-4-isoxazolepropionic acid receptor

AP: Amyloid Plaques

Aq: Aqueous

ATP: Adenosine triphosphate

BBB: Blood Brain Barrier

CAT: Chloramphenicol acetyltransferase

CIR: Cerebral ischemia/reperfusion

CNS: Central Nervous System

CT: Computed tomography

DNA: Deoxyribonucleic Acid

DMEM: Dulbecco's Modified Eagle Medium

DMSO: Dimethyl sulfoxide

Em: Emission

FDA: Food and Drug Administration

GABA: Gamma aminobutyric acid

GPX: Glutathione peroxidase

GTP: Guanosine triphosphate

HD: Huntington's disease

Hrs: Hours

5-HT: 5-Hydroxy Tryptamine

IAPP: islet amyloid polypeptide

IR: Infrared

LB: Lewy Bodies

MAO: Monoamine Oxidase

MK-801: Dizocilpine

MP: Melting Point

MPO: Myeloperoxidase

MPP+: 1-methyl-4-phenyl pyridinium

MRI: Magnetic resonance imaging

MS: Multiple Sclerosis

MTT: 3-[4,5-dimethylthiazol-2-yl]-2,5-diphenyl tetrazolium bromide

MW: Molecular Weight

NAD: Nicotinamide Adenine Dinucleotide

NBD: 4-chloro-7-nitrobenzofurazan

ND: Neurodegenerative Diseases

NFT: Neurofibrillary tangles

NIM: Nimodipine

NIR: Near Infrared

NMDA: N-methyl-D-aspartate receptor

NMR: Nuclear Magnetic Resonance

OI: Optical Imaging

PCP: Phencyclidine

PCU: Pentacycloundecane

PD: Parkinson's Disease

PET: Positron emission tomography

RNA: Ribonucleic acid

RNS: Reactive Nitrogen Species

ROS: Reactive Oxygen Species

Rt: Room Temperature

SERT: Serotonin transporters

SPECT: Single-photon emission computed tomography

SOD: Superoxide dismutase

TLC: Thin Layer Chromatography

TMS: Tetramethylsilane

US: Ultrasound

UV: Ultraviolet

VGCC: Voltage Gated Calcium Channel

Units

ºC = Degree Celsius

g = Grams

mmol = Millimoles

W = Watt

ml = Millilitres

% = Percentage

Psi = Pounds per square inch

cm^{-1} = Per centimetre

g/mol = Gram per mole

MHz = Megahertz

ppm = Part per million

Hz = Hertz

mg = Milligrams

µM = Micromolar

Abstract

Neurodegenerative diseases (ND) are chronic and progressive in nature, and characterized by the gradual loss of neurons in various regions of the central nervous system (CNS). ND include Alzheimer's disease (AD), Parkinson's disease (PD), Huntington's disease (HD), multiple sclerosis (MS), amyotrophic lateral sclerosis (ALS) and cerebral ischemia/reperfusion (CIR). They have various progressive neurodegenerative pathologies that can result in several severe functional impairments for patients, and ultimately lead to serious health-related issues. According to more recent data, AD accounts for the most common cause of dementia and is believed to contribute to approximately 60–70% of cases. AD is thus seen as the most common form of dementia.

There are various mechanisms involved in neuronal cell death, whether necrotic or apoptotic in nature, but one of the most notable is the lethal triplet. This triplet consists of metabolic compromise, oxidative stress, and excitotoxicity. Although not the only processes that can cause cell death, one or a combination of these processes are usually involved. A large part of this triplet involves excessive Ca^{2+} influx through Voltage gated calcium channels (VGCC) and N-Methyl-D-Aspartate (NMDA) receptor overstimulation.

Polycyclic cage derivatives are hydrocarbon chemical compounds that resemble a cage like shape or structure. Well known chemical structures such as PCP, amantadine and NGP1-01 are all cage like moieties. These cages have been proven to exhibit neuroprotective properties, while also inhibiting NMDA receptors and/ or calcium channels. Furthermore, they tend to exhibit a generally low side effect profile. These cages also have the potential to cross the blood brain barrier (BBB) permeability. Moreover the use of fluorescent molecules in ND can be highly advantageous, as they can generate high-resolution images; they tend to have a high sensitivity and can be a cost-effective way of monitoring diseases. Combining the neuroprotective, NMDA and VGCC activity of cage moieties with fluorophores can result in multi-functional agents in ND.

For this purpose six compounds were synthesised, including polycyclic cage derivatives, fluorophores and fluorophore-cage conjugates. The structures of these

compounds were confirmed using NMR, IR and MS. The synthesised compounds were evaluated for cytotoxicity, neuroprotection and most importantly NMDA and VGCC inhibitory activity. For the VGCC inhibition assay Nimodipine and NGP1-01 were used as reference compounds, yielding 69.55% and 59.14% inhibition respectively, while all the test compounds showed a moderate to high degree of inhibition. Compound **3** had the highest inhibition at 77.76%. The assay proved to be statistically significant ($P < 0.0001$). MK-801 and NGP1-01 were used as reference compounds for the NMDA assay. They showed a percentage inhibition of 59,57% and 42,27% respectively. Again compound **3** showed the best activity at 73.68% inhibition. For this assay most compounds also showed significant results and the assay was found to be statistically significant ($P < 0.01$). Compound **3**, **4** and **7** were fluorophore-cage conjugates and all proved to have moderate to high degrees of dual VGCC and NMDA activity.

The true potential use of these compounds as neuroprotective, NMDA and VGCC inhibitory agents have been proven to some degree, however the efficiency of these compounds and safety in patients is yet to be established and should be further researched. It has also been proven that these compounds maintained the fluorescent nature of the fluorophores conjugated to the cage moieties, and as such have potential as fluorescent ligands in disease monitoring and detection. The compounds could serve as lead structures in studies with a more comprehensives series for the development of novel fluorescent polycyclic agents in ND.

TABLE OF CONTENTS

List of Tables and Figures:

CHAPTER 1

INTRODUCTION

1.1 Background

Neurodegenerative diseases (ND) are chronic and progressive in nature, and are characterized by the gradual loss of neurons in specific areas of the central nervous system (CNS), such as the frontal cortex and substantia nigra. A few examples of such diseases include Alzheimer's disease (AD), Parkinson's disease (PD), Huntington's disease (HD), multiple sclerosis (MS), amyotrophic lateral sclerosis (ALS) and cerebral ischemia/reperfusion (CIR) (Giacoppo *et al.*, 2015). They have various progressive neurodegenerative pathologies that can result in several severe functional impairments for patients, and ultimately lead to serious health-related issues. According to more recent data, AD accounts for the most common cause of dementia and is believed to contribute to approximately 60–70% of cases. AD is thus seen as the most common form of dementia. It was reported 2019 that there are more than 50 million people living with dementia globally. This figure is believed to increase to 152 million by 2050 (Adelina, 2019).

Most of these neurological conditions are not curable, and can even progress and become worse with the process of ageing. These diseases present a range of signs and symptoms, usually leading to functional limitations, and affecting the quality of life of individuals suffering from the disorder, as well as their families (Giacoppo *et al.*, 2015). The pathogenesis of these diseases often have similar features, such as the abnormal accumulation and aggregation of disease-specific proteins, such as amyloid-β plagues, protein misfolding and aggregation in previously unaffected cells or areas, genetic mutations and/or environmental factors. The symptoms can happen as a result of oxidative or metabolic stress. The various factors involved in the pathogenesis of these diseases, together with age, play an integral role in the onset, progression and severity of the disease (Herrero and Morelli, 2017).

Dementia also has a huge economic impact, resulting in a worldwide cost of US$818 billion in 2015. (Prince *et al.*, 2016) In 2006 the world health organisation (WHO)

reported that “a large body of evidence shows that policy-makers and health-care providers may be unprepared to cope with the predicted rise in the prevalence of neurological and other chronic disorders and the disability resulting from the extension of life expectancy and ageing of populations globally” (World Health Organization, 2006).

AD and PD are the two most common neurodegenerative diseases (Tokuchi *et al.*, 2016). Yet both and many other neurodegenerative disorders have very different clinical and pathological features (Tokuchi *et al.*, 2016). AD is a prototypical dementing illness that is associated with cortical dysfunction, amyloid plaques, neurofibrillary tangles and cholinergic basal forebrain degeneration, while PD is a movement disorder, associated with degradation and dysfunction in the basal ganglia, Lewy bodies, and substantia nigral dopaminergic neurons of the brain (Starkstein *et al.*, 1996; Weintraub *et al.*, 2007).

The main objective when treating patients suffering from neurological conditions has mostly been single target treatments. PD treatment for example focuses on restoring the function of striatal dopamine (Dondorp *et al.*, 2009). However, lately the focus for treating these disorders has shifted to alternative approaches that involve neuroprotection, rather than only focussing on treating symptoms that become worse as the disease progresses. Effective therapy in ND conditions should not only prevent disease progression, but also cure the motor and cognitive dysfunction associated with them. Presently, there are no drugs that effectively meet these requirements, as the drugs currently marketed focus on symptomatic treatment of the relevant condition (Madrid *et al.*, 2006; Finazzi and Arosio, 2014).

Current therapies in the field of neurodegeneration act by targeting specific sites or pathways that are involved in the pathology of the disease. These include acetylcholinesterase (AChE) inhibitors such as rivastigmine (Exelon®) and N-methyl-D-aspartate (NMDA) receptor antagonists such as memantine (Namenda®), both FDA approved drugs in AD. In the case of PD, monoamine oxidase-B inhibitors such as selegiline (Eldepryl®) and rasagiline (Azilect®), and dopamine agonists like bromocriptine (Cycloset®) (Rang *et al*. 2012) are used in treating this disorder.

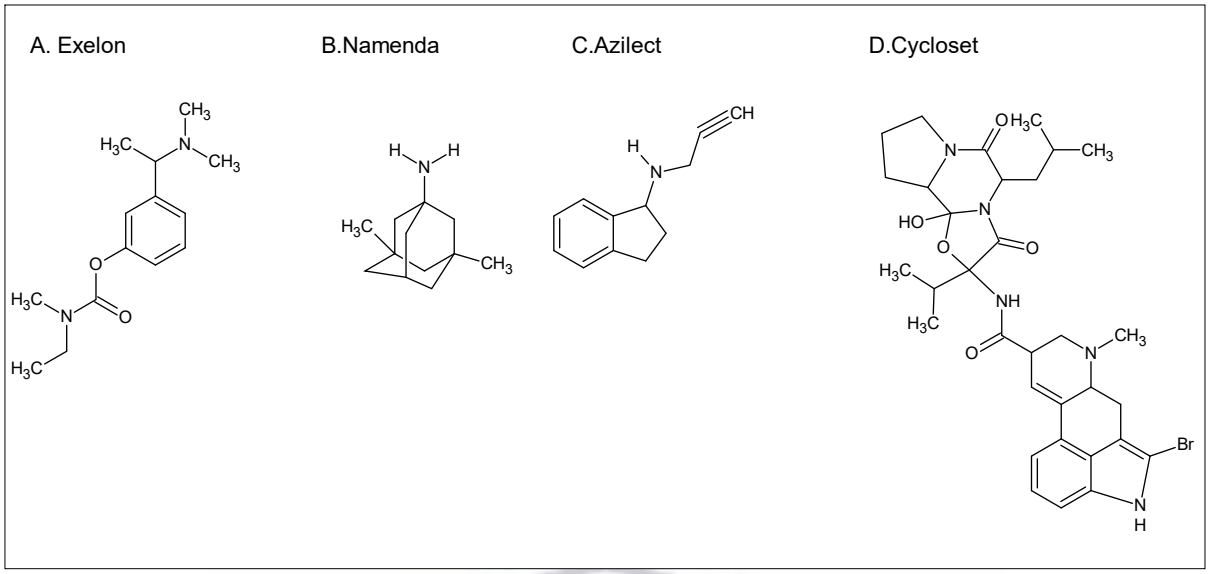

Figure 1.1: Structures of FDA approved drugs for various ND.

1.2 Rationale

A study conducted in Europe alone, estimated that the annual economic cost of neurological diseases (dementia, epilepsy, migraine and other headaches, multiple sclerosis, Parkinson's disease and stroke) amounted to € 139 billion (approximately US$ 180 billion) in 2004. This excluded indirect costs and omitted intangible costs (WHO report). One of the main difficulties with regards to diagnosing these neurodegenerative disorders is the fact that they do not develop overnight. These disorders exhibit a progression and decline that is not linear, and usually cognitive function fluctuates between patients, and may also differ when it comes to patient evaluations. (Korczyn, 2016) (Werner and Korczyn, 2008) This alone makes early and effective diagnosis of these diseases extremely difficult.

1.2.1 Fluorescent ligands and imaging

Molecular imaging with fluorescent molecules, known as fluorophores, is currently a focus in molecular imaging research. Using fluorophores in imaging is advantageous because they can generate high-resolution images, they usually have a high sensitivity and precision, they can be non-invasive and more importantly cost-effective, while having minimum or in many cases no influence on cellular functions (Boustany and Boppart, 2010). In the last decade molecular imaging as a field has emerged, developed and progressed remarkably, due to the ability for site-specific

and molecule-specific imaging, resulting in a vast number of applications and opportunities (Specht *et al*., 2016).

In science and medicine various different techniques are being used for imaging and diagnosis of different types of diseases. These can include computed tomography (CT), planar scintigraphy, positron emission tomography (PET), single photon emission computed tomography (SPECT), magnetic resonance imaging (MRI), ultrasound (US) and optical imaging (OI). Some of these techniques are invasive while others such as PET, SPECT and MRI are used because of their non-invasive nature of molecular imaging. These techniques all have differences in terms of the types of probes, detection methods, their spatial/temporal resolution, sensitivity and tissue penetration depth (Alberti, 2012; Arslan Ali, 2015).

Fluorophores being used as fluorescent probes exhibit a number of specific properties such as a specific excitation/emission wavelength range, Strokes shift and spectral bandwidth being imposed by the fluorescent imaging instrument. The fluorescent signal for a given fluorophore is dependent on the efficiency with which it absorbs and emits photons, and also its ability to undergo repeated excitation/emission cycles (Joubert, 2007).

It has been found that fluorophores designed for molecular imaging should aim to be in the near infrared region (NIR). Using fluorophores that emit light in this wavelength is superior over using fluorophores in the visible window due to a reduction of photon absorption in biological tissue, interference from auto-fluorescence and increasing resolution and penetration depth (Hong *et al*., 2017). Hence for the purpose of this the fluorescent ligands NBD, dansyl chloride and the dicyano fluorophore have been assessed and shown to be effective fluorophores for application in ND. The structures of these fluorophores and their emission wavelengths can be seen in figure 1.2.

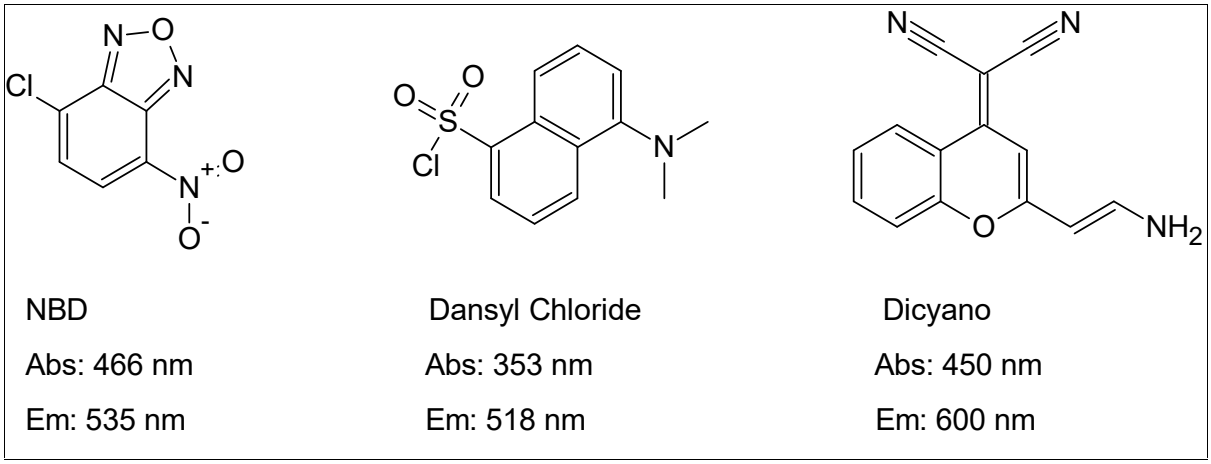

Figure 1.2: Fluorophores and their respective emission wavelengths.

1.2.2 Polycyclic Cages

Polycyclic cage derivatives are hydrocarbon chemical compounds that resemble a cage like shape or structure, usually saturated, and includes chemical structures such as PCP, amantadine and NGP1-01(Fig 1.3). These structures have been of particular interest to chemists for their potential in the field of medicine has been explored because of this (Ito *et al.*, 2007; Egunlusi, 2014). These cages have been shown to exhibit neuroprotective properties, while also inhibiting NMDA receptors and/ or calcium channels, and also generally having a low side effect profile. Furthermore they show good blood brain barrier (BBB) permeability. All these factors make them a group of structures with a high potential as lead derivatives for drug design and development (Lipton, 2007). The neuroprotective nature of these structures is of particular importance and occurs by not only slowing down cell death, but also preventing it. Compounds such as memantine acts on the NMDA receptor and prevents over activation and thus excessive activity, while maintaining normal NMDA receptor activity. With this neuroprotective potential, it has resulted in a lot of focus on memantine and other cage derivatives in the field of medicinal chemistry (Johnson and Kotermanski, 2006; Lipton, 2007; Wenk, 2007; Egunlusi, 2014).

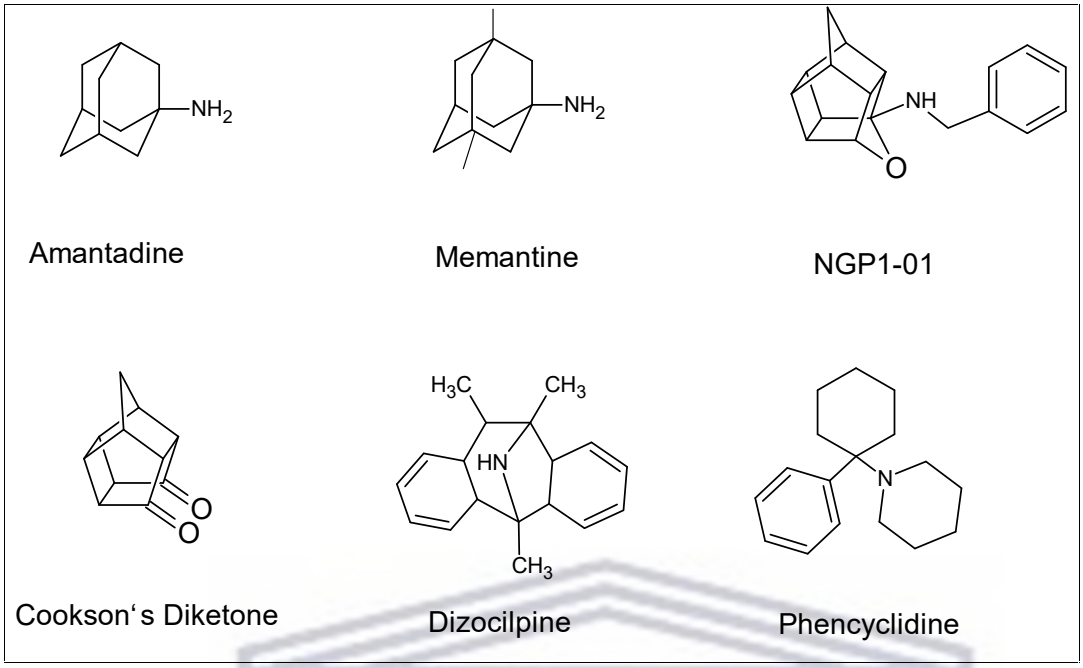

Figure 1.3: Chemical structures of PCP, NGP1-01 and polycyclic derived molecules with neuroprotective effects.

Furthermore several pentacyloundecane cage derivatives have also been reported to have neuroprotective activity, while also being good synthons due to the ability to conjugate other chemical structures. These modifications tend to improve the pharmacokinetic and pharmacodynamic properties of the molecules. They also exhibit NMDA receptor inhibition as well as L-type voltage gated calcium channel (VGCC) blocking activity. This dual inhibitory mechanism that we see in structures like NGP1-01 (Fig. 1.3), mean polycyclic cage derivatives are potential drug candidates in both prophylaxis and the treatment of neurodegenerative disorders (Van der Schyf and Youdim, 2009). As a result of this, various cage derivatives have been developed and synthesised extensively for this purpose (Geldenhuys *et al.*, 2004; Joubert *et al.*, 2011).

1.3 Aim

A series of novel pentacylcloundecane derivatives were developed which are similar in structure to that of NGP1-01, but with varying carbon linkers, and conjugated fluorophores. NMDA receptor and VGCC inhibitions are known to be useful in the treatment of ND. The final compounds were evaluated for fluorescence, cytotoxicity, neuroprotective ability and finally the ability to inhibit Ca^{2+} influx through NMDA and

VGCC modulation. NMDA receptors and VGCC are integral targets in glutamate related neurotoxicity and thus directs our focus with regards to disease treatment and prevention. Furthermore, the fluorescent nature of the molecule directs the research to a disease diagnosis and monitoring focus. Thus, a compound that can detect the disease early enough, while treating it to prevent the progression and ultimately dysfunction of the patient from occurring, would be a significant advancement in the field.

Designing a drug which acts on multiple targets, through various biological pathways involved in the apoptotic process, (or which has more than one mechanism of action) can completely revolutionise the treatment of neurological disorders. This can possibly lead to the discovery of an effective neuroprotective, or even curative agent. The multi-functional or multitargeted approach explored in this study may be of great importance. Even though these compounds could act on multiple targets, the goal will be to ensure these compounds are selective for these specific receptors. This selectivity will help to minimise side effects. Since these compounds will also have fluorescent properties, it is possible to visualise the pharmacokinetics and binding sites of the compounds using fluorescent imaging techniques. Furthermore being able to see a drug cross the BBB, interact with drug binding pockets and/or its deposition, might allow the visualisation and early detection of neurodegenerative disorders. This may be accomplished through binding to specific targets or deposits responsible for the progression of neurodegenerative disorders, such as amyloid-β plaques, NMDA receptors and/or VGCC. Table 1 below highlights the series of compounds designed for synthesis and evaluation in this study.

1.2 Concluding remarks

This exploratory study will be used to develop an agent that is not only effective in disease detection and/or treatment, but also in monitoring and prevention. Drugs targeting neurodegeneration currently available on the market only offer symptomatic relief without stopping the progression of the disease. However through blocking over activation of NMDA receptors and VGCCs, agents that are more beneficial in this field can be developed. Attaching a fluorophore that can assist with disease monitoring and understanding is a potential option that would be beneficial. This

process of conjugating an active compound to a fluorophore is an applicable concept and applied to different neurodegenerative diseases such as AD and PD.

Table 1.1: Ketal and Aza derivatives that were designed

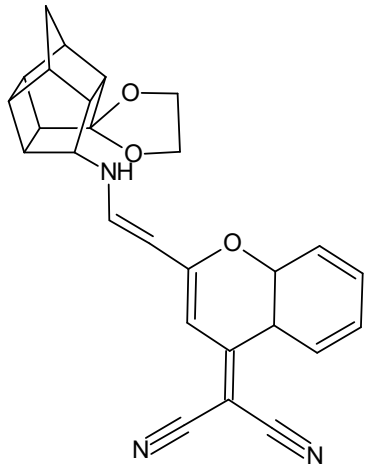	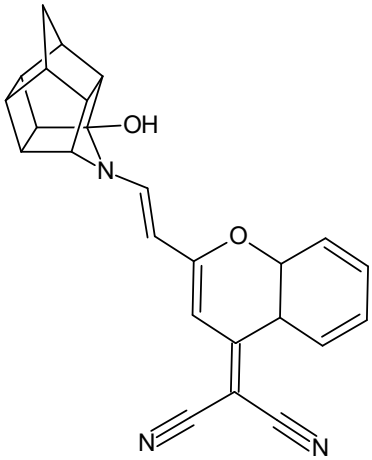
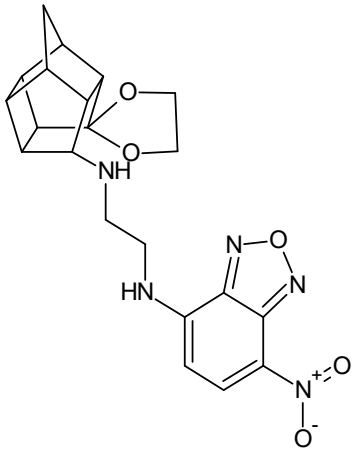	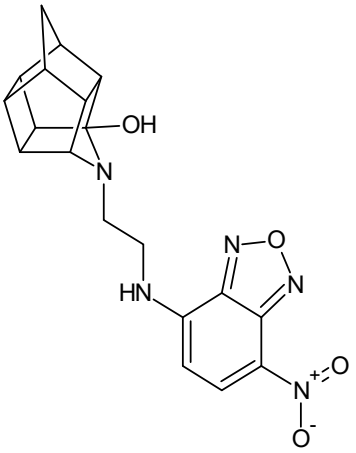
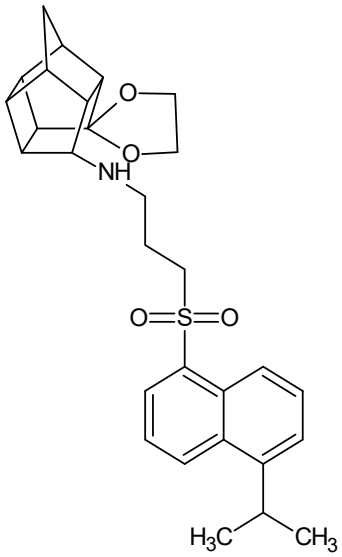	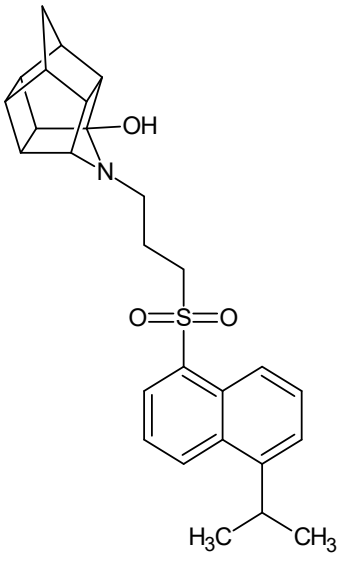

CHAPTER 2

2. LITERATURE REVIEW

2.1 Neurodegenerative disorders

Neurodegeneration occurs when neurons in the CNS, the brain in particular, are destroyed by several mechanisms (Araki *et al.*, 2001). The pathology of these ND are progressive and irreversible, and the abnormal loss of neurons from specific regions of the brain is a main characteristic of them (Alexi *et al.*, 2000). Cells affected in these specific regions become necrotic (cellular death due to injury) or apoptotic (programmed cellular death) (Connor and Dragunow, 1998). When these regions become damaged or apoptotic, a neurotransmitter imbalance occurs in a specific region of the brain, ultimately leading to the signs and symptoms that arise in these diseases(Alexi *et al.*, 2000; Zindo *et al.*, 2014a). These ND include among others Huntington's disease (HD), Alzheimer's disease (AD) and Parkinson's disease (PD). Of the vast number of neurodegenerative disorders, PD and AD are the most common, more so in the elderly (Calon and Cole, 2007; Egunlusi, 2014). Symptoms of these disorders usually start to occur around the age of sixty and progresses from there (Landrigan *et al.*, 2005). Disorders such as ALS and HD are much more rare in comparison to AD and PD, however these are fatal with little to no effective treatment options (Mayeux, 2003). Some manifest at ages as young as infancy and happen irrespective of age (Mayeux, 2003).

Although all classified as neurodegenerative diseases, it is observed that they all, even the more common ones AD and PD, have very different clinical, as well as pathological features (Tokuchi *et al.*, 2016). With AD we see a prototypical dementing illness that is related to a cortical dysfunction, amyloid-β plaques and neurofibrillary tangles formation, and cholinergic basal forebrain degeneration. However with PD, basal ganglia dysfunction, the presence of Lewy bodies, and degeneration in the substantia nigra of dopaminergic neurons are observed (Tokuchi *et al.*, 2016). The quality of life of patients suffering from these diseases is significantly diminished as their normal functionality and well-being is compromised. This is seen even more so among the ageing population, and it is a huge problem

worldwide (Alexi *et al.*, 2000). There has been a large amount of research, money and time put into this area of disorders, especially towards identifying causative factors.

The current treatment options that are available are used more for the management of these disorders and not curing them. These disorders have a profound impact on the life of both the affected patient and their families (Tarrants *et al.*, 2010). As a result of this significant impact, it has become crucial to create drugs that can stop the progression and destruction we see in this abnormal neuronal breakdown process, as well as assist in treating them, and helping monitor and diagnose them early and effectively (Schweichel and Merker, 1973).

2.1.1 Alzheimer's Disease

AD is a form of dementia that is related to neurodegeneration occurring with age and a number of other factors. AD involves progressive memory loss, as well as a decline in ability to communicate, and multiple other cognitive impairments. Worldwide there are more than 35 million cases, making it one of the most common types of neurodegenerative disorders (Lardenoije *et al.*, 2015; Selkoe, 2012). Between 40-80 people in every 1000 people suffer from AD, and the average years of living with the diseases is only 9 years (Mayeux, 2003). Moreover the extent to which the disease affects the families, caretakers and community of the sufferer, contributes to the global burden of AD. Globally the annual cost of dementia and AD is estimated at around 1 trillion US dollars, and it is expected to double by 2030 (Adelina, 2019).

AD is extremely complex and multifaceted disorder. Genetic, epigenic and environmental factors all play a role in the resulting dysfunction in homeostasis of the brain, and it can be seen with inflammation, cell cycles and many other processes and pathways in the brain (Mastroeni *et al.*, 2010). The cognitive decline, mood instability, and various behavioural and physical instabilities occur due to cortical degeneration as well as subcortical degeneration (Bediou *et al.*, 2008; Lardenoije *et al.*, 2015). It is also important to note that with AD the neural degeneration occurs in specific regions of the brain and not the entire brain (Hardy, 2006). The main areas affected by AD is the frontal cortex, temporal lobe, parietal lobe, hippocampus, entorhinal cotex and finally the cingulate gyrus (Wenk, 2007).

Current treatment for AD focuses on the management of symptoms, and even though many pre-clinical and clinical trials have been done on treatment options, the focus still lies on target and drug discovery. These treatment options only slow the disease progression, and cannot stop it or cure the disease (Mastroeni *et al.*, 2010). Approved options for treatment, as mentioned before includes AChE inhibitors such as rivastigmine (Fig 1.3), galanthamine and donepezil, or NMDA antagonists like Memantine (Fig 1.3), while other possible agents are still in the pipeline for development.

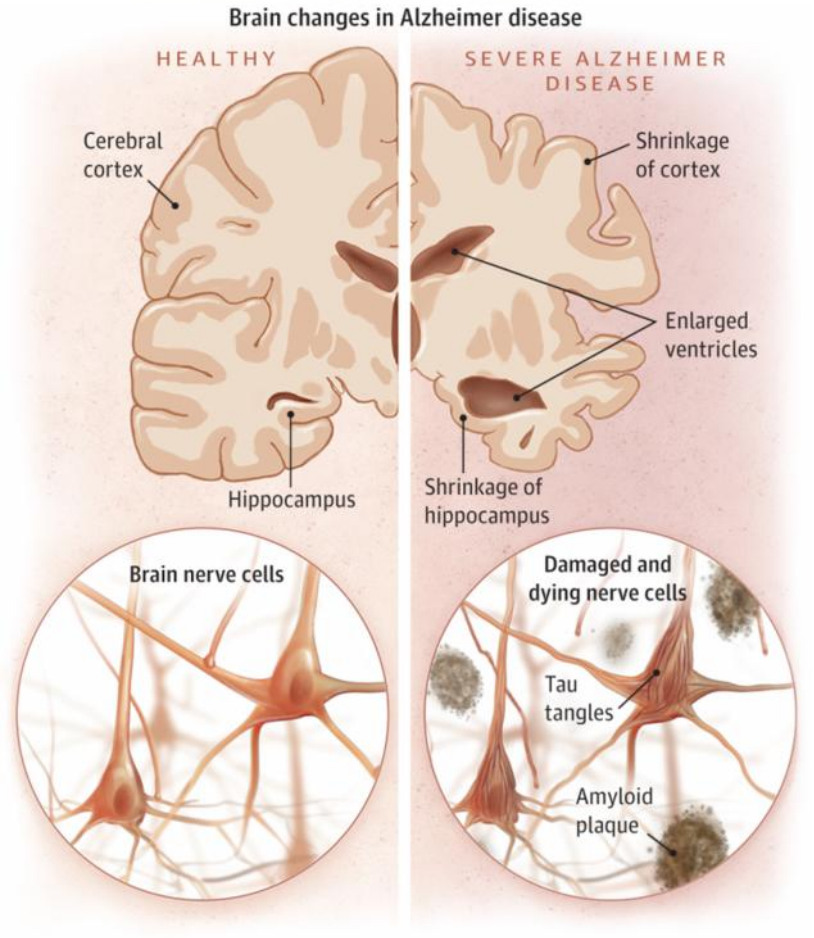

Figure 2.1: Changes observed in AD brain and neurons, compared to healthy brain (Arslan Ali, 2015)

2.1.2 Parkinson's Diseases

PD is the second most common ND disorder after AD, and involves progressive degeneration of dopaminergic neurons in the substantia nigra. Approximately 10 to

20 out of every 1000 people suffer from the disease. Duration of the illness usually last about 2 to 20 years, depending on severity, and then leads to death as a result of multiple complications. PD has been found to be more common in the male population (Mayeux, 2003). When it comes to PD genetic predisposition is reported to be a high risk factor, although age and environmental factors also play an important in role PD and its development and progression (Veldman *et al.*, 1998).

PD is known for its symptoms relating motor dysfunction, but cognitive dysfunction and ultimately cognitive impairment takes place in most, if not all cases of the cases, to some degree. This is one of the reasons PD and AD are often mentioned together or compared. One similarity between the two diseases is the degeneration of the nucleus basalis of Meynert in the brain. This region is related to the cholinergic innervation of the brain, and is believed to be responsible for some of the cognitive dysfunction and memory related changes seen in these diseases (Korczyn, 2016).

Even though a few similarities are seen between PD and AD, they do have very different histopathologies. In AD the regions of the brain mainly affected include the frontal cortex and hippocampus of the brain, while in PD it is the substantia nigra, and dopaminergic pathway. Dopaminergic neurons play a crucial role in initiating motor movements in the body, and thus the progression of PD. When these neurons are damaged or lose function, the effectiveness of movement and related activities is affected, and these are seen as the main resulting symptom in PD. The degradation of these neurons result in symptoms such as tremors, bradykinesia which is the slowness of movements and gait disturbances, which is disturbances in the ability to walk (Jankovic, 2008). These motor disturbances are also accompanied by psychiatric symptoms, autonomic impairments and some cognitive dysfunctions. These symptoms are all intrinsic to the disease and may occur prior to or after the motor related symptoms (Aarsland *et al.*, 1999). The symptoms observed in PD that are not related to motor function are due to imbalances in specific neurotransmitters in the brain. These are the serotonergic, noradrenergic and cholinergic neurotransmitters. These imbalances are accompanied by the presence of Lewy bodies (LBs) occurring in certain areas of the brain (van de Berg *et al.*, 2012). LBs are distributed throughout the CNS, more specifically in the case of PD, the substantia nigra. There are two types of LBs, called brainstem as well as cortial LBs. Brainstem LBs are intra-cytoplasmic, and spherical or elongated in shape, while

Cortical LBs tend to be irregular in shape (Wakabayashi *et al.*, 2007). LBs, regardless of the type, consist of filamentous structures similar to neurofilaments but thicker in nature. In patients with PD, the number of LBs in the substantia nigra is higher, and it corresponds to the level of neuronal depletion. It is also suggested that neurons with high levels of LBs are in the process of dying. Furthermore Cortical LB specifically could be involved in cognitive impairment seen in patients with PD (Wakabayashi *et al.*, 2007).

2.1.3 Other NDs

NDs can differ with regards to their clinical presentations, underlying physiology, and histopathology, but still have overlapping features. This is seen in lesser known NDs such as ALS and HD. ALS is a ND characterized by progressive degeneration of motor neurons (Hawley *et al.*, 2019). HD on the other hand is an autosomal dominant progressive ND. These and multiple other NDs do not receive as much attention as AD and PD as a result of the significantly higher prevalence of AD and PD. However over the last few years, awareness and incidence of the less well known NDs have increased.

HD is characterized by movement, cognitive and neuropsychiatric dysfunction and has symptoms similar to both AD and PD. (Clarimón *et al.*, 2018). HD is extremely rare with and estimated worldwide prevalence of only 2.7 cases per 100 000 people. Diagnosis occurs in the middle stages of life, around 40 years old. High rates of depression, suicide and suicide attempts are also associated with HD (Clarimón *et al.*, 2018). The histopathology of HD involves neurodegeneration in the striatum as well as the white matter and neocortex. Neurodegeneration in these areas relate to the motor symptoms as well as the cognitive side of the disease (Groen *et al.*, 2010).

ALS on the other hand overlaps with PD with regards to involvement of motor neurons specifically. Similar to both AD and PD, ALS can be genetic in nature (familial) or non-familial. It is also slightly more common in men. ALS is more likely to occur in the middle to later stages of life, and generally progresses to a fatal degree in less than five years. Similar to AD, glutamate and calcium ion related excitotoxicity is the main mechanism in neuronal cell death within ALS (Checkoway *et al.,* 2011; Logroscino *et al.*, 2005; Sen *et al.*, 2005). With the histopathology of ALS,

intracytoplasmic bodies with neurofilaments and spheroids containing enzymes and ions are involved in formation of reactive oxygen species (ROS) (Checkoway *et al.,* 2011; Nordlund and Oliveberg, 2006).

Table 2.1: Comparison between different NDs

ND	Characteristic Pathology	Symptoms	Approved Treatment Options
AD	Neurofibrillary tangle formation, Amyloid-β aggregation, glutamate receptor dysfunction and calcium ion imbalances.	Dementia, loss of cognitive function, mood alterations, memory loss.	Rivastigmine, memantine
PD	Neurotransmitters imbalances, Lewy bodies occurrence.	Tremors, bradykinesia, gait disturbances, autonomic impairments and some cognitive dysfunctions.	Selegiline, rasageline
HD	CAG gene coding deregulation.	Movement, cognitive and neuropsychiatric dysfunction.	Tetrabenazine amantadine, riluzole
ALS	Glutamate receptor dysfunction and calcium ion imbalances, as well as genetic factors, proteins involved in RNA processing and excitotoxic damage.	Muscular weakness, loss of muscle, speech and breathing difficulty, mild cognitive impairment.	Riluzole

2.2 Mechanisms involved in Neurodegeneration

Neurodegenerative diseases for the most part have a common mechanism of degeneration or neuronal damage. The etiopathology of these diseases is complex and heterogeneous (Geldenhuys *et al.*, 2011; Egunlusi, 2014). When it comes to the mechanisms and pathogenesis of the different neurodegenerative diseases, a number of common features arise. One of the common features is when disease specific proteins, such as amyloid-β (Aβ) or tau-proteins accumulate, and aggregation occurs at an abnormal rate, ultimately leading to the loss of cell function. Further evidence has also shown that these abnormal levels of aggregated protein can spread from one cell to another, and also from a specific area in the brain to

another area. This in turn induces protein misfolding, leading to the aggregation, resulting in previously unaffected cells or environments being drawn in. It is important to note that genetic mutations, and environmental factors, such as oxidative stress can promote or induce this protein misfolding and aggregation that is seen in neurodegenerative diseases (Herrero and Morelli, 2017). Underlying mechanisms of some of these disorders themselves are still not well understood in many cases (Herrero and Morelli, 2017). As mentioned previously both genetic and environmental factors are initiators of ND.

Neuronal cells which are prone to degeneration either become apoptotic or necrotic (Feuvre *et al.,* 2002; Egunlusi, 2014). In patients suffering from ND, intrinsic cell death or suicide takes place. This is a programmed process known as apoptosis, and takes place in the CNS (Schweichel and Merker, 1973). Oxidative stress, excitotoxicity and metabolic compromise are but a few mechanisms involved in triggering a number of pathways which lead to apoptosis.

2.2.1 The lethal triplet

The key mechanisms involved in neuronal cell death, whether necrotic or apoptotic in nature, are often referred to as the lethal triplet (Joubert *et al.,* 2007). This triplet consists of metabolic compromise, oxidative stress, and excitotoxicity. Although not the only processes that can cause cell death, one or a combination of these processes are usually involved.

2.2.1.1 Oxidative Stress

Oxidative stress refers to the physiological reaction that takes place in the body as a result of the increasing and progressive damage caused by free radicals that are not properly neutralised by endogenous antioxidants. The process is believed to be linked to ageing or diseases (Halliwell, 2001). It is usually an imbalance in the level of these free radicals and/or the amount of natural antioxidants that are meant to be present within the cell and body. This imbalance leads to oxidative damage of the cell as well as its components, and ultimately causing neurotoxicity and cell death (Gilgun-Sherki *et al.,* 2001; Crouch *et al.*, 2008; Gonsette, 2008). AD and often other neurodegenerative diseases are associated with ROS and these free radicals. The imbalances mentioned before often causes damage to cellular components and/or

biological molecules through peroxidation. This, in turn results in apoptosis (Uttara *et al.*, 2009).

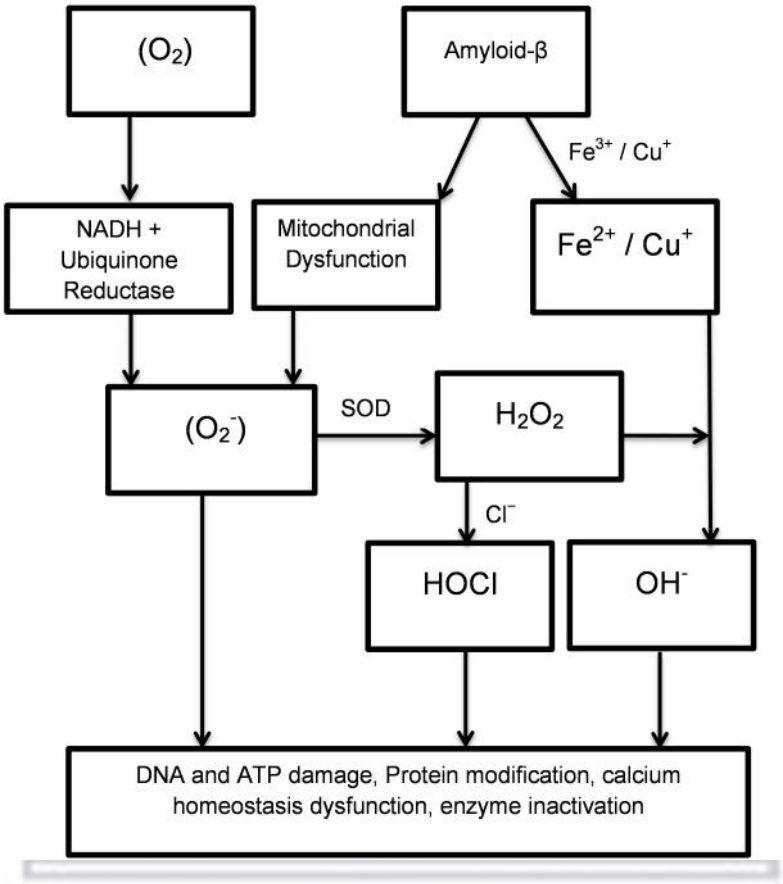

Figure 2.2: Chemical and molecular mechanisms in cell death (Lü *et al.*, 2010).

Free radicals are formed when compounds that contain one or more unpaired electrons usually become more reactive in nature. Common free radicals include the superoxide radical (O^-). This free radical is extremely reactive due to a reaction where one electron escapes from the electron transport chain in the mitochondrial membrane (Teponnou, 2017; Halliwell, 2001). Nicotinamide Adenine Dinucleotide (NAD), which is a cofactor found in all living cells, when in its reduced form NADH, together with the enzymes ubiquinone reductase and ubiquinone cytochrome C, forms an enzymatic complex. This complex catalyses the reaction of oxygen with the escaped electron, and forms the superoxide radical. Antioxidant enzymes such as SOD (superoxide dismutase) assist in converting the superoxide radical to hydrogen peroxide, a free radical that is much less harmful. Hydrogen peroxide can however still form a reaction with copper (Cu^+) or iron (Fe^{2+}) causing the hydroxyl radical (OH^-

) to form. This free radical is also a very strong ROS. The reaction between chlorine and ROS can lead to the formation of hypochlorous acid (HOCl), through a reaction catalysed by myeloperoxidase (MPO). However if hydrogen peroxide is in the presence of antioxidants such as either glutathione peroxidase (GPX) or antioxidant enzyme catalase (CAT), it is converted to water (Lü *et al.*, 2010). It is the imbalance or lack of enzymes or antioxidants such as GPX or CAT that ultimately result in the accumulation and damaging effect free radicals have on cells.

Amyloid-β (Aβ) plaque formation has also been linked with the production of ROS and there is much research on the role of Aβ in ND. Aβ plagues form and ultimately play a role in ND through a process often referred to as the Aβ cascade hypothesis. The cascade starts with missense mutations of dysregulation of APP, PS1 or PS2 genes. This dysregulation results in increases Aβ production and accumulation (Hardy and Selkoe, 2002). Aβ then interacts with a number of metal ions such as (Cu^{2+}, Fe^{3+} and Zn^{2+}) and this interaction results in reduced forms of these ions namely Cu^{+} / Fe^{2+} / Zn^{+}. Once in this form the metal ions can now interact with hydrogen peroxide and produce the previously mentioned OH^{-} (Uttara *et al.*, 2009). Throughout the body we find multiple sources of ROS such as by products from monoamine oxidase (MAO) activities. Hydrogen peroxide is one of these by-products, and as mentioned before can from ROS that causes oxidative stress and cellular damage, in this case mitochondrial and cytoplasmic dysfunction (Sturza *et al.*, 2013). Having ROS in the body is extremely important, due to the fact that they often act as antimicrobials, as well as playing a key role in degrading foreign matter (Nimse and Pal, 2015). The problem is that ROS are capable of producing a vast number lethal cellular effects. ROS can cause the depletion of ATP within cells, cause increased levels of cellular Ca^{2+}influx elevation and various other processes that can lead to the process of cellular degeneration process (Raffray and Gerald M., 1997). Within a healthy body antioxidant enzymes such as carotenoids, or the presence of components such as Vitamin E or C, tends to neutralise or inactivate ROS (Uttara *et al.*, 2009).

Oxidative stress plays a large role in AD pathology, specifically with regards to free radical attack, mitochondrial dysfunction, nucleic acid damage and protein oxidation. Oxidative stress ultimately leads to the damage of DNA, RNA, proteins and lipids

and cells and neurons on multiple levels. This ultimately results in apoptosis and disease states (Lü *et al.*, 2010).

2.2.1.2 Excitotoxicity

Excitotoxicity plays a major role in neurodegeneration in both acute and chronic CNS diseases. Ca^{2+} ions are seen as the key mediators involved in the excitotoxic process and the damage caused by it. These ions act as intracellular messengers, and control various cellular functions such as membrane excitability, exocytosis and also synaptic activity. Because they play such a key role, there is a constant extremely complex balance between the influx and efflux of Ca^{2+} ions at the cell's ion channels. These levels are controlled by neurons and they enable the signalling cascade, regulated by these ions to occur under normal physiological conditions. Once there is an excessive influx or efflux of these ions from intracellular stores, the Ca^{2+} regulatory mechanism can be overloaded, leading to the Ca^{2+} dependant processes to be activated at the wrong time. This can lead to metabolic derangements that effect cell death (Choi, 1988; Tymianski and Tator, 1996; Sattler and Tymianski, 2000).

Glutamate is the key or major neurotransmitter involved in the process of excitotoxicity in the CNS. The release of glutamate stimulates both ionotropic and metabotropic receptors resulting in these postsynaptic responses. The main ionotropic receptors are NMDA, AMPA and kinase receptor subtypes. These receptors form an ion channel pore when they are stimulated or activated. Activation specifically causes cellular Ca^{2+}, Na^{+} and K^{-} ions permeability. Excitotoxic effects occur through activation of the glutamate receptor and calcium channel on neuronal cells. When metabotropic receptors are activated, there is an indirect link to the same ion channels. It is observed that activation causes stored Ca^{2+} ions to be mobilised. This occurs through a number of mechanisms that is dependent on GTP-binding protein dependant mechanisms (Tymianski and Tator, 1996; Arundine and Tymianski, 2003). GTP or trimeric G-proteins binding proteins play a crucial part in signal transduction pathways for multiple hormones and neurotransmitters, in this case glutamate. Research has shown that most if not all subtypes of the glutamate receptors are involved mediating or causing neurotoxicity on some level (Arundine and Tymianski, 2003). This is the reason we see the connection between excessive

levels of Ca^{2+} influx into cells and glutamate related damage or injury to neurons (Arundine and Tymianski, 2003).

This form of primary or direct excitotoxicity occurs when the NMDA receptors get over activated by abnormal or excessive amounts of glutamate. This causes Ca^{2+} influx, but because of the excessive levels of glutamate there is an intracellular Ca^{2+}overload (Lipton, 2007). Sensitive VGCC are also activated, adding to the cumulative effect of the intracellular overload. This process results in a disturbance in the cellular Ca^{2+} homeostasis. As a result of the disturbances of specific enzymes get activated. The processes of these enzymes result in the previously discussed 'free radicals being formed, which ultimately leads to neuronal cell damage and death.

The second type of excitotoxicity is referred to as indirect excitotoxicity. In this process glutamate receptor stimulation is normal and unchanged. However cell death in this case occurs due to the postsynaptic neuron being damaged or weakened. There can be multiple reasons for this damage or weakness to be present in a neuron. If there is mitochondrial dysfunction as mentioned previously, it can be a result of oxidative stress, and low levels of ATP production can occur. Normal cellular processes cannot take place because of the low levels of ATP. This means the energy for cell activity is not sufficient. This cascade of events causes damage to the neuron and cell apoptosis occurs eventually (Fulvio Celsi *et al.,* 2009).

2.2.1.3 Metabolic Compromise

Metabolic compromise can also be referred to as bioenergetics impairment. Bioenergetics refers to cell energy metabolism. Metabolic compromise in other words refers to a deficiency in the ability to provide the required energy levels for normal cellular function. For the brain to function at optimal capacity, it require a lot of energy and it consumes approximately 20% of body basal oxygen for this purpose. If there is disruption or an imbalance in the homeostasis of the oxygen, energy levels and metabolisms of the CNS and the brain, it can easily result in disease states, whether these changes are small or not. Differences in neuronal function lead to possible cell death and neurodegeneration. (Grimm and Eckert, 2017) Metabolic compromise occurs when cells or neurons are deprived of the

cellular substances, including oxygen, required for optimum cellular function. For this reason the mitochondria plays a crucial role. It is often referred to as the cellular powerhouses, providing ATP as cellular energy. It produces the energy that is essential for most cellular processes, specifically regulation of intracellular Ca^{2+} homeostasis, synaptic plasticity and the synthesis of vital neurotransmitters (Grimm and Eckert, 2017). In multiple neurodegenerative diseases such as PD and HD it had been found that there are reduced levels of mitochondrial enzymes. This enzymatic deficit results in metabolic injuries and ultimately reduced or complete loss of function in the mitochondria. This leads to lower levels of ATP in cells, in this case neurons. In diseases such as PD, we see this depletion of ATP which mostly in the basal ganglia, resulting in cell death and neurodegeneration. ATP depletion plays a significant role in metabolic compromise, as it means cellular ion pumps which are dependent on ATP cannot function. This means depolarisation of these neurons cannot occur(Greene and Greenamyre, 1996).

As the mitochondria functions less optimally, and the ionic integrity of the cell becomes compromised, the ability of the mitochondria to buffer itself from the intracellular Ca^{2+} and other ions becomes hindered. This causes Ca^{2+} accumulation in the mitochondria, as well as affecting Ca^{2+} homeostasis in the cell, resulting in increased levels of oxygen and nitrogen free radicals, further damaging the neuron due to the cytotoxic nature of these free radicals (Stout *et al.*, 1998).

Figure 2.3 indicates how the lethal triplet and more specifically the mitochondria influences brain ageing and damage to the CNS and neurons. Increased levels of oxidative stress plays a crucial role in these disorders, while high levels of ROS depletes the antioxidant system. When at homeostasis these processes leads to normal ageing, but as soon as the pathological threshold is passed due to processes involved in the lethal triplet, it triggers multiple processes inducing neurodegeneration (Grimm and Eckert, 2017).

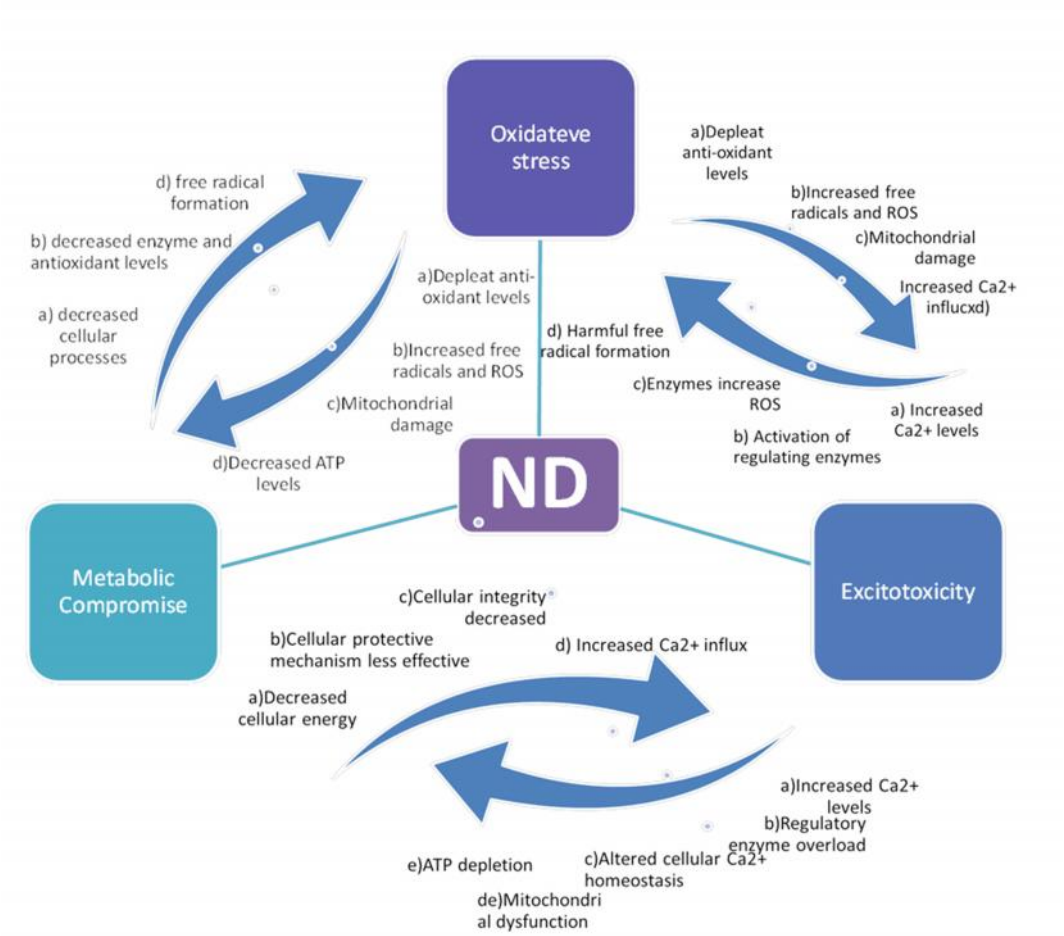

Figure 2.3: The lethal triplet

2.2.2 Apoptosis and Necrosis

Apoptosis is known or referred to as the chain of enzymatic processes that take place resulting in energy-dependent and programmed cell death (Raffray and Gerald M., 1997; Egunlusi, 2014). Apoptosis is the most common form of neuronal cell death (Krantic *et al.*, 2005). Necrosis on the other hand usually occurs to a high number of cells at once, resulting from a high degree of injury or stress. Often this injury will be severe, unexpected and sudden in nature, and is caused by detrimental agents or cellular injury. It affects the cell homeostasis to the point where cellular function is lost irreversible and uncontrollable enzymatic processes take place. This causes high levels of inflammation and eventually cell death (Raffray and Gerald M., 1997; Egunlusi, 2014).

Apoptosis, as a process, is slow and part of normal growth and differentiation of cells and organ systems in both vertebrates and invertebrates. It is centred on matching neuronal populations to target size. Apoptosis is believed to mostly be controlled by a limiting supply of target-derived trophic factors, but is also controlled by afferent stimulation (Martin *et al.*, 1998). Apoptosis consists of two main pathways, referred to as an intrinsic and extrinsic pathway of neuronal cell death.

The intrinsic pathway is related to UV exposure, mitochondrial damage as a result of ROS and reactive nitrogen species (RNS), excitotoxicity due to increased Ca^{2+} influx, and finally hypoxia. Due to some or all of these processes or environments, cytochrome C is released into the cytosol. This results in the subsequent formation of the apoptosome and finally effector caspases activation. The second or extrinsic path occurs when the binding of specific ligands happens to apoptotic initiating receptors that belong to the family of tumour necrosis factors. This binding between receptor and ligand causes the activation of effector caspases (Waldmeier, 2003; Artal-sanz and Tavernarakis, 2005).

Necrosis, on the other hand, is much more rapid. The cell inflammatory process that takes place as mentioned before, leads to swelling and ultimately the rupture of the cell plasma membrane, damaging the integrity of the cell. The process of necrosis is not as well understood as that of apoptosis, but it is believed that intracellular Ca^{2+} influences necrosis when occurring at accelerated rates. Unlike apoptosis, caspases are not believed to be involved in necrosis (Artal-sanz and Tavernarakis, 2005).

2.3 Polycyclic Cages

Polycyclic cage compounds play an essential role in synthetic organic chemistry due to their unique properties which stem from their rigid structures. As a result of this they have a key role in the design and synthesis of both natural and non-natural products. The C-C bonds within the cage and their angles result in a unique synthetic architecture. The use of polycyclic cages and derivatives thereof has been a focus in the field of drug design for many years (Joubert *et al.*, 2011; Onajole *et al.*, 2012). Compounds such as adamantine and pentacycloundecane (PCU) have become a focal point in drug design since the discovery of anti-viral properties of amantadine (Onajole *et al.*, 2012). These structural derivatives have the ability to

improve drug lipophilicity, a crucial aspect when it comes to drug transport across cellular membranes, the CNS and the BBB. Furthermore, it has been found that polycyclic derivatives slow down or lower bio-degradation of drugs once in the body when it gets subjected to biological systems. This ensures these compounds have longer pharmaceutical effects (Onajole *et al.*, 2012). Some of the cages such as amantadine, and PCU are also extremely rigid in conformation, which means they are often able to maintain their conformational entropy when binding or interacting to proteins or receptors, and as a result of this maintaining their pharmacological activity. Polycyclic cages are highly beneficial in drug design as they can also improve and change both pharmacokinetic and pharmacodynamic properties of other chemical compounds (Oliver *et al.,* 1991). Memantine is one example, where the adamantane cage is structurally altered to synthesise a compound that is clinically well tolerated, has a low affinity, and is an uncompetitive NMDA receptor antagonist (Geldenhuys *et al.*, 2004). Another example is NGP-101, a PCU derivative with significant NMDA antagonist activity, but also neuroprotective properties (Zindo *et al.*, 2014a). Polycyclic compounds as seen in Figure 1.3, can be used as a building block or privileged structures by attaching side chains and resulting in improved properties such as the lipophilicity of a drug (Oliver *et al.*,1991).

Polycyclic cages have many more biological activities. Besides the use of amantadine in PD, PCU derivatives have anticataleptical activity, while others such as D3-trishomocubanes have anti-oxotremorine and anticataleptic activity. Some cages have also shown a degree of anti-TB activity (De Vries, 2006).

2.4 Potential mechanisms of action and target sites

2.4.1 N-methyl-D-aspartate receptor

As previously mentioned, excitotoxicity plays a large role in a various neurodegenerative diseases and their progression.. This suggests that it can be a common pathway or process to target in ND. This process of excitotoxicity takes place as a result of over-activation of receptors for excitatory neurotransmitters such as the NMDA and α-amino-3-hydroxy-5-methyl-4-isoxazolepropionate (AMPA) receptors. Ionotropic glutamate receptors like NMDA receptors, regulate quick

responses to the major excitatory neurotransmitters that are found in the CNS (Egunlusi, 2014).

NMDA and kainic acid act as excitotoxins when binding to NMDA receptors. When these receptors are activated in high levels, it ultimately results in excitotoxicity. It creates numerous toxic and damaging consequences to cells, which include disturbing Ca^{2+}homeostasis, formation of free radicals, and finally interfering with mitochondrial permeability and function (Oliver *et al.,* 1991).

NMDA receptors regulate the plasticity of the synapses through controlling Ca^{2+} entry through the NMDA receptor. Excessive activation of these receptors results in cellular death through a number of cytoplasmic as well as nuclear processes taking place within the cell. It is because of this reason that drugs that block or regulate NMDA receptors have therapeutic relevance, especially in ND (Cookson *et al.*, 1964).

An important aspect about the structure of the NMDA receptor is that it has an S-nitrosylation site. In the extracellular region of the receptor the N-terminus can be found as illustrated in Figure 2.4. This is referred to as the modulatory site of the NMDA receptor. At this site activity of the NMDA receptor is controlled through the process known as S-nitrosylation. During this reaction a nitric oxide group in covalently bonded to a cysteine sulfhydryl. It causes down regulation of the receptor and decrease channel opening and activity, preventing excessive amounts of $Ca^{2+}$from entering the cell, ultimately having a neuroprotective effect (Schyf, 1989).

Although neurodegenerative diseases may result due to multiple different mechanisms, processes and factors, the fact that neuronal injury occurs due to overstimulation of glutamate receptors, usually NMDA, is a common denominator between these diseases (Marchand *et al.*, 1988).

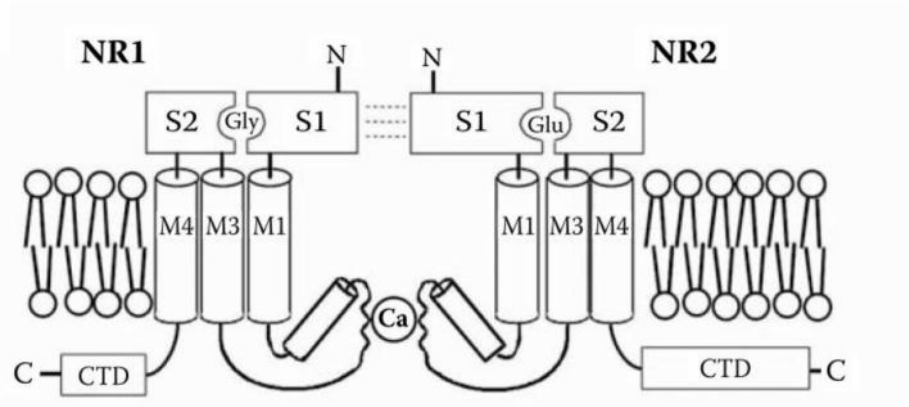

Figure 2.4: The structure of the NMDA receptor (lanke ML, 2009).

2.4.2 Voltage-gated calcium channels (VGCCs)

Evidence that Ca^{2+} overload is implicated in NDs and ultimately acts as a neuron death-triggering signal has been extensively researched and proven. VGCC are present in many different cell types, and play an important physiological role in these cells. Roger Simon discovered in 1984 that after an ischemic insult event there is a significant increase in Ca^{2+} build-up within the hippocampus. This resulted in interest forming around the role and involvement of Ca^{2+} overload in neurodegeneration (Cataldi, 2013). VGCC regulate Ca^{2+} influx into the cell, when membrane depolarisation takes place, and is thus a controlling agent with regards to the amount of Ca^{2+} moving into the cell. These channels in other words act as secondary messengers when it comes to initiating cellular activity (Catterall and Few, 2008). VGCCs initiate the synaptic transmission that takes place in cells. This results in signalling between synapses, within neurons (Tsien *et al.*, 1988; Dunlap *et al.,* 1995; Catterall and Few, 2008). How effectively neurotransmitters are released from neurons are dependent on Ca^{2+} entering the neuron. This entry firstly initiates the fast release of glutamate, acetylcholine, and GABA, and furthermore ensures these neurotransmitters continue to be released (Catterall and Few, 2008). Presynaptic Ca^{2+} channels conduct currents in order to initiate synaptic transmission in neurons. Efficiency and effectiveness of neurotransmitter release is dependant Ca^{2+} entry. This high level dependence of neurotransmission on Ca^{2+} entry, means the presynaptic Ca^{2+} channel is extremely sensitive and a crucial target for control and regulation.

VGCCs are thus closely related to the NMDA receptor activity, and more importantly implicated in excitotoxicity, and many neurodegenerative disorders. Extensive research has been done which shows that drugs acting on VGCCs are beneficial neurodegenerative diseases (Van der Schyf *et al.,* 1986). These drugs are effective because they block Ca^{2+} that enters cells through VGCC. Apoptosis is more likely to arise from higher or abnormal levels of Ca^{2+} entering the cell. When a significant increase in Ca^{2+} entry occurs, it can result in saturation of mitochondria's buffering capacity, disrupting mitochondrial homeostasis. This causes damage to the mitochondria, and eventually neuronal death.

2.4.3 5-HT

5-hydroxytryptamine, also referred to as serotonin is a monoamine neurotransmitter, specifically linked to emotions of well-being and happiness. It does however have a complex and multifaceted function in the brain and body, influencing multiple biological as well as physiological processes. Some of these processes include controlling aspects of the memory and cognition centres of the brain. This complex serotonin system undergoes degeneration in both normal aging as well as AD, and it has been proven by multiple neuropathological and neuroimaging studies (Smith *et al.*, 2017). These studies proved neurofibrillary tangle formation and neuronal loss in specific cell bodies which originate in serotonin projections, known as the raphe nuclei cell bodies (Curcio and Kemper, 1984; Smith *et al.*, 2017). Post mortem studies of AD patients also showed a significant decrease in the level of serotonin and metabolites of the neurotransmitter such as 5-hydroxyindoleacetic acid in the cortex of the brain when compared to controls. This was accompanied by decreased serotonin transporters (SERT), 5-HT2A and 5-HT1A receptors (Palmer *et al.*, 1988; Smith *et al.*, 2017). The shortage or decreased levels of serotonin is to be more widespread than other monoaminergic and cholinergic neurotransmitters in AD specifically (Palmer *et al.*, 1988; Stout *et al.*, 1998; Smith *et al.*, 2017). The widespread influence of the serotonin system is even seen in receptors, as neuroimaging studies have proven the cortical 5- HT2A receptors are less in AD, globally (Blin *et al.*, 1993), while lower levels of cortical and hippocampal 5-HT1A receptor availability is also seen. This decrease in the serotonin receptors in the cortical and hippocampal regions of the brain can be associated with cognitive impairment seen in AD. Furthermore it results in decreased metabolism of glucose in

the hippocampal region of the brain and ultimately relates to the neuropathology of AD (Kepe *et al.*, 2006; Smith *et al.*, 2017). Other studies showed lower SERT in the striatal, midbrain and temporal cortex regions of the brain when compared to control groups (Ouchi *et al.*, 2009; Marner *et al.*, 2012).

Serotonin deficiency has also been seen in other ND. PD is an ND with complex motor dysfunctions, yet multiple non-motor symptoms also occur in these patients. These include depression, anxiety disorders and abnormalities in sleep patterns (Prediger *et al.*, 2012; Troeung *et al.,* 2013; Chen and Marsh, 2014), while other studies also show attention deficit, learning impairments and a decline in recognition memory (Lewis *et al.*, 2003; Wood, 2012; Leal *et al.*, 2019). Studies have shown that these non-motor symptoms play a significant role in the health-related quality of life of the patient and ultimately the progression of disability for patients suffering from PD (Den Oudsten *et al.,* 2007; Soh *et al.,* 2011; Leal *et al.*, 2019). In some cases of PD the non-motor symptoms have been observed before the motor symptoms (Elgh *et al.*, 2009; Benito-León *et al.*, 2011; Chen and Marsh, 2014). As studies have shown these non-motor symptoms of PD do not respond to dopaminergic medication (Chaudhuri *et al.,* 2006; Prediger *et al.*, 2012), non-motor dysfunction is believed to be caused by other neurotransmitters, such as serotonin and acetylcholine. The influence of the altered serotonergic system have been seen in both clinical and preclinical studies, specifically in the physiological and emotional processes of PD patients (Ohno *et al.,* 2013; Faggiani *et al.*, 2018). The non-dopaminergic progression of PD is still unclear in many ways, and as a result current therapies for PD do not address symptoms that are non-motor related (Pavese *et al.*, 2011; Politis and Loane, 2011).

2.3.4 Amyloid-Beta

There is a lot of research implicating protein misfolding and aggregation in ND. Aβ misfolding, the ultimate growth by gradual accumulation of Aβ and other proteins like α-Syn, tau, IAPP, polyglutamine and superoxide dismutase are well known to be underlying causes and factors in ND as AD, HD, PD and ALS (Soto, 2003; Knowles *et al.,*2014; Rajasekhar *et al.*, 2017).

The term amyloid originates from the expression “corpora amylacea”, first noted around 1854 by a German physician and scientist known as Rudolph Virchow. He

found small corpuscles with atypical microscopic appearance around some blood vessels within the CNS of elderly subjects (Sipe and Cohen, 2000). In 1859 it was discovered that these amyloids are high in nitrogen content, and as a result of this, it changed study of amyloids to another path. Amyloids were now investigated as proteins, and more importantly this meant they are susceptible to conformational change forming ultimately amyloid fibrils (Sipe and Cohen, 2000).

It has since been found that amyloid peptides accumulate in AD, causing amyloid plaques (AP) to form. When mis-folded Aβ peptides, mostly Aβ42 and hyperphosphorylated tau proteins undergo aggregation, insoluble Aβ plaques and neurofibrillary tangles(NFT) form in the brain (Hamley, 2012; Rajasekhar *et al.*, 2017). As the plaques form there is a significant increase in VGCC currents, resulting in neuronal cell death in AD. Studies have shown a significant increased potentiation of L- and N- type VGCC currents when exposed to AP. More recently research revealed that AP also inhibit P-type currents, and could as a result of this be related to the cognitive impairment seem in AD (Nimmrich *et al.*, 2008). AP occur in different forms, and the status of it affects the way in which AP modify VGCC currents. AP oligomers for instance activates VGCC more than non-toxic aggregated forms (Ramsden *et al.,* 2002). Even though the exact mechanism by which AP increase VGCC currents is not know, it is believed to be as a result of free radical generation in L-type VGCC activation (Ueda *et al.*, 1997).

Aβ-plaques and aggregates play a vital role in AD diagnosis, specifically because it can be used as a selective target in distinguishing AD from multiple other dementia related diseases (Spires-Jones and Hyman, 2014). Most cases of AD only get diagnosed once the cognitive state and capabilities of a patient was tested, and this only becomes possible when the disease has progressed and there is significant and irreversible brain degeneration. Making a diagnosis tool that targets sites with AP can be crucial in managing AD (McKhann *et al.*, 1984).

2.5 Fluorescence

The design and use of fluorescent agents, ligands or probes, and the associated imaging techniques has received significant attention over the last few years. A major aspect of this has been heading towards agents with emission wavelengths in the deep-red to near-infrared regions (NIR)(Li *et al.*, 2016). Fluorophores or

fluorescent dyes that emit light in the NIR, have a wavelength of around the >600 nm region. They are considered crucial in biological and clinical applications. The reason for focussing on agents in the NIR, is because they cause minimal photodamage to biological tissue and specimens. Agents emitting light in this region also show outstanding deep tissue penetration. Lastly, with agents emitting light in the NIR minimum interference is seen from the natural fluorescence emitted by biological substances or molecules in living systems, known as auto fluorescence (Zhang *et al.*, 2015). Autofluorescence is defined as the natural emission of light by biological structures, usually mitochondria and lysosomes, when they have absorbed light.

Fluorescent agents such fluorophores, fluorescent ligands, or fluorescent probes give us the ability visualize and form images of cellular activities. The process is becoming increasingly convenient, detailed and advanced, as it allows researchers to describe but also do a visualisation of different biological phenomena. Imaging technology based on fluorescence are not only effective techniques, but also incredibly useful and cost effective in the cellular imaging field (Li *et al.*, 2016).

Fluorescence is an optical phenomenon based on a principle where an external energy source supplies energy a specific body. This body or fluorescent molecule absorbs this energy from the external source and emits a fluorescent signal at a specific wavelength (Wood, 1994). The process occurs in three main stages, and can only take place in certain molecules, with specific properties allowing them to absorb energy from the source but also emit it. These molecules are usually poly-aromatic hydrocarbons or heterocyclic hydrocarbons and are thus referred to as fluorophores (Wood, 1994).

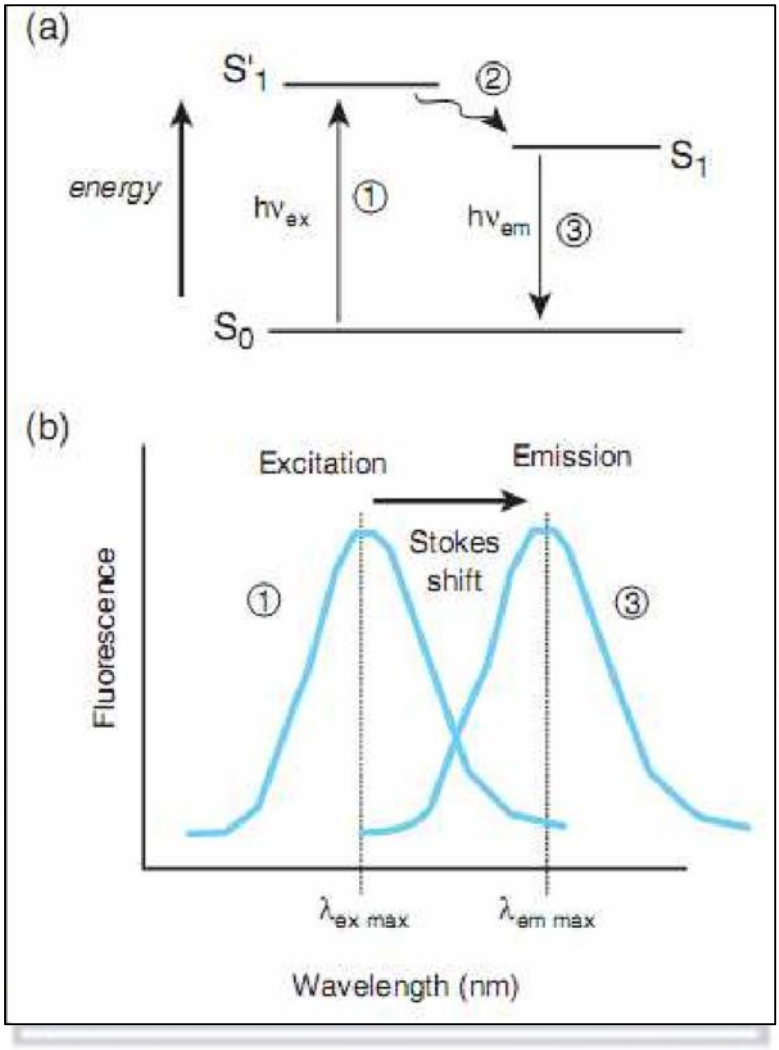

Figure 2.5: (a) The drop in energy from the first stage of fluorescence to the final stage, (b) and the accompanying stokes shift observed (Al-khafaji, 2017).

The first stage of fluorescence is known as excitation. During excitation the external energy source supplies a photon of a specific energy, either through an incandescent lamp or a laser. The fluorophores then absorbs this energy, which results in an excited energy state (Figure 2.5 (a) 1). The second stage of the fluorescent process is known as the excited-state lifetime, indicated by 2 in Figure 2.5. The molecule can only exist in this state for a finite time, during which conformational changes occur within the fluorophore. The third and last stage of the process is known as fluorescence emission. The molecule or fluorophore emits a photon during this stage, which results in the fluorophore returning to its ground energy state from the excited state achieved in stage two (Figure 2.5 (a) 1). As

energy from the excited-state lifetime dissipates in this stage, the energy of this photon is lower. The lower energy accounts for longer wavelength, compared to the excitation photon, as the relationship between energy and wavelength is inversely proportional.

The loss or difference in energy seen between the excitation and emission stages is referred to as the Stokes shift, and can thus be defined as the difference, between the peak excitation (absorption) and the peak emission wavelengths (Wood, 1994). The Stokes shift phenomenon explains how a fluorophore or fluorescent molecule is excited at a specific wavelength, and then it emits light at a longer wavelength (Figure 2.5 (b)). This process is seen as a constant or general rule in fluorescent molecules and is also referred to as a red Stokes shift (Wood, 1994). Blue stokes shifts can also occur due to a phenomenon known as Raman scattering. When Raman scattering occurs, the incoming excitation light or energy interacts with the sample which results in scattered light. This scattered light is lessened in energy by the vibrational modes of the chemical bonds of the specimen (Wang and Zhang, 2014).

2.4.1 Fluorescent ligands and methods of disease detection

PET, SPECT and MRI-based techniques are just a few disease detection techniques that have been developed for detecting and imaging the brain and specific regions of it (Adlard *et al*., 2014). PET, Positron emission tomography is nuclear imaging technology, and is often referred to as molecular imaging. It is used as an important tool to visualise or image protein aggregates in the brain. The disadvantage of PET is that it is expensive and hazardous to humans. This is because of the use of radiolabeled nuclei in the imaging process (Zhu *et al.,* 2014). As a result of many imaging techniques showing similar as well as other risk factors, more attention has been shifted to focus on developing fluorescent probes and ligands, more specifically those on the NIR fluorescence region, as mentioned earlier in this chapter. The reason for this is that these probes are usually easily synthesised, they tend to be less expensive, have a long shelf-life, can be easily identified in the body as they have minimal interference from auto-fluorescence and finally they show a significant and good tissue penetration depth, which will assist in receiving information from deep inside a specimen or target site. All of these factors make fluorescent ligands in this region perfect candidates to be used diagnostic and imaging agents for diseases

(Rajasekhar *et al.*, 2017). There are also various fluorescent imaging techniques, and devices designed to detect fluorescence and other probes because of this. Firstly there are spectrofluorometers and microplate readers, of which both measure the fluorescent properties of bulk samples (Chen, Dzitoyeva and Manev, 2012). Fluorescence microscopes, another imaging device, resolves fluorescence as a function of spatial coordinates in two or three dimensions for microscopic objects (Roe, 1990). Flow cytometers can measure the fluorescence per cell in a flowing stream, known as flow cytometry (Haugland *et al.,* 2002). Other types of instrumentation used in fluorescence detection include capillary electrophoresis apparatus, DNA sequencers and microfluidic devices. All these instruments produce their results in terms of different variables and have different specifications with regards to the intensity or type of fluorescent signal. One example of this can be seen with photobleaching that is often problematic in fluorescence microscopy, because it does not result in a significant impediment in flow cytometry. These fluorescent instruments and techniques are of great importance in various fields of medicine, research and every day testing. They are thus often used in disease detection, but also have various other applications (Haugland *et al.,* 2002).

There are multiple reports and a vast number of research being done on probes, designed to bind to different protein aggregates, or targets in the human body, and are considered as candidates for use in disease detection. A problem seen with many of these probes or ligands are the lack specificity for the desired target, and thus they are not suitable for selectively detecting and diagnosing specific diseases. The urgency to design and develop more aggregate or target specific imaging agents or ligands, is well documented. These agents can be used in understanding disease progression and help study the effect, and effectiveness of therapeutic agents and treatment plans for specific diseases. (Rajasekhar *et al.*, 2017).

The combination of these fluorophores or probes used with the imaging instruments lead to the development of multiple assays used in disease detection and diagnosis or research. Examples of current uses of fluorescence include assays for biomolecules, metabolic enzymes and DNA sequencing. Research done in biomolecule dynamics, more specifically cell signalling and adaptation has also been developed (Applications and Sciences, 2005). The use of fluorescence plays an essential role in disease diagnosis and detection, by making use of, for example

fluorescence microscopy. Microorganisms such as bacteria, viruses and fungi can be detected using fluorescence, and in some cases specifically identified.. Fluorescent antibodies and fluorescent acid-fast stains are usually used with detection of these organisms. An example more closely related to AD is the AP deposits which form in the brain. Since it has been found that there are fluorophores that can bind to these deposits, it could make early disease detection and prevention of disease progression possible (Zhu, Ploessl and Kung, 2014).

2.5 Conclusion

As discussed throughout this chapter there are a number of mechanisms involved in NDs. The aggregation and misfolding of proteins, combined with the lethal triplet of excitotoxicity, mitochondrial dysfunction, oxidative stress combine or in some cases act individually in both the activation and progression of these diseases, ultimately leading to neuronal cell death. Due to the lack of effective treatment options that can cure these diseases, or detect then early enough, it is crucial to focus on the development and synthesis of compounds that may act at multiple target sites, or have multiple functionality. Designing agents for the treatment, diagnosis and monitoring of disease progression is essential in ND. Furthermore, agents that can possible have further activity to reverse the neuronal damage as well as protect against more degeneration.

The polycyclic cage derivatives such as the PCU scaffold and other cages such as amantadine, memantine and NGP1-01, have shown great potential in this field, due to their inhibitory activity against NMDA-mediated Ca^{2+}influx and VGCC inhibition. The highly lipophilic nature of these cages, ensure effective movement through the BBB. The additional advantage of these cages are that they can act as carriers for other moieties, such as fluorescent agents across the BBB. The combination these agents could lead to the development of compounds with better pharmacokinetic and pharmacodynamic properties, and ultimately agents for effective treatment in neurodegenerative disorders.

CHAPTER 3

3.1 General Synthesis

The general synthesis for the proposed series of fluorescent-polycyclic ligands consisted out of a number of microwave and conventional synthesis procedures. The fluorophores selected for conjugation are presented in Figure 3.1. The synthetic procedures are shown in scheme 3.1. The synthesis of the final fluorescent-polycyclic ligands was accomplished by starting from the synthesis of Cookson's diketone (pentacyclo[5.4.0.0^{2,6}.0^{3,10}.0^{5,9}]undecane-8,11-dione). This diketone was then converted to the ketal moiety as seen in *Step 1*. An amine linker was conjugated to the free carbonyl moiety using a microwave assisted amination reaction as seen in *Step 2*. The respective fluorophores (Figure 3.1) were subsequently conjugated to the primary amine. This yielded the imine derivatives, which was then further reduced using $NaBH_4$ to produce the secondary amine derivatives of the fluorescent-polycyclic ligands as shown in *Step 3*. The compounds from *Step 3* were then converted to the second series using a trans-annular cyclization reaction as seen in *Step 4*.

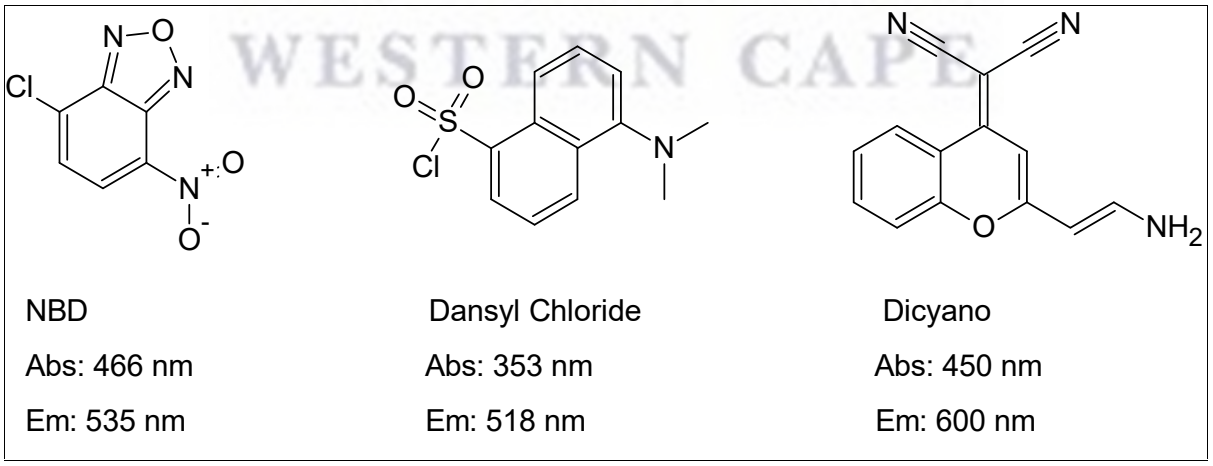

NBD	Dansyl Chloride	Dicyano
Abs: 466 nm	Abs: 353 nm	Abs: 450 nm
Em: 535 nm	Em: 518 nm	Em: 600 nm

Figure 3.1: Fluorophores and their respective emission wavelengths. (Zhang *et al.*, 2015) (Haugland *et al.*, 2002).

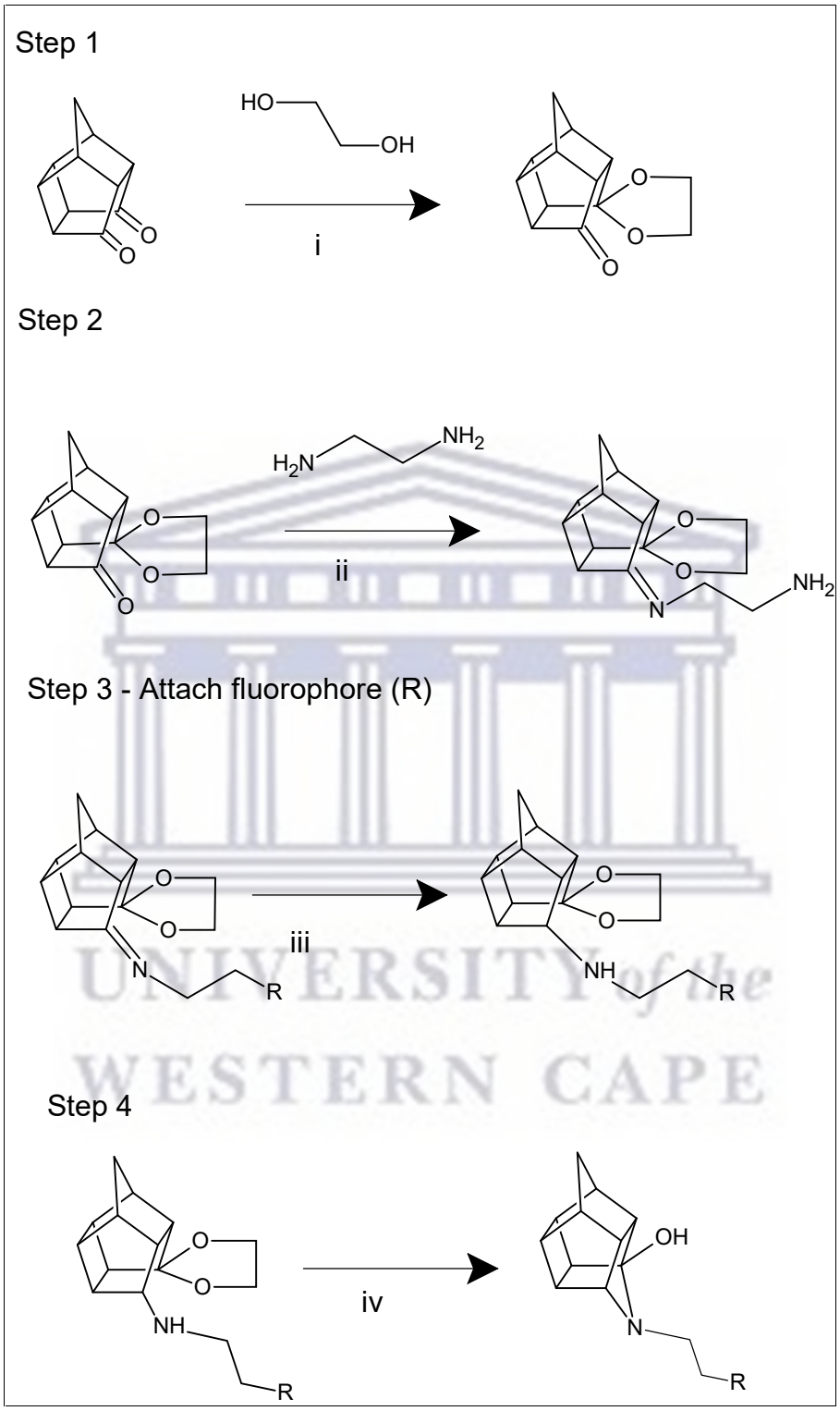

Figure 3.2: General synthesis of the fluorescent-polycyclic ligands. Reagents and conditions: (i) benzene, rt, 5 hrs; (ii) ethanol, microwave irradiation, 150 W, 150 psi, 5 hrs; (iii) ethanol/$NaBH_4$, rt, 8 hrs;(iv) acetone, 3 M HCl (aq).

3.2: Standard experimental procedures

3.2.1: Reagents and chemicals

All reagents used during the synthesis were purchased from Merck (St Louis, MO, USA) and Sigma-Aldrich® (Darmstadt, Germany). These reagents were used without further purification. The solvents used were dried using standard methods.

3.2.2: Instrumentation

Infrared (IR) absorption spectrophotometer:

Infrared spectra were obtained on a Perkin Elmer Spectrum 400 spectrometer, fitted with a diamond attenuated total reflectance (ATR) attachment.

Melting point (MP) determination:

Melting points were determined using a Stuart SMP-300 melting point apparatus and standard capillary tubes.

Mass Spectrometry (HR-MS):

Mass Spectrometry data were obtained from Stellenbosch University, Mass Spectrometry Unit, using a Waters Synapt G2, ESI probe. This was done at a Cone Voltage of 15 V. Samples were infused in methanol.

Nuclear magnetic resonance (NMR) spectroscopy:

^{1}H and ^{13}C spectra were determined using a Bruker Avance III HD spectrometer at a frequency of 400 MHz and 100 MHz, respectively. Tetramethylsilane (TMS) was used as internal standard. Deuterated chloroform ($CDCl_3$) was used as solvent. Reported chemical shifts are in parts per million with an internal standard ($\delta = 0$) and the $CDCl_3$ peaks as reference.

Abbreviations used to indicate the multiplicity of respective signals are as follows:

- s-singlet
- bs-broad singlet
- d-doublet
- dd-doublet of doublets
- t-triplet
- m-multiplet.

Microwave synthesis system:

All microwave synthesis was performed using a CEM DiscoverTM focused closed vessel microwave synthesis system. Standard microwave vessels and magnetic stirrers were used. Parameters adjusted were watts (W), pressure (psi) and time.

3.2.3: Chromatographic techniques

All mobile phases were prepared on a volume-to-volume (v/v) based and used for both thin layer chromatography (TLC) and column chromatography. The prism model described by *Nyiredy et al. (1985),* was used for these preparations. Visualisation of TLC was done using a UV light at 254 nm and 366 nm, as well as iodine vapour and nihydrin (1.5%).

3.2.4: Fluorescent scanning

Fluorescence for each final compound was determined using a Synergy™ Mx Monochromator-based fluorescent Microplate Reader. A concentration of 1 µM in 100% DMSO of the compounds were used to determine the fluorescent excitation and emission λ for each compound. The scan ranged from a wavelength of 250 nm to 700 nm.

3.3 Synthetic Procedures:

3.3.1 PCU:

Pentacyclo[5.4.0.0^{2,6}.0^{3,10}.0^{5,9}]undecane-8,11-dione

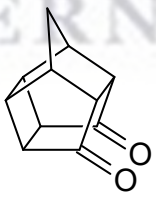

Method:

Benzoquinone (10 g, 9.25 mmol) was dissolved in 100 ml benzene on an external ice bath to cool the solution to 5 °C. The mixture was protected from light with aluminium foil. Cyclopentadiene (12.23 g, 9.25 mmol) was freshly monomerised and added stoichiometrically to the reaction mixture, while keeping the reaction temperature between 5 °C and 18 °C. The reaction was monitored with TLC using hexane:DCM = 3:1. Upon completion, the reaction mixture was removed from the

external ice bath and stirred at room temperature for an additional 1 hour, while still protected from light. Activated charcoal was then added to the mixture and it was stirred at room temperature for a further 30 minutes. The activated charcoal was removed through filtration, and benzene was removed *in vacuo*, yielding a yellow oil. The remaining solvent was evaporated overnight in a fume hood, resulting in the formation of yellow Diels-Alder adduct crystals (16.25 g). The crystals were then dissolved in ethyl acetate (4 g/100 ml) and irradiated with UV light for 6 hours, using a photochemical reactor. After 6 hours, decolouration of the solution had occurred and cyclisation of the Diels-Alder adduct was complete. The ethyl acetate was evaporated yielding a yellow wax. The wax was purified through Soxhlett extraction, using cyclohexane to produce the final cage as a fine light yellow-white powder (Cookson *et al.*, 1964).

Physical Characteristics:

$C_{11}H_{10}O_2$; MW: 174.1959 g/mol; Melting point: 242 ºC; Yield: 13.020 g, 80 %. The physical and structural characteristics of these crystals correlated with that in Cookson *et al.*, 1964. **[^{1}H-NMR = Spectrum 1]**

3.3.2 Compound 1:

Spiro[1,3-dioxolane-2,8'-pentacyclo[5.4.0.0^{2,6}.0^{3,10}.0^{5,9}]undecan]-11'-one

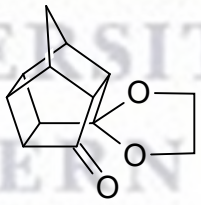

Method:

PCU (2 g, 11.6 mmol) was dissolved in benzene (20 ml). Ethylene glycol (0.72 g, 11.6 mmol) and p-toluesulfonic acid monohydrate (22.07 mg, 0.116 mmol) was added to the solution. The mixture was then refluxed under Dean Stark conditions for 5 hours. The solution was then allowed to cool to room temperature and neutralised by adding aqueous $NaHCO_3$ solution in a drop-wise manner. The pH of the solution was monitored using pH indicator strips. The benzene was then removed *in vacuo*. The compound was extracted and separated from the aqueous using dichloromethane (DCM). This was repeated three times using 15 ml DCM. The

organic layers where combined and dried by stirring with $MgSO_4$ for 30 minutes. This yielded a yellow brown oil, which was recrystallized from hexane to yield the ketal cage compound. The final compound was purified via column chromatography (using ethyl acetate:DCM in a ratio of 1:3). It yielded light white-brown crystals(Oliver *et al.,* 1991).

Physical Characteristics:

$C_{13}H_{14}O_3$; MW: 218.2485 g/mol; Melting point: 71 ºC; Yield: 0.978 g, 4.471 mmol, 39 %. The physical characteristics of these crystals correlated with that in Oliver *et al.,* 1991.

Structural Elucidation:

Infrared spectrum: 2979 cm^{-1}: (dioxolane), 1740 cm^{-1}: (aromatic C-H), 1687 cm^{-1}: (C=O) **[Spectrum 4]**. ^{1}H-NMR (400 MHz, $CDCl_3$) δ (ppm): 3.82-3.96 (m, 4H), 2.94-2.99 (m, 1H), 2.79-2.84 (m, 2H), 2.41-2.68 (m, 5H), 1.59-1.89 (AB-q, 2H, *J* = 11.2 Hz) **[Spectrum 2]**. ^{13}C-NMR (100 MHz, $CDCl_3$) δ (ppm): 215.2, 113.9, 65.7, 64.6, 53.0, 50.7, 45.9, 42.9, 42.4, 41.5, 41.4, 38.8, 36.4 **[Spectrum 3]**.

3.3.3 Compound 2:

N^1-{spiro[1,3-dioxolane-2,8'-pentacyclo[5.4.0.0^{2,6}.0^{3,10}.0^{5,9}]undecan]-11'-ylidene}ethane-1,2-diamine

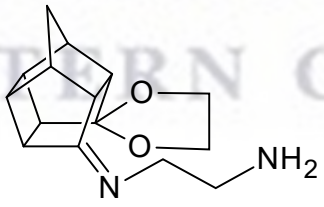

Method:

Compound **1**, (0.9880 g, 4.57 mmol) was dissolved with diaminoethane (1.53 ml, 22.88 mmol) in a 10 ml ethanol solution. The solution was then microwave irradiated for 3 hours at 60 W, 100 °C and 80 psi. This yielded a light brown liquid, from which the compound was extracted with DCM (3 x 10 ml). The organic layers were combined and washed with brine (3 x10 ml). The organic layer was dried over anhydrous magnesium sulphate ($MgSO_4$). The mixture was then filtered and the DCM removed *in vacuo*. The crude mixture was purified by column chromatography

using an ethanol and ammonia solution/methanol/DCM solution at a ratio of (1:9:90) as eluents, to give a light-yellow wax(Joubert *et al.*, 2013a).

Physical Characteristics:

$C_{15}H_{20}N_2O_2$; MW: 260.3315 g/mol; Melting point: Wax; Yield: 0.499 g, 1.920 mmol, 42.7 %.

Structural Elucidation:

Infrared spectrum: 3250 cm^{-1}: (N-H), 1748 cm^{-1}: (aromatic C-H), 1342 cm^{-1}: (C-O) **[Spectrum 7]**. HR-ESI $[M+NH_4]^+$: calc. 287.363 exp. 279.1010 **[Spectrum 8]**. ^{1}H-NMR (400 MHz, $CDCl_3$) δ (ppm): 3.87-3.93 (m, 4H), 3.79-3.84 (m, 2H), 2.76-2.96 (m, 4H), 2.52-2.65 (m, 4H), 2.45-2.49 (m, 1H), 2.38-2.43 (m, 1H), 1.54-1.86 (AB-q, 2H, *J* = 10.8 Hz) **[Spectrum 5]**. ^{13}C-NMR (100 MHz, $CDCl_3$) δ (ppm):154.1, 114.9, 65.7, 63.8, 53.8, 51.6, 50.5, 45.3, 43.8, 42.7, 40.9, 39.6, 37.3, 32.1 **[Spectrum 6]**.

3.3.4 Compound 3:

5-(dimethylamino)-N-[2-({spiro[1,3-dioxolane-2,8'-pentacyclo[5.4.0.0^{2,6}.0^{3,10}.0^{5,9}]-undecan]-11'-yl}amino)ethyl]naphthalene-1-sulfonamide

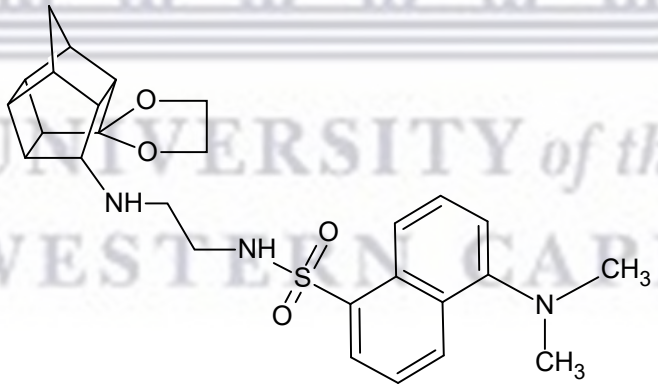

Method:

Compound **2** (0.1 g, 0.39 mmol) was dissolved in 10 ml THF (10 ml). Dansyl chloride (0.1 g, 0.39 mmol) was added and the solution was left to stir at room temperature for 6 hours. Following the stirring a yellow precipitate formed that was filtered yielding 0.098 g (0.198 mmol) of the imine PCU-dansyl as a yellow solid. This compound was dissolved in EtOH (5 ml) with $NaBH_4$ (0.04 g, 0.8 mmol), and the mixture was stirred at room temperature for 8 h. The EtOH was evaporated in vacuo and H_2O (10 ml) was added. The final mixture was extracted with DCM (3 x 10 ml).

The combined organic extracts were washed with brine (10 ml) and concentrated *in vacuo*. This yielded compound **3** as a light yellow oil (Joubert *et al.*, 2013).

Physical Characteristics:

$C_{27}H_{33}N_3O_4$; MW: 495.63 g/mol; Melting point: Oil; Yield: 0.031 g, 0.063 mmol, 17 %. Absorption λ: 350 nm, Emission λ: 450 nm

Structural Elucidation:

Infrared Spectrum: 3344 cm-1: (N-H), 1574 cm^{-1}: (Aromatic C-H), 1453 cm^{-1}: (S=O), 1277 cm^{-1}: (C-O) **[Spectrum 11]**. HR-ESI [M+ CH_3OH + H]$^+$: calc. 528.663, exp. 527.181 **[Spectrum 12]**. ^{1}H-NMR (400 MHz, $CDCl_3$) δ (ppm): 8.50-8.53 (d, J = 9.2 Hz, 1H), 8.11-8.20 (m, 2H), 7.44-7.56 (m, *J* = 7.6 Hz, 2H), 7.15-7.18 (d, *J* = 7.6 Hz, 1H), 5.40-5.44 (d, *J* = 12.4 Hz, 1H), 3.84-4.04 (m, 4H), 3.64-3.70 (m, 1H), 2.85-2.886 (m, 8H), 2.18-2.74 (m, 8H), 1.148-1.658 (AB-q, 2H, *J* = 10.8 Hz) **[Spectrum 9]**. ^{13}C-NMR (100 MHz, $CDCl_3$) δ (ppm): 151.2, 134.9, 128.4, 127.5, 127.0, 125.9, 123.6, 121.1, 114.5, 67.9, 54.9, 64.5, 53.0, 50.7, 45.9, 45.5, 42.8, 42.2, 41.9, 40.6, 38.8, 36.5, 30.3 **[Spectrum 10]**.

3.3.5 Compound 4:

N^1-(7-nitro-2,1,3-benzoxadiazol-4-yl)-N^2-{spiro[1,3-dioxolane-2,8'-pentacyclo[5.4.0.0^{2,6}.0^{3,10}.0^{5,9}]undecan]-11'-yl}ethane-1,2-diamine

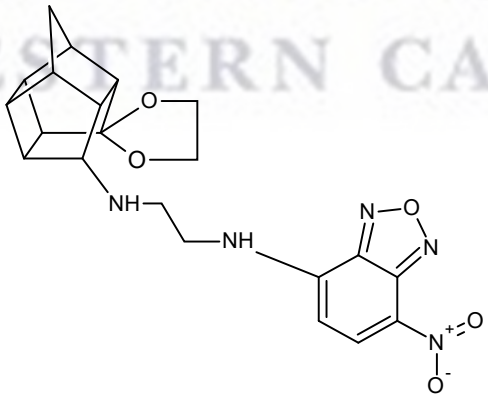

Method:

Compound **2** (0.1 g, 0.385 mmol) was dissolved in 10 ml THF. NBD (0.78 g, 0.38 mmol) was added and the solution was left to stir at room temperature for 6 hours. Following the stirring a yellow precipitate formed that was filtered yielding (0.078 g,

0.184 mmol) of the imine PCU-NBD as a yellow-brown solid. This compound was dissolved in EtOH (5 ml) with $NaBH_4$ (0.04 g, 0.8 mmol), and the mixture was stirred at room temperature for 8 h. The EtOH was evaporated *in vacuo* and H_2O (10 ml) was added. The final mixture was extracted with DCM (3 x 10 ml). The combined organic extracts were washed with brine (10 ml) and concentrated in vacuo. This yielded compound **4** as a dark yellow-brown oil (Joubert *et al.*, 2013).

Physical Characteristics:

$C_{21}H_{23}N_3O_5$; MW: 425.44 g/mol; Melting point: Oil; Yield: 0.021 g, 0.049 mmol, 12 %. Absorption λ: 485 nm, Emission λ: 530 nm

Structural Elucidation:

Infrared Spectrum: 2956 cm^{-1} (N-H), 1450 $cm^{-}1$: (N=O), 1450 cm^{-1}: (aromatic C=O), 1267 cm^{-1} (C-O) **[Spectrum 15]**. HR-ESI [M+ CH_3OH + H]$^+$: calc. 458.473, exp. 461.2442 **[Spectrum 16]**. ^{1}H-NMR (400 MHz, $CDCl_3$) δ (ppm): 8.46-8.49 (d, J = 10.8 Hz, 1H), 7.64-7.67 (d, J = 7.6 Hz, 1H), 3.83-3.97 (m, 4H), 3.69-3.77 (m, 2H), 2.43-2.98 (m, 7H), 2.26-2.34 (m, 1H), 1.99-2.05 (m, 1H), 1.84-1.93 (m, 2H), 1.23-1.26 (AB-q, J = 3.2 Hz, 6.8 Hz, 2H) **[Spectrum 13]**. ^{13}C-NMR (100 MHz, $CDCl_3$) δ (ppm): 152.1, 134.3, 130.7, 129.6, 128.6, 123.2, 118.5, 115.4, 72.4, 65.6, 63.1, 47.3, 46.7, 45.5, 44.7, 43.7, 43.1, 39.9, 39.3, 38.9 **[Spectrum 14]**.

3.3.6 Compound 5:

2-{2-[(1E)-2-aminoethenyl]-4H-chromen-4-ylidene}propanedinitrile

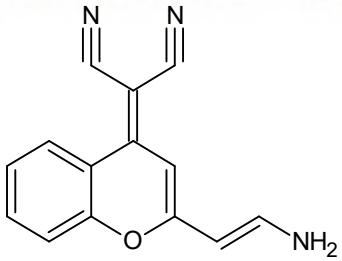

The synthesis of compound **6** involved an additional step which was to synthesise the dicyano-fluorophore itself, compound **5** (*Figure 3.3*).

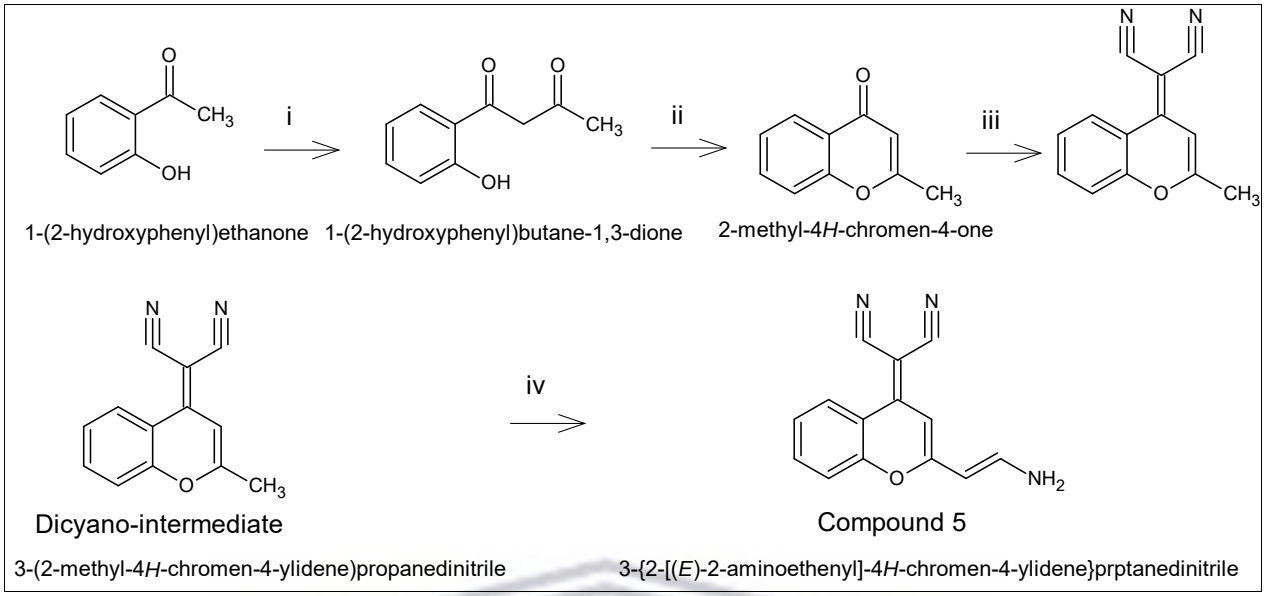

Figure 3.3: Synthetic route of the final fluorophore, compound **5**. Reagents and conditions: (i) AcCl, pyridine, DCM; t-BuOK, THF, (ii) 98% H_2SO_4, AcOH; (iii) malononitrile, Ac_2O; (iv) 3-amino-2-propenal, piperidine, CH_3CN.

3.3.6.1 2-(2-methyl-4H-chromen-4-ylidene)propanedinitrile

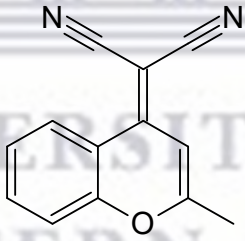

Method:

1-(2-Hydroxyphenyl)ethan-1-one (20 ml, 166 mmol) and pyridine (26.8 ml, 332 mmol) was dissolved in 80 ml DCM. To this solution AcCl (14.1 ml, 199 mmol) was added in a drop wise manner. This mixture was then stirred at room temperature for 16 h. The first intermediate of the fluorophore was then extracted with EtOAc and washed with 40 ml 6 N HCl (aq) followed by brine. The solution was dried over Na_2SO_4 and concentrated under reduced pressure. This yielded a brown-red oil that was crystallized to the crude product with petroleum ether and EtOAc (5:1). The crystals were then dissolved in 120 ml THF and 19.7 g of t-BuOK (176 mmol) was added to the same flask. This mixture was refluxed for two hours, forming a bright

red mixture. The mixture was then poured into ice to rapidly cool down, and extracted with EtOAc. The organic layer was washed with water followed by brine, and finally dried with Na_2SO_4. This solution was concentrated *in vacuo* and crystallized using an EtOH and petroleum ether solution yielding brown crystals as 1-(2-Hydroxyphenyl) butane-1, 3-dione. These crystals were dissolved with 3.3 ml 98% H_2SO_4 in 50 ml AcOH and refluxed for 30 min. The orange solution was then poured into ice and extracted with DCM. The organic layer extracted was washed with 10% Na_2CO_3 (aq) followed by water and then dried over Na_2SO_4 and concentrated. The crude product was crystallized in a mixture of EtOAc and petroleum ether to yield 2.581 g of 2-methyl-4H-chromen-4-one. (2 g, 12.5 mmol) 2-methyl-4H-chromen-4-one was refluxed with malononitrile (0.99 g, 15 mmol) in AcOH for 14 h. Water was added into the solution and refluxed for an additional 30 min. The solution was concentrated under reduced pressure and purified by column chromatography using (petroleum ether: DCM 3:1 followed by petroleum ether: DCM 2:1) as eluent. 3-(2-methyl-4H-chromen-4-ylidene)propanedinitrile was collected as an orange solid powder.

Physical Characteristics:

$C_{13}H_8N_2O$; MW: 208.25 g/mol; Melting point: 300 ºC. The physical characteristics were identical to those indicated in (Zhang *et al.*, 2015). Yield: 0.91 g, 3.85 mmol, 31 %

Structural Elucidation:

^{1}H-NMR (400 MHz, $CDCl_3$) δ (ppm): 8.90-8.92 (m, 1H), 7.75-7.69 (m, 1H), 7.42-7.48 (t, J = 8 Hz, 2H), 5.70-5.72 (s, 1H), 2.42-2.46 (t, 3H) **[Spectrum 17]**.

3.3.6.2 Compound 5:

2-{2-[(1E)-2-aminoethenyl]-4H-chromen-4-ylidene}propanedinitrile

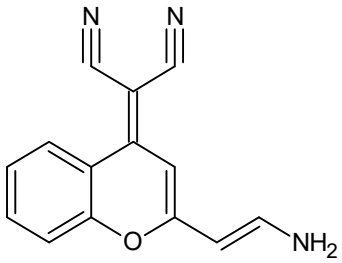

Method:

3-(2-Methyl-4H-chromen-4-ylidene)propanedinitrile (0.05 g, 0.212 mmol) and 3-amino-2-propenal (0.015 g, 0.22 mmol), with 150 ml piperidine in 5 ml CH_3CN was refluxed for 16 h. The mixture was cooled to room temperature and extracted it with DCM and concentrated *in vacuo* to yield a dry orange powder.

Physical Characteristics:

$C_{14}H_9N_3O$; MW: 263.29 g/mol; Melting point: 300 ºC+. Yield: 0.009 g, 0.34 mmol, 16 %. Absorption λ: 450 nm, Emission λ: 620 nm.

Structural Elucidation:

Infrared Spectrum: 3375 cm^{-1} (N-H), 2865 cm^{-1}: (nitrile), 1450 cm^{-}, 1337 cm^{-1} (Aromatic C-O) **[Spectrum 20]**. HR-ESI $[M+_2Na-H]^+$: calc. 308.271, exp. 309.135 **[Spectrum 21]**. ^{1}H-NMR (400 MHz, $CDCl_3$) δ (ppm): 8.90-8.93 (d, J = 12 Hz, 1H), 7.69-7.76 (m, 1H), 7.43-7.50 (m, 2H), 6.95-7.00 (d, J = 8.4 Hz, 1H), 6.88-6.93 (d, J = 8.0 Hz, 1H), 6.71-6.72 (s, 1H) **[Spectrum 18]**. ^{13}C-NMR (100 MHz, $CDCl_3$) δ (ppm): 168.8, 162.3, 161.7, 136.6, 134.8, 130.8, 126.1, 125.7, 119.1, 118.7, 118.5, 105.4, 50.1, 47.5 **[Spectrum 19]**.

3.3.7 Compound 6:

2-{2-[2-({spiro[1,3-dioxolane-2,8'-pentacyclo[5.4.0.0^{2,6}.0^{3,10}.0^{5,9}] undecan]-11'-yl}amino)ethenyl]-4a,8a-dihydro-4H-chromen-4-ylidene}propanedinitrile

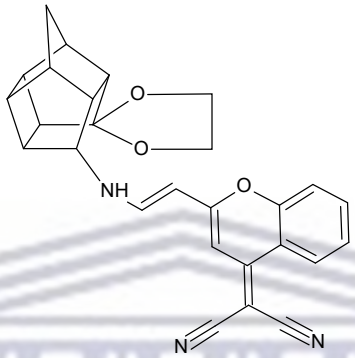

Method:

Compound **1** (0.01 g, 0.046 mmol) and compound **5** (0.009 g, 0.034 mmol) were reacted under microwave conditions. These reactants were dissolved in EtOH (5 ml) at a maximum temperature of 100 ºC, 150 W and a pressure of 150 psi for 30 min. This yielded what was expected to be the imine intermediate mixture. The mixture was allowed to cool down and dissolved in EtOH (5 ml). $NaBH_4$ (0.005 g, 0.136 mmol) was added to the mixture. The mixture was stirred at room temperature for 8 hours after which the EtOH was evaporated under reduced pressure. H_2O (10 ml) was added to the mixture, and compound 6 was extracted with CH_2Cl_2 (3 x 10 ml). The combined organic extracts were then washed with brine (10 ml) and concentrated *in vacuo*.

Physical Characteristics:

$C_{27}H_{23}N_{33}$; MW: 437.49 g/mol.

Structural Elucidation:

Compound **6** was not successfully synthesised due to the inability link the fluorophore to the cage moiety. The extremely low yields of the fluorophore also made it more difficult to synthesise compound **6**. Increased starting materials did not significantly increase the yield of the fluorophore, but rather the amount of wastage and by-products. For this reason, repeating the synthesis of the fluorophore multiple

times, or on a larger scale to produce a higher yield of the fluorophore was not feasible. Compound **5** was completely lost in the synthesis and the resulting NMR was identified as only compound **1**. Compound **5** was however still tested in the biological assays, Chapter 4, to identify whether or not it has activity for future reference.

3.3.8 Compound 7:

5-(3-{[5-(propan-2-yl)naphthalen-1-yl]sulfonyl}propyl)-5-azahexacyclo[5.4.1.$0^{2,6}$.$0^{3,10}$.$0^{4,8}$.$0^{9,12}$]dodecan-4-ol

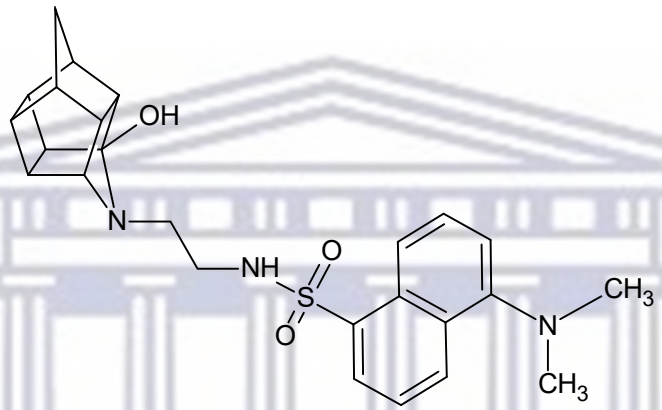

Method:

Compound **3** (0.02 g, 0.04 mmol) was dissolved in acetone (10 ml), and 4 M aq HCl (8 ml) was added to the mixture. The mixture was stirred at room temperature for 6 hours. The mixture was then diluted with H_2O (120 ml) and basified to pH 14 using 1 M aq. NaOH. Compound 7 was extracted using DCM (3 x 10 ml), and dried with Na_2SO_4. The product was then concentrated *in vacuo*. This yielded the compound **7** as an amber yellow oil. The compound could not be further purified using column chromatography due to extremely low yield.

Physical Characteristics:

$C_{25}H_{29}N_3O_3$; MW: 451.58 g/mol; Melting point: Oil; Yield: 0.01 g, 022 mmol, 6 %. Absorption λ: 350 nm, Emission λ: 450 nm.

Structural Elucidation:

Infrared Spectrum: 3465 cm^{-1}: (N-H), 3407 cm^{-1}: (O-H), 1574 cm^{-1}: (Aromatic C-H), 1453 cm^{-1}: (S=O), 1277 cm^{-1}: (C-O) **[Spectrum 24]**. HR-ESI $[M+NH_4]^+$: calc. 469.615, exp. 462.275 **[Spectrum 25]**. ^{1}H-NMR (400 MHz, $CDCl_3$) δ (ppm): 8.50-

8.53 (d, J = 8.8 Hz, 1H), 8.22-8.37 (m, 2H), 7.45-7.59 (m, 2H), 7.16-7.20 (d, *J* = 7.0 Hz, 1H), 3.01-3.07 (m, 2H), 2.94-2.97 (m, 1H), 2.86-2.89 (s, 6H), 2.65-2.73 (m, 2H), 2.33-2.59 (m, 8H), 1.74-1.90 (AB-q, 2H, *J* = 10.4 Hz, 2H) **[Spectrum 22]**. ^{13}C-NMR (100 MHz, $CDCl_3$) δ (ppm): 152.1, 134.2, 130.6, 129.9, 129.6, 129.3, 128.7, 123.1, 118.7, 115.8, 115.2, 115.3, 72.3, 65.5, 62.9, 46.9, 46.7, 45.5, 44.7, 43.6, 43.1, 39.9, 39.0, 38.9, 34.9 **[Spectrum 23].**

3.3.9 Compound 8:

5-{2-[(7-nitro-2,1,3-benzoxadiazol-4-yl)amino]ethyl}-5-azahexacyclo[5.4.1.$0^{2,6}$.$0^{3,10}$.$0^{4,8}$.$0^{9,12}$]dodecan-4-ol

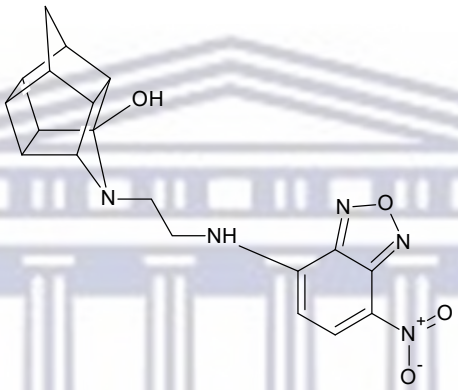

Method:

Compound **4** was dissolved in acetone (10 ml) and 4 M aq HCl (8 ml) was added to the mixture. This mixture was stirred at room temperature for 6 hours. The mixture was then diluted with H_2O (120 ml) and basified to pH 14 with 1 M aq. NaOH. The compound was extracted with DCM (3 x 10 ml), dried with Na_2SO_4 and concentrated *in vacuo*. The reaction was unsuccessful as it did not yield a compound. As a result of this compound **8** was not successfully synthesised.

The synthesis of compound **4**, had an extremely low yield (0.021 g, 0.049 mmol, 12 %). The likely reason for the failure to successfully synthesise compound **8**, is because the quantity of compound **4** was not enough. This was also seen in the Transanular cyclisation of compound **3** to compound **7**. Compound **3** had a low yield of only 17 %, and this resulted in an even lower yield for compound **7** of 6 %.

Compound 9:

2-{2-[(1E)-2-{4-hydroxy-5-azahexacyclo[5.4.1.$0^{2,6}$.$0^{3,10}$.$0^{4,8}$.$0^{9,12}$] dodecan-5-yl}ethenyl]-4a,8a-dihydro-4H-chromen-4-ylidene}propanedinitrile

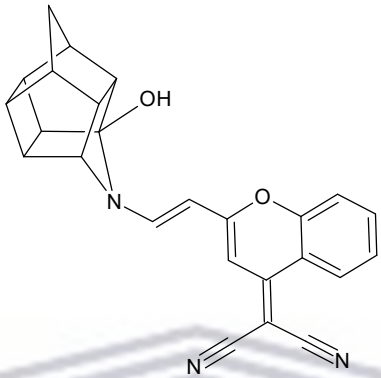

Due to the inability to synthesise compound **9**, because the yield of the fluorophore, compound **5**, transannular cyclisation of compound **9** could not be performed. As a result of this, compound **10** was not successfully synthesised.

3.4 Conclusion

A total of six compounds were successfully synthesised using multi-step synthetic procedures (Figure 3.4). Compound **6**, **8** and **9**, were not successfully synthesised due to extremely low yields that did not allow for purification, and as such the ability to properly analyse the NMR and IR data. The structure of the successfully synthesised compounds were confirmed using MS, IR and NMR analysis. In future, optimisation of the synthesis procedure and improved purification methods can be developed to synthesise compound **6**, **8** and **9**. The initial cage and derivatives thereof showed moderate yields, with **1** and **2** giving yields of 39% and 42%, respectively. Compounds **3** and **4**, as well as the fluorophore **5**, and the aza-derivative **7**, all showed very low yields. A large part of the low yields seen with these compounds was due to significant purification needed, as well as the formation of by-products. Furthermore, the final transannular cyclization step was not performed for **8** and **9**, because of the extremely low yields obtained for **4** and inability to synthesise **6**. However, as initial proof of concept the aza, and ketal derived polycyclic ligands were used in further biological studies in order to see if the

conjugation of the fluorophores still maintain the biological properties known for these cage molecules.

For the purpose of this study, the synthesised compounds were subjected to NMDA, VGCC, cytotoxicity and neuroprotective assays. The results of these assays are discussed in Chapter 4.

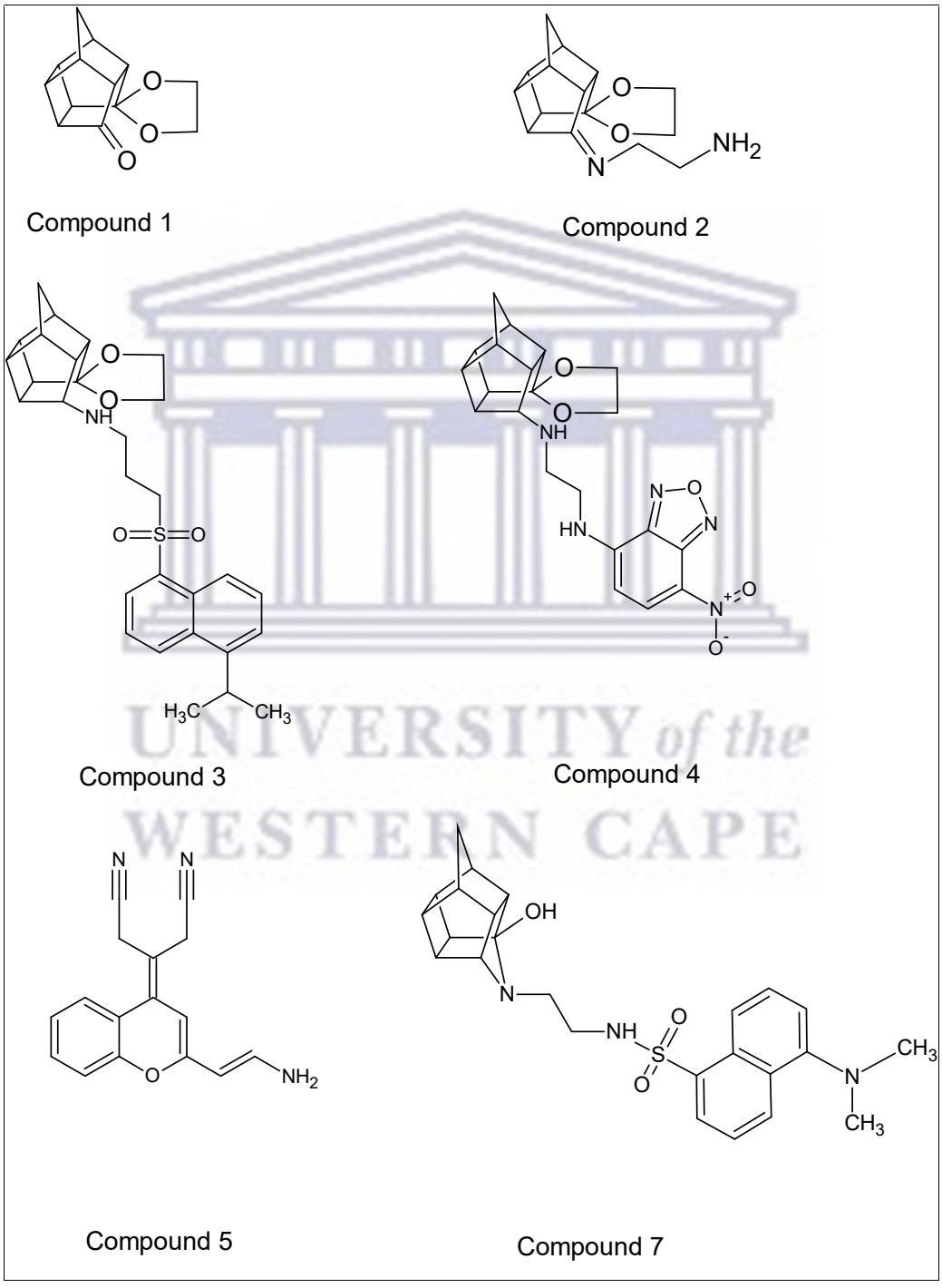

Figure 3.4: Successfully synthesised compounds.

Chapter 4

4.1 Introduction

Biological evaluations of test compounds **1-5** and **7** were performed in using four different assays. Firstly a cytotoxicity test to identify the cellular survival in the presence of the test compounds and whether or not these compounds are toxic for cells was done through an MTT assay. The second assay is a neuroprotection test on cells to identify if cellular death is attenuated in the presence of the test compounds when these cells are exposed to an agent that is known to induce neurotoxicity, in this case, 1-methyl-4-phenyl pyridinium (MPP+).

Assays three and four, the VGCC and NMDA modulation assays, are almost identical and aim to determine if the test compound will be effective in blocking Ca^{2+} influx into cells through either VGCC or NMDA receptors, ultimately as agents for further development in neurodegenerative disorders. This assay model was developed in our laboratory in collaboration with the Department of Medical Bioscience at UWC, and is described in this chapter. No ethical approval was required for the assays performed and described in the chapter.

All assays were conducted using SH-SY5Y neuroblastoma cell lines. The cells were cultured in DMEM (Dulbeco Modified Eagles Medium). This medium was replaced every two to three days and cells were always kept at 37 °C, with humidified air that was 95% air and 5% CO_2.

4.2 Assays

4.2.1. Cytotoxicity Assay

Compounds **1-5** and **7** were assayed for cell viability on SH-SY5Y human neuroblastoma cells using a standard 3-[4,5-dimethylthiazol-2-yl]-2,5-diphenyl tetrazolium bromide (MTT) assay method (Zindo *et al.*, 2014b). The SH-SY5Y cells were plated in flat bottom 96 well plates in growth medium at a density of 7,500

cells/well. The cells were allowed to adhere to the plate surface for 24 hours. The test compounds were then introduced to each well by replacing the growth medium with different concentrations of each compound. This assay was performed at concentrations of 10 µM, 50 µM and 100 µM, to measure the metabolic activity of the cells and ultimately if and how cytotoxic the test compounds are. The cell viability was tested spectrophotometrically after exposing them to the aforementioned concentrations of the respective test compounds for 48 hours. Vehicle control cells for this assay was treated with dimethyl sulfoxide (DMSO), and served as a reference for 100% cell viability. DMSO was used to dissolve the test compounds. Once incubation for 48 hours was complete, 10 µL of MTT solution (5 mg/mL) was added to each well. Further incubation was done for 4 hours. The purple formazan that formed was solubilized with 100 µL DMSO, and plates were read spectrophotometrically to determine absorbance. This was done at 570 nm with a BMG Labtech POLARStar Omega multimodal plate reader.

4.2.1.1 Compound Preparation

Each test compound was prepared in 100 µL of DMSO at a stock concentration of 50 mM.

4.2.2 Neuroprotection Assay

As with the cytotoxicity test SH-SY5Y cells were used to perform the neuroprotection assay. A well-known and used cellular model was used to perform this assay. This assay involves inducing neurotoxicity in the SH-SY5Y neuroblastoma cells through (MPP+) (Zindo *et al.*, 2014b). MPP+ is used due to the highly toxic effects it has on neurons. It is well documented in the use of inducing neurodegeneration in various *in vitro* as well as *in vivo* models. It is believed that MPP+ induces neurodegeneration through oxidative stress and ultimately apoptosis.

4.2.2.1 Compound Preparation

Each test compound was prepared in 100 µL DMSO to make a 50mM solution, similar to the cytotoxicity assay.

4.2.3 VGCC and NMDA Assay

These assays both utilised a fluorescent ratiometric indicator, Fura-2 AM. The Synergy™ Mx Monochromator-based fluorescent Microplate Reader was used to

scan and analyse the fluorescence from the cells in combination with Gen 5™ data analysis software.

The assay measures the relative changes in intracellular Ca^{2+} levels that occur after cell membrane depolarisation. A dual wavelength ratiometric approach is used to detect excitation of both Ca^{2+}-bound and free concentrations. This is done at both 340 nm and 380 nm, while emission is measured at 510 nm. A ratio of the fluorescent intensities at both excitations, allows for quantification of Ca^{2+} ion levels within the cells(Zindo *et al.*, 2014).

4.2.3.1 Compound, control and buffer solution preparation

Each compound was prepared in 10 µL of a 50 mM solution and added to 990 µL of DMSO to have a final concentration of 0.5 mM. The positive test controls for the VGCC assay (nimodipine and NGP1-01 as well as the positive controls for the NMDA assay (MK-801 and NGP1-01 was prepared in the same manner.

Two identical buffer solutions were required for the assays:

- The Krebs-Hepes solution (Ca^{2+} Free Buffer). This consisted of 118 mM NaCl, 4.7 mM KCl, 1.18 mM MgCl, 20 mM HEPES and 30.9 mM glucose.
- The Ca^{2+} containing buffer consisted of 118 mM NaCl, 4.7 mM KCl, 1.18mM MgCl, 2 mM $CaCl_2$, 20 mM HEPES and 30.9 mM glucose.

Each assay required an additional depolarising buffer, specific to the relative assay.

The VGCC depolarising buffer consisted of 5.4 mM NaCl, 770 mM KCl, 10 mM $NaHCO_3$, 1.4 mM $CaCl_2$, 0.9 mM $MgSO_4$, 5.5 mM glucose monohydrate, 0.6 mM KH_2PO_4, 0.6 mM Na_2HPO_4 and 20 mM HEPES.

The NMDA/glycine depolarising buffer contained 0.1 mM $CaCl_{2.2}H_2O$, 0.55 mM NMDA, 0.55 mM Glycine, 118 mM NaCl, 4.7 mM KCl, 30.9 mM glucose monohydrate and 20 mM HEPES.

The pH for all for buffers were adjusted to 7.4 using 4 M solutions of NaOH and HCl.

4.2.3.3 VGCC Assay Method (KCl-mediated VGCC depolarisation)

The Ca^{2+} influx through VGCC was tested using SH-SY5Y neuroblastoma cell lines, to determine the ability and potential of the test compounds to block these channels.

The cells grown were sub-cultured into 96-well black plates to a density of 1 x 10^5 cells per well, at 37 °C, and in 100 µL of DMEM. The cells were plated 24 hours prior to the actual assay to allow them to adhere to the plates. Fura-2 AM was loaded with the cells after the 24 hours. This was done by removing the DMEM solution and adding 5 µM Fura-2/AM-DMEM solution (9990 µL of DMEM and 10 µL of Fura-2/AM). The cells were then incubated for another hour at 37 °C. The Fura-2/AM DMEM solution was then removed from each well, and the well was washed with Ca^{2+} Krebs-Hepes solution. 98 µL of Ca^{2+} containing buffer was then added to each well and the cells were incubated for further 30 minutes at 37 °C. Then 2 µL of test compound dissolved in DMSO was plated to into each -well to a final concentration of 10 µM. Two positive controls were used, nimodipine (NIM), a known L-type VGCC blocker commercially available, as well as NGP1-01, a well-known and tested polycyclic amide. The plated cells with the respective test compounds and controls were then inserted into the plate reader. In the reader the cells were incubated at 37°C for 10 minutes, shaking the plate slightly every minute. After the 10 minutes, 10 µL of the VGCC depolarising solution was added. The fluorescence was then measured over 35 seconds to determine the Ca^{2+} influx after depolarisation. The test compounds were compared to a control where the cells were not exposed to any VGCC blocking agent and which represented 100 % Ca^{2+} influx.

4.2.3.2 NMDA Assay Method (NMDA/glycine-mediated receptor stimulation)

To assess the compounds' ability to block Ca^{2+} influx *via* the NMDA receptor channels, a similar method as in the VGCC assay was used. However, a concentrated NMDA/Glycine solution, instead of KCl, was used to stimulate Ca^{2+} influx through the NMDA receptors specifically. This assay also had two positive controls. NGP1-01 was again used, while the second positive control was MK-801, a commercially available non-competitive antagonist of NMDA receptors. SH-SY5Y neuroblastoma cell lines were used, and the cells were sub-cultured into 96-well black plates to a density of 1 x 10^5 cells per well, at 37 °C, and in 100 µL of DMEM. The cells were then plated 24 hours prior to the actual assay to allow them to adhere to the plates. Fura-2 AM was loaded with the cells after the 24 hours, identical to the VGCC assay. This was done by removing the DMEM solution and adding 5 µM Fura-2/AM-DMEM solution (9990 µL of DMEM and 10 µL of Fura-2/AM). The cells were incubated for another hour at 37 °C. The Fura-2/AM DMEM solution was then

removed from each well, and the well was washed with Ca^{2+} Krebs-Hepes solution. 98 µL of Ca^{2+} containing buffer was then added to each well and the cells were incubated for a further 30 minutes at 37 °C. 2 µL of test compound dissolved in DMSO was plated to into each well, resulting in a final concentration of 10 µM for each compound. The 96-well black plate containing the cells with the test compounds as well as controls were then inserted into the plate reader. In the reader the cells were incubated at 37 °C for 10 minutes. During this time shaking of the plate occurred every minute. After 10 minutes, 10 µL of the NMDA/Glycine depolarizing buffer was added. The fluorescence was then measured over 35 seconds to determine the Ca^{2+} influx after depolarisation.

The test compounds were assayed at 10 µM for NMDA assays. The percentage NMDA receptor inhibition of each compound was calculated relative to the control which represented 100 % Ca^{2+} influx.

4.2.4 Statistical analysis

The data analysis, calculations as well as graphs were all done using Prism 6 (GraphPhad, Sorrento Valley, CA). All bar charts included are shown as a % of the control and each bar represents the mean ± SD.

One way analysis of variance ANOVA was performed on the data to indicate significant differences between test compounds.

$P < 0.05$ was considered to be statistically significant and is represented on graphs by *. Further degrees of significance was indicated as follows: **$P < 0.01$, ***$P < 0.001$, ****$P < 0.0001$.

4.2.5 Materials

Chemicals used for all assays were of analytical grade or spectroscopy grade. These chemicals were purchased from Merck (St Louis, MO, USA) and Sigma-Aldrich® (Darmstadt, Germany).

4.3 Results

4.3.1 Cytotoxicity

As seen in Figure 4.1 all the compounds were compared to 100% growth in the control. None of the test compounds showed significant cytotoxicity at 10 µM, as all had cell viability above 85%. The general trend showed a slight decrease in cell survival at 50 µM, except for compound **5**, which maintained an almost constant cell viability at all three concentrations. The general trend, as expected, showed a further decrease in cell viability as the concentration of each test compound was increased to 100 µM. As a result, it can be seen that the concentration in most cases was indirectly proportional to cell survival, in other words as the concentration increased, the cell viability decreased. An interesting observation was that at all concentrations the derivatives of the ketal-cage, compound **1**, became less cytotoxic irrespective of the structure conjugated to the cage. This can be seen in Table 4.1, where the percentage viability is the lowest for compound **1** irrespective of the concentration. This was the general trend except for compound **2**, which showed a higher degree of cytotoxicity than compound **1** at all concentrations.

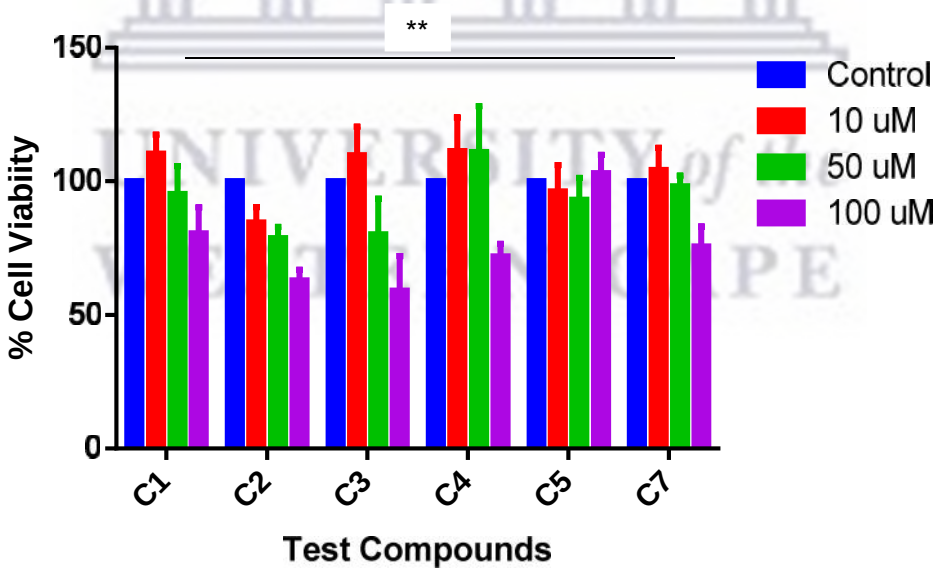

Figure 4.1: Cytotoxic effects of tested compounds at 10 µM, 50 µM and 100 µM. The data represents the mean ± SD of the treated cells vs the untreated Control cells. The experiment was performed three times and analysed using one-way ANOVA. The assay was found to be statistically significant with a P-value of 0.0064, when the mean cell viability of the cell treated with the test compounds were compared to the control of 100% cell viability.

Table 4.1: Mean ±SD % Cell Viability for test compounds.

	10 µM	50 µM	100 µM
C1	110±7	95±10	81±10
C2	85±6	79±4	63±4
C3	110±11	80±13	59±13
C4	111±12	111±16	72±5
C5	96±10	93±8	103±7
C7	104±8	98±4	76±7

4.3.2 Neuroprotection

For this assay the SH-SY5Y cells were seeded onto a 96-well black plate and treated with test compounds dissolved in DMSO. After two hours, MPP^+ was added to the cells to induce neurotoxicity. The cells were then incubated for 48 hours. During this time the cells were in the presence of the test compounds as well as 2000 µM MPP+. The neuroprotective effect of each compound was evaluated through the MTT mitochondrial function assay. As with the cytotoxicity assay, vehicle control cells were treated with only DMSO, to represent 100% cell survival. The percentage neuroprotection was calculated as a percentage of the control. It can be seen in Figure 4.2 that all the test compounds exhibited significant neuroprotective properties when compared to the cells treated with only MPP^+. The most significant level of neuroprotection was seen for compound **1**. As a result of this, it could be expected that conjugating fluorophores to the PCU cage, merely maintained or slightly decreased the ability of the cages to protect the neurons.

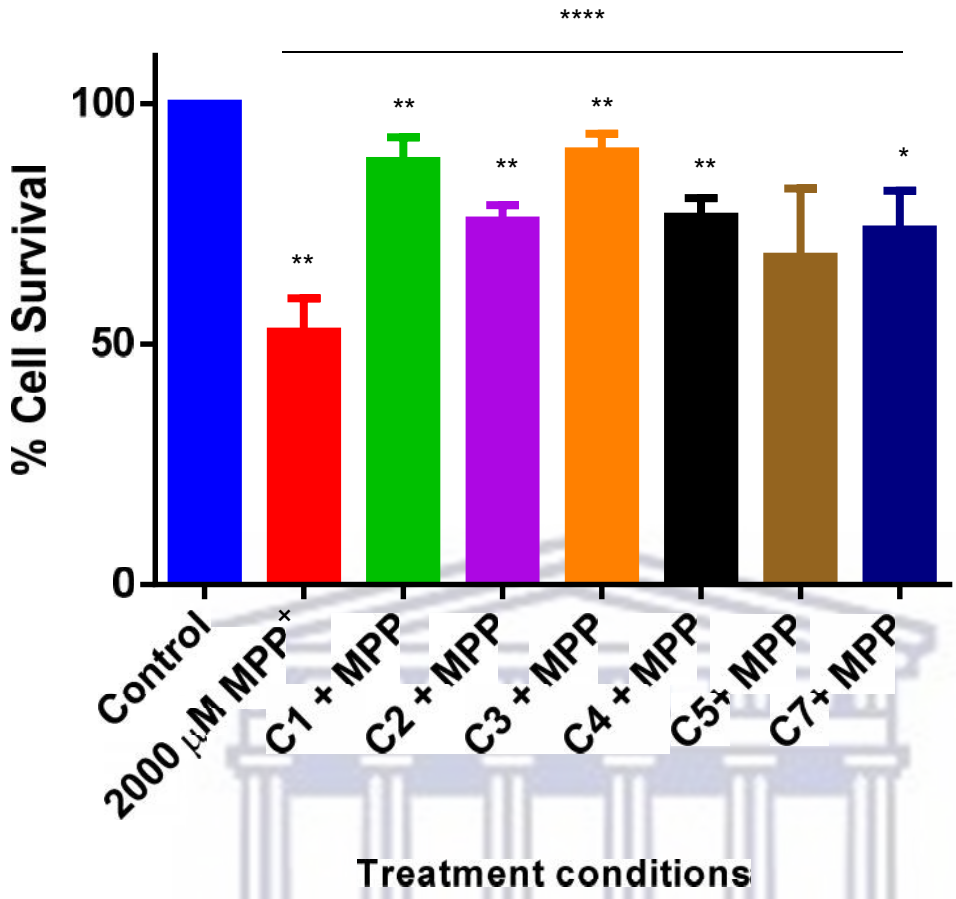

Figure 4.2: Neuroprotective effects of tested compounds at 10 µM. The data represents the mean ± SD of the treated cells vs the untreated Control cell. The experiment was performed three times and analysed using one-way ANOVA. The level of significance is expressed as *P < 0.05, **P < 0.01, ***P < 0.001, ****P <0.0001.

4.3.3 VGCC

Compound 1-7 were evaluated for VGCC inhibition by measuring Ca^{2+} influx into SH-SY5Y neuroblastoma cell lines using the fluorescent technique as described in section 4.2.3. Fura-2 AM, a ratiometric fluorescent indicator, was used to determine the change in intracellular Ca^{2+} concentration after depolarisation of the VGCC. The influx of Ca^{2+} of test compounds, relative to a control, which represents 100% influx was used to determine of the degree of inhibition produced by the test compounds. The positive controls for this assay was Nimodipine and NGP1-01. Nimodipine, a commercially available L-type Ca^{2+} channel blocker, is used because it passes the BBB readily and binds with a high affinity to these channels (Marchetti & Usai, 1996). NGP1-01 has also been shown to block VGCC, but to a lesser degree.

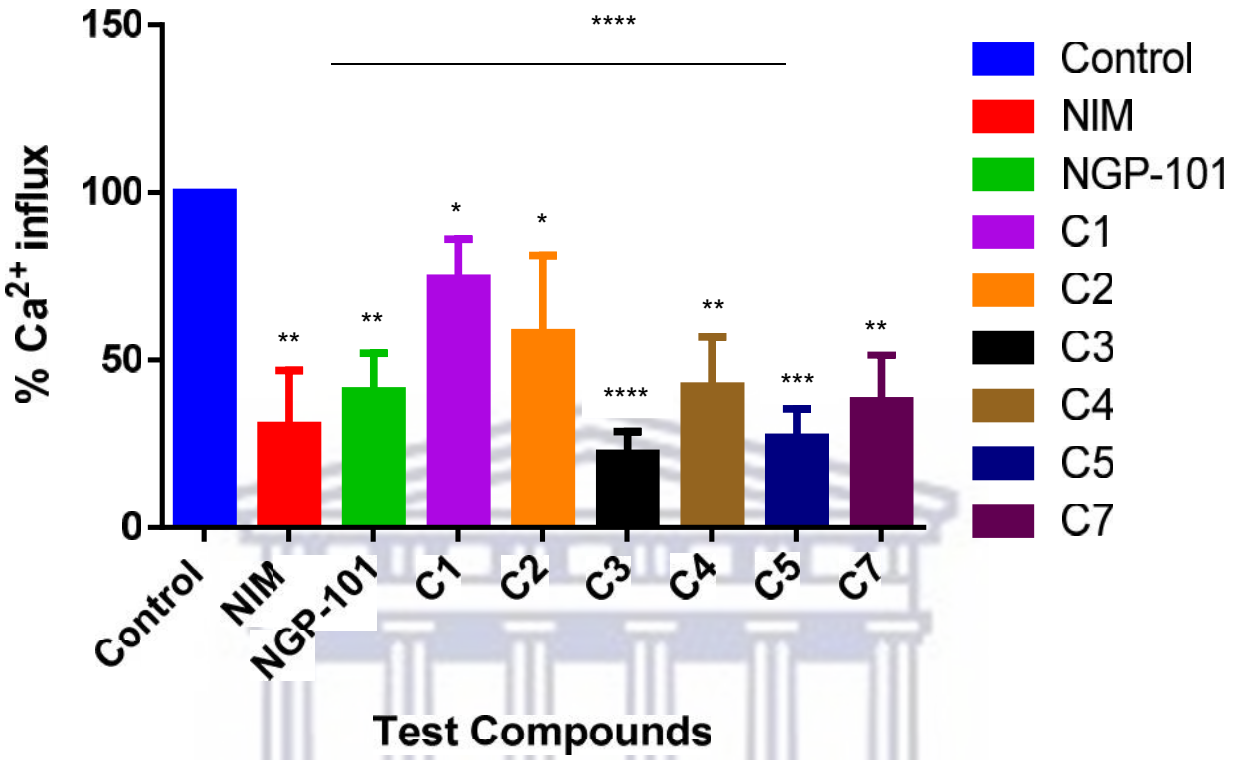

Figure 4.3: Effect of the test compounds and positive controls, Nimodipine (NIM) and NGP1-01 (NGP) on the Ca^{2+}influx through VGCC. VGCC blocking effects of tested compounds were measured at 10 µM. The data represents the mean ± SD of the treated cells as a percentage of Ca^{2+} influx relative to the 100% influx of untreated control cells. The experiment was performed in triplicate and analysed using one-way ANOVA. The level of significance is expressed as *P < 0.05, **P < 0.01, ***P < 0.001, ****P <0.0001.

Table 4.2: Percentage VGCC Ca^{2+} influx inhibition of test compounds.

Control	0
Nimodipine	69,54±16**
NGP1-01	59,14±11**
C1	25,60±12*
C2	41,85±23*
C3	77,76±6****
C4	57,79±15**
C5	73,09±8***
C7	62,18±13**

*Control = DMSO only *P < 0.1 **P < 0.05 ***P < 0.001 ****P <0.0001*

As seen in table 4.2, and figure 4.3, all compounds including the reference compounds yielded statistically significant results. The positive controls yielded expected results, with nimodipine inhibiting Ca^{2+} influx to a very high degree at 69.54%, while NGP1-01 also showed a slightly lower, but still high degree of inhibition at 59.14%. There was a clear increase of activity with the conjugation of the fluorophores to the PCU. The inhibition of Ca^{2+} influx increased from 25.60% with Compound **1** to 41.85% with compound **2**. This gives an indication that the NH_2 group on the linker interacts with the VGCC in some way. A further increase in activity was seen when attaching the fluorophores. Compound **3**, **4** and **7** all exhibited a higher degree of inhibition than compound **2**. These fluorophore-PCU conjugates also displayed either a similar level of inhibition (compound **4**), or higher degree of inhibition than the positive control NGP1-01. Nimodipine showed better activity than all the test compounds, except compound **3**, that had an inhibitory concentration of 77.76%. Similar to previous studies it was seen that compounds with bi-aromatic fluorophores showed significant VGCC activity (Joubert *et al.*, 2011a). There was a significant decrease in activity between compound **3** and its aza-derivative, compound **7**. Even though previous studies have found that in some cases the exposed hydroxyl group increases VGCC activity (Egunlusi, 2014), this was not observed in the case of compound **3** and **7**. The increase in activity is more than likely do to the flexibility of compound **3** as a result of not having the aza-bond. This flexibility better allows the compound to move and bind to the VGCC. Compound **5**, the fluorophore alone also showed a high level of inhibition at 73.09%. This is more than likely due to the nitrile groups seen in this compound. Studies have shown the compounds containing nitrile groups exhibit good VGCC blocking activity (Joubert *et al.*, 2011a). Due to the high level of inhibition seen with Compound **5**, it is expected that the proposed compounds **6** and **9**, the PCU derivatives of this fluorophore will have great potential as VGCC inhibiting agents, should they be synthesised successfully.

4.3.4 NMDA

In the NMDA assay, the inhibition of the NMDA receptor was studied by determining the relative change of Ca^{2+} influx compared to the control that has no NMDA receptor blocking agent and as such represented 100% influx.

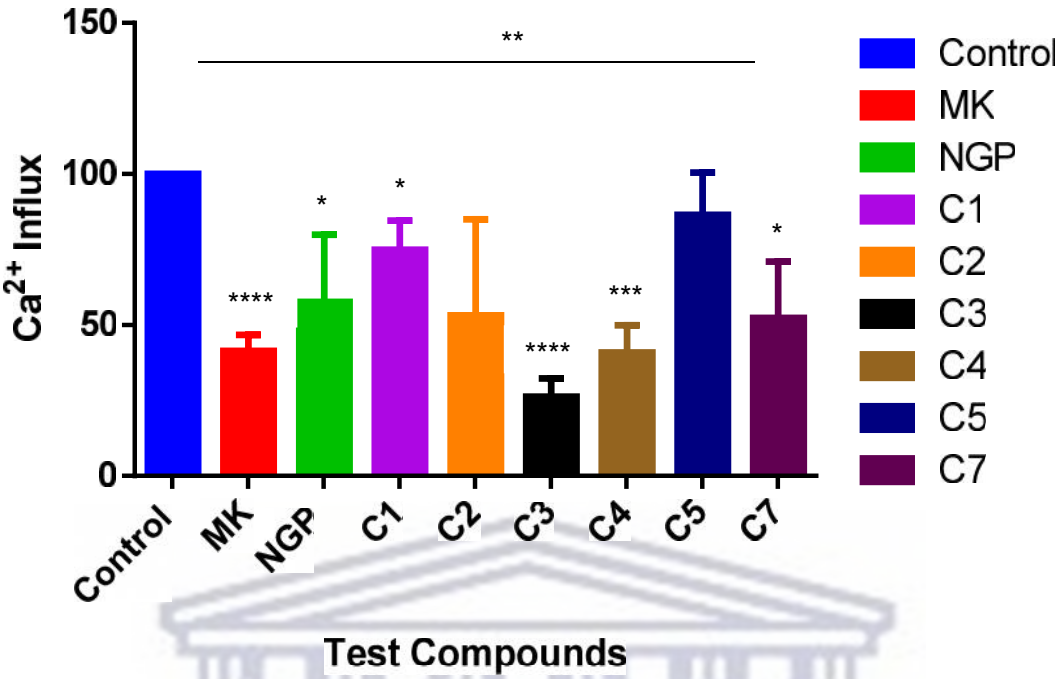

***Figure 4.4**: Effect of the test compounds and positive controls, MK-801(MK) and NGP1-01(NGP) on the Ca^{2+}influx through NMDA channels. NMDA receptor antagonism of tested compounds were measured at 10 µM. The data represents the mean ± SD of the treated cells as a percentage of Ca^{2+} influx relative to the 100% influx of untreated control cells. The experiment was performed in triplicate and analysed using one-way ANOVA. The level of significance is expressed as *P < 0.05, **P < 0.01, ***P < 0.001, ****P <0.0001.*

The lower the percentage influx compared to the control, the better the inhibition Ca^{2+} influx and activity of the test compound. The experiment was performed in triplicate, and the results are given as an average inhibition over the three experiments. The test compounds were prepared to have a final concentration of 10 µM, and their activity relative to the control can be seen in Figure 4.3.

Table 4.3: Percentage NMDA receptor Ca^{2+} influx inhibition by test compounds.

Control	0,00
MK-801	59,57±5****
NGP1-01	42,27±22*
C1	25,08±10*
C2	46,83±32
C3	73,68±6****
C4	59,07±10***
C5	13,55±14
C7	47,71±19*

*Control = DMSO only *P < 0.1 **P < 0.05 ***P < 0.001 ****P <0.0001*

As expected, the positive controls MK-801 and NGP1-01 both showed significant inhibitory activity (table 4.2), with 59.57% and 42.27% respectively. This is supported by the fact that both these compounds are known to block NMDA receptors. MK-801 is however known to have a high affinity for the PCP binding site of the NMDA receptor and this is likely to be the reason for the higher percentage of inhibition compared to NGP1-01 (Black *et al.,* 1996). The synthesised compounds all showed some level of statistically significant activity when compared to the control, except compound **1** and compound **5**. Compound **5** showed the lowest activity, with 13.55% Ca^{2+} influx inhibition. Compound **3** showed the best activity with 73.68% inhibition, outperforming both the positive controls in this assay. It is seen that there is a gradual increase in the activity of the PCU cage moiety as it is modified. There is a clear increase from compound **1** to compound **2**, from 25.08% to 46.83%. This suggests that the primary amine at the end of the link attached to the ketal cage could allow the cage improved interaction and binding with the NMDA receptor channel. The large SD seen for compound **2** specifically does mean that this increase in activity seen between compound **1** and **2** could not be as significant as the results indicate. Another increase in activity was seen when the fluorophores were conjugated to compound **2**, to yield compounds **3**, **4** and **7**. These compounds showed activity of 73.68%, 59.07% and 47.71% inhibition respectively. The increase in activity seen here is also variable, due to the previously stated large SD seen for compound **2**. Irrespective of this, there was still a clear increase seen in activity between the ketal PCU derivative, compound **1** and the fluorophore PCU derivatives. The increase in activity with these compounds could be due to a number of reasons. Firstly the increase in LogP as seen in Table 4.4, means these compounds have a significantly higher degree of lipophilicity compared to that of compound **1** and **2**. The increased lipophilicity means these compounds are more easily able to cross biological membranes. Similar results have been reported previously (Joubert *et al.*, 2011a). In this study it was also reported that an increase in molecular weight correlated to an increase in activity, more than likely due to the ability of the conjugated fluorophores to interact with residues in the NMDA receptor binding pocket. Similarly it was seen that compounds **3**, **4** and **7** have fluorophores attached that correlates to the higher molecular weight, but more importantly the ability to interact with residues in the NMDA receptor pocket. In this study it was found that the bi-aromatic groups could be involved in these interactions. Compounds **3** and **7**

contain two benzene rings, while compound **4** has a benzene ring attached to pentane ring. These rings are expected to contribute to the activity seen with these compounds. There was however a significant decrease in activity seen between compound **3** and compound **7**. The difference between these two compounds is the transannular cyclisation resulting in the formation of the aza-PCU derivative, from the ketal-PCU derivative. This conversion means the ketal is now effectively replaced with a hydroxyl group that is located on the cage. This hydroxyl group might allow the compound to form additional interactions in the receptor site, however this significantly decreases the LogP value of the compound, and as such the activity. Furthermore the formation of the aza-bond on the cage means that compound **7** is much more rigid than compound **3**. This more than likely means the compound is not able to bend and fit into the receptor pocket as effectively, and ultimately results in the decreased activity. Compound **5** was the only compound in the final series that did not have a PCU moiety. The fluorophore alone meant a lower LogP and ultimately lipophilicity, and decreased activity. There was however still some activity seen, probably due to the bi-aromatic nature of the compound. The multiple exposed nitrogen groups on the fluorophore could also have been the reason for some interactions within the receptor channel. Based on the results from the successfully synthesised compounds, there are grounds to believe the proposed aza-derivative of compound **4** could also show a moderate degree of NMDA inhibition. Compounds **6** and **9**, the proposed PCU- **5** conjugates could thus have a high degree of activity, should they be synthesised successfully. Significant variation in the results of the NMDA assay indicates that more replicates of this specific assay could be done in order to confirm the findings of these results and findings. Even though a large SD was seen with compound **2** and **5,** the assay was still statistically significant.

4.4 Conclusion

Table 4.4: Combined analysis of test compounds

Compound	MW	LogP	% Cell Viability	% Cell Survival	% VGCC inhibition	% NMDA inhibition	λex (nm) DMSO	λem (nm) DMSO
	g/mol		10 µM	1 µM	10 µM	10 µM	1 µM	1 µM
MK-801	221,3	3,68± 0,39	x	x	X	59,57±5	x	x
NGP1-01	265,35	1,68± 0,36	x	x	69,54±11	42,27±22	x	x
Nimodipine	418,44	3,85± 0,59	x	x	42,48±16	X	x	x
Compound 1	218	0,1±0,59	110.39±7	88,02±5	25,60±12	25,08±10	x	x
Compound 2	260	1,56±0,62	84.72±6	75,64±3	41,85±23	46,83±32	x	x
Compound 3	495,63	3,78± 0,56	109,77±11	90,1±4	77,76±6	73,68±6	350	450
Compound 4	425,44	1,55± 1,14	111,26±13	76,64±4	57,79±15	59,07±10	485	530
Compound 5	263,3	0,01± 0,63	96,32±10	68,12±14	73,09±8	13,55±14	420	550
Compound 7	451,58	2,42± 0,49	104,30±8	73,83±8	62,18±13	47,71±19	350	450

The procedures used in this chapter allowed for successful evaluation of the synthesised compounds for cell cytotoxicity, neuroprotection and more specifically VGCC and NMDA related Ca^{2+} inhibition. The test compounds we analysed to indicate their potential NMDA receptor and VGCC inhibitory activities by comparing them with reference compounds known to be active. The potential NMDA receptor and VGCC inhibition of the synthesised compounds was successfully established, while the possible structure-activity relationships of the active compounds were discussed. The PCU-fluorophore derivatives showed great promise, especially compound **3,** which showed the highest neuroprotection while also showing good VGCC and NMDA inhibitory activity. The results provided insight into the activity of these compounds and show promise in the establishment of these or similar structures as fluorescent ligands in drug design and evaluation.

Chapter 5

Conclusion

5.1 General

Neurodegeneration occurs when neurons in the CNS, and the brain in particular, are destroyed by a complex network of mechanisms (Araki *et al.*, 2001). ND are progressive and irreversible, and the treatment options available for these diseases target the management of these disorders, rather than aiming to cure them. These diseases have a profound impact on the life of both the affected patient and their families (Tarrants *et al.*, 2010). Due to this significant and global impact of ND, it has become crucial to create drugs that can stop the progression and destruction we see in ND. Detecting these diseases, preventing them or even stopping the progression of ND is a strong motivator behind research in this field. Ultimately, to be able to treat ND, and helping monitor and diagnose them early and effectively is vital (Schweichel and Merker, 1973).

One of the greatest obstacles when treating ND is in the complexity of the neurodegenerative processes. It is not one simple process, but rather a complex system with multiple pathways of neurodegeneration. The development of molecules that prevent, stop or reverse the degenerative processes is a complex process in itself as there are all these different pathways that need to be considered. There is a need for a neuroprotective agent, which simultaneously possesses multifunctional activity for these different pathways to possibly cure these disorders. The lethal triplet of neurodegeneration is key mechanisms involved in neuronal cell death. Metabolic compromise, oxidative stress, and excitotoxicity are three crucial targets in the fight against ND. Two major pathways involved in the lethal triplet are VGCC and NMDA receptors. They have shown to be responsible to a large degree, for the excessive Ca^{2+} influx and ultimately neurodegeneration seen in neurons. Designing an agent that targets these pathways, while also showing neuroprotective properties is crucial in ND. The need for a multifunctional agent that could also assist in more effective disease treatment is evident. The addition of monitoring and detecting the progression of the disease due to the fluorescent nature of a compound, could be

even more useful. With this in mind, this project embarked on designing, synthesising and evaluating several fluorescent cage derivatives that show potential for use in the detection, prevention, treatment and cure of ND.

5.2 Synthesis and Chemistry

Five polycyclic cage derivatives, some with conjugated fluorophores, and an additional dicyano fluorophore were successfully synthesised for the purpose of biological evaluation. These compounds can be seen in figure 5.1. The lead compound, Cookson's diketone, also known as PCU, was initially synthesised and purified to a pale yellow-white power. This synthesis had an extremely high yield of 13.020 g, 80 %. The ketal-derivative of PCU was synthesised by refluxing under Dean Stark conditions to produce compound **1** as light white-brown crystals with a yield of 39% after purification. An amine linker was then conjugated to compound **1**, to yield compound **2**, a light yellow wax and had a yield of 42%. This was done using a microwave assisted amination reaction at 100 °C, 80 psi and 60 W for 3 hrs. The respective fluorophores were then conjugated to the primary amine of compound **2**, yielding imine-fluorophore derivatives. These derivatives were then further reduced using $NaBH_4$ to produce the secondary amine derivatives of the fluorescent-polycyclic cages known as, compounds **3** and **4**. These Ketal-PCU fluorophore derivatives were both oils, compound **3** yellow in colour and compound **4** being brown. Both compounds had low yields of 17% and 12.8% respectively. Compound **3** then underwent a transannular cyclisation reaction, yielding compound **7**. Compound **7** was a light yellow oil, and had the lowest yield at 6%. Compound **5** was a fluorophore successfully synthesised for conjugation to PCU. Compound **5**, was a solid orange powder and had a yield of 16%, but the mass of this yield only amounted to 0.009 g. Successful conjugation of compound **5** to compound **1** via microwave assisted reductive amination could not be successfully achieved due to this low yield. Purification of these compounds proved to be a great challenge as a result of extremely low yields. All compounds except **1** and **2** had yields below 17%. Various unidentified by-products or impurities further complicated purification and the synthesis of additional ketal and aza derivatives. Purification and recrystallization processes assisted in being able to identify the successfully synthesised compounds via NMR, IR and MS spectra. These processes also further lowered the yields resulting in the inability to synthesise more derivatives. As a result of the high level

of by-products accompanied by low yields meant it was impossible to synthesise compounds **6**, **8** and **9**. The synthesis of compound **6** and **8** were attempted but not successful as no product was yielded. The synthesis of **9** could not be performed due to the inability to synthesise compound **8**. With improved synthetic processes and more importantly purification techniques, the synthesis of these compounds could be feasible.

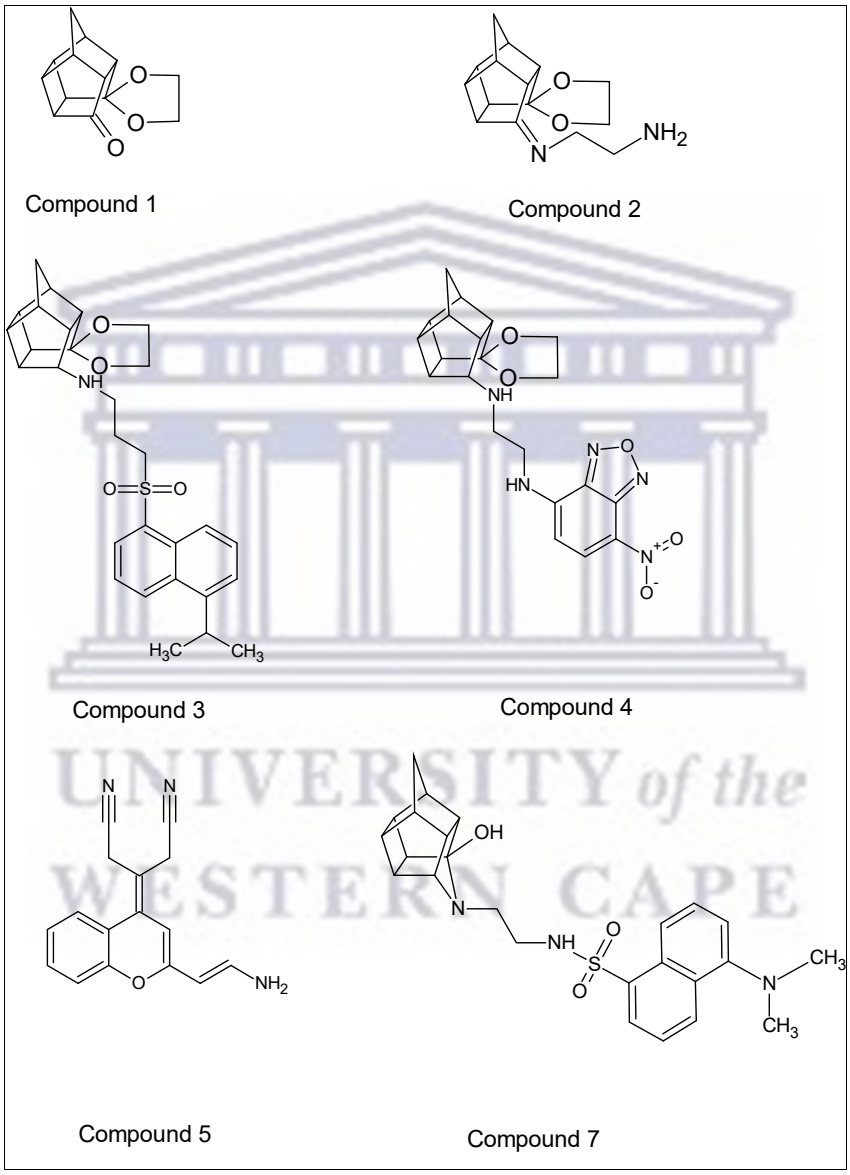

Figure 5.1: Structures of the successfully synthesised compounds.

5.3 Biological Evaluation

In this study four different assays were successfully performed on the synthesised compounds. Firstly a cytotoxicity assay was performed. Compounds **1-5** and **7** were assayed for cell viability on SH-SY5Y human neuroblastoma cells, a standard MTT

assay. Compound concentrations of 10 μM, 50 μM and 100 μM were used. None of the compounds were found to be cytotoxic at 10 μM or 50 μM. At 100 μM a slight reduction in cell viability was seen, with only compound **1**, **3** and **5** showing more cytotoxic effects with cell viability under 75%, with 63%, 59% and 72% respectively. The results for this assay were statistically significant ($P < 0.01$).

The second assay was a neuroprotection assay, and also performed on SH-SY5Y cells. The assay involved inducing neurotoxicity in the cells through MPP+ in these SH-SY5Y neuroblastoma cells (Zindo *et al*., 2014). The toxic effects induced by MPP+ causes neurodegeneration through oxidative stress. The cells were incubated with test compounds at 10 μM as well as 2000 μM MPP+. All the compounds showed some degree of neuroprotection when compared to the cell survival percentage seen with cells exposed to only MPP+. The highest level of neuroprotection was seen with compounds **1** and **3**. This assay also yielded results that were statistically significant with a P value less than 0.0001.

The VGCC and NMDA assays performed were similar as both used SH-SY5Y neuroblastoma cell lines again. Both assays assessed the ability of the test compound to block Ca^{2+} influx via VGCC and NMDA receptor channels respectively. The VGCC assay used a KCl solution for depolarisation, whereas a concentrated NMDA/glycine solution was used in the NMDA assay for depolarisation. NGP1-01 was used as a reference compound in both assays, while MK-801 was also used in the NMDA assay and nimodipine in the VGCC assay.

In the VGCC assay compound **3** showed the highest concentration of Ca^{2+} influx inhibition at 77.76%. A gradual increase in activity was seen when conjugation occurred on the ketal PCU, compound **1**. This showed that the addition of linkers and fluorophores have great potential in improving and further utilising the cage derivatives in VGCC antagonism. Significant activity was seen with compound **2**, **3**, **4** and **7**, all the cage derivatives. Lastly the fluorophore compound **5** also showed activity at 73.09% indicating it has great potential to be used as a fluorophore with VGCC activity and possibly as part of a cage derivative. The assay was also statistically significant with a P value less than 0.001.

The NMDA assay yielded very similar results to the VGCC assay. Again, compound **3** has the greatest activity at 73.68% inhibition. Here it was also seen that the

conjugation on Compound **1** increased the activity as compound **2**, **3**, **4** and **7** all showed higher activity. Compound 5 was the only compound that showed extremely low NMDA activity at 13.55%

This study confirmed the dual antagonism of VGCC and NMDA receptor related Ca^{2+} influx with compounds **3**, **4** and **7**. It was also seen that flexibility around the amide bond in the ketal derivatives is better than that of the rigid nature of the same bond in the aza derivative, as it more than likely allows for better interaction and bond formation in the receptor pockets. Furthermore these polycyclic cage-like molecules show great potential as expected and could be further analysed and explored as different derivatives to develop compounds that can be used as treatment options for neurodegenerative disorders.

5.4 Closing Remarks

A series of polycyclic cage derivatives were successfully synthesised. Their fluorescence, neuroprotective as well as potential inhibitory activities on VGCC and NMDA receptors were tested and demonstrated. Compounds **3**, **4** and **7** proved to not only have a high degree of fluorescence and neuroprotection, but also clear dual VGCC and NMDA activity. As such these compounds can serve as possible lead compounds to develop a more comprehensive series with more derivatives and fluorophores. Further expansion on this series will also help clarify structure activity profiles and mechanisms related to the activity seen with these compounds.

Although these compounds were found to have the fluorescent, VGCC and NMDA properties discussed in this thesis, their readiness for clinical use, as well as safety in humans still needs to be proven. Further *in vitro* and *in vivo* studies with regards to fluorescent ability and VGCC and NMDA ability of these compounds must still be tested to establish the true potential of these compounds as imaging tools in neurodegenerative/protective research.

Bibliography

Aarsland, D., Larsen, J.P., Karlsen K., Lim, N.G. (1999) 'Mental symptoms in Parkinson's disease are important contributors to caregiver distress.', *International journal of geriatric psychiatry*. England, 14(10), pp. 866–874.

Adelina, C. (2019) 'The costs of dementia: advocacy, media and stigma.', *Alzheimer's Disease International: World Alzheimer Report 2019*, pp. 100–101.

Al-khafaji, Z. (2017) 'Study of Genetic Variations of 15 Autosomal short Tandem Repeats (STRs) and Amelogenin Loci to Establish Database for Iraqi Population Biotechnology for Postgraduate Studies Study of Genetic Variations of 15 Autosomal short Tandem Repeats (STRs) doi: 10.13140/RG.2.2.15139.35360.

Alberti, C. (2012) 'From molecular imaging in preclinical / clinical oncology to theranostic applications in targeted tumor therapy', pp. 1925–1933.

Alexi, T. *et al.* (2000) 'Neuroprotective strategies for basal ganglia degeneration : Parkinson ' s and Huntington ' s diseases', 60.

Godlewski, M., Turowska, A., Jedynak, P., Martinez, D., Nevalainen, H. (2009). Fluorescence Applications in Biotechnology and Life Sciences.

Araki, T. *et al.* (2001) 'Neuroprotective effect of riluzole in MPTP-treated mice', *Brain Research* (918), pp. 176–181.

Arslan Ali, M. (2015) 'Alzheimer Disease', *Ajhmr*, 1(1), p. 2019. Available at: http://www.nhs.uk/Conditions/Alzheimers-disease/Pages/.

Artal-sanz, M. and Tavernarakis, N. (2005) 'Proteolytic mechanisms in necrotic cell death and neurodegeneration', *FEBS* (579), pp. 3287–3296. doi: 10.1016/j.febslet.2005.03.052.

Arundine, M. and Tymianski, M. (2003) 'Molecular mechanisms of calcium-dependent neurodegeneration in excitotoxicity', *Cell Calcium* 34, pp. 325–337. doi: 10.1016/S0143-4160(03)00141-6.

Benito-León, J. Louis, E.D., Posada, I.J., Sánchez-Ferro, Á., Trincado, R., Villarejo,

A., Mitchell, A., Bermejo-Pareja, F. (2011) 'Population-based case–control study of cognitive function in early Parkinson's disease (NEDICES)', *Journal of the Neurological Sciences*, 310(1), pp. 176–182. doi: https://doi.org/10.1016/j.jns.2011.06.054.

Black, M., Lanthorn, T., Small, D., Mealing, G., Lam, V. & Morley, P. (1996) 'Study of potency, kinetics of block and toxicity of NMDA receptor antagonists using fura-2', *European Journal of Pharmacology*, (317), pp. 377–381.

Blin, J. *et al.* (1993) 'Loss of brain 5-HT2receptors in Alzheimer's disease: In vivo assessment with positron emission tomography and (18)setoperone', *Brain*, 116(3),

pp. 497–510. doi: 10.1093/brain/116.3.497.

Boustany, N. N. and Boppart, S. A. (2010) ‘Microscopic Imaging and Spectroscopy with Scattered Light’. doi: 10.1146/annurev-bioeng-061008-124811.

Calon, F. and Cole, G. (2007) ‘Neuroprotective action of omega-3 polyunsaturated fatty acids against neurodegenerative diseases: Evidence from animal studies’, *Prostaglandins, Leukotrienes and Essential Fatty Acids*, 77(5), pp. 287–293. doi: https://doi.org/10.1016/j.plefa.2007.10.019.

Cataldi, M. (2013) ‘The Changing Landscape of Voltage-Gated Calcium Channels in Neurovascular Disorders and in Neurodegenerative Diseases’, *Current Neuropharmacology*, 11(3), pp. 276–297. doi: 10.2174/1570159x11311030004.

Catterall, W. A. and Few, A. P. (2008) ‘Calcium channel regulation and presynaptic plasticity.’, *Neuron*. United States, 59(6), pp. 882–901. doi: 10.1016/j.neuron.2008.09.005.

Chaudhuri, K. R., Healy, D. G. and Schapira, A. H. V (2006) ‘Non-motor symptoms of Parkinson’s disease: diagnosis and management’, *The Lancet Neurology*. Elsevier, 5(3), pp. 235–245. doi: 10.1016/S1474-4422(06)70373-8.

Checkoway, H., Lundin, J. I. and Kelada, S. N. (no date) ‘Neurodegenerative diseases’.

Chen, H., Dzitoyeva, S. and Manev, H. (2012) ‘Effect of aging on 5-hydroxymethylcytosine in the mouse hippocampus.’, *Restorative neurology and neuroscience*. Netherlands, 30(3), pp. 237–245. doi: 10.3233/RNN-2012-110223.

Chen, J. J. and Marsh, L. (2014) ‘Anxiety in Parkinson ’ s disease : identification and management’, pp. 52–59. doi: 10.1177/1756285613495723.

Choi, D. W. (1988) ‘Glutamate neurotoxicity and diseases of the nervous system’, *Neuron*, 1(8), pp. 623–634. doi: https://doi.org/10.1016/0896-6273(88)90162-6.

Clarimón, J. *et al.* (2018) ‘HTT gene intermediate alleles in neurodegeneration: evidence for association with Alzheimer’s disease’, *Neurobiology of Aging*. Elsevier Inc, 76, pp. 215.e9-215.e14. doi: 10.1016/j.neurobiolaging.2018.11.014.

Connor, B. and Dragunow, M. (1998) ‘The role of neuronal growth factors in neurodegenerative disorders of the human brain’, *Brain Research Reviews*, 27(1), pp. 1–39. doi: https://doi.org/10.1016/S0165-0173(98)00004-6.

Cookson, R. C. *et al.* (1964) ‘586. Photochemical cyclisation of diels–alder adducts’, *Journal of the Chemical Society (Resumed)*. The Royal Society of Chemistry, (0), pp. 3062–3075. doi: 10.1039/JR9640003062.

Crouch, P. J. *et al.* (2008) ‘Mechanisms of A [illegible] mediated neurodegeneration in Alzheimer ’ s disease’, 40, pp. 181–198. doi: 10.1016/j.biocel.2007.07.013.

Curcio, C. A. and Kemper, T. (1984) ‘Nucleus Raphe Dorsalis in Dementia of the Alzheimer Type: Neurofibrillary Changes and Neuronal Packing Density’, *Journal of Neuropathology & Experimental Neurology*, 43(4), pp. 359–368. doi:

10.1097/00005072-198407000-00001.

Dondorp, A. M. *et al.* (2009) 'Artemisinin resistance in Plasmodium falciparum malaria.', *The New England journal of medicine*. United States, 361(5), pp. 455–467. doi: 10.1056/NEJMoa0808859.

Dunlap, K., Luebke, J. I. and Turner, T. J. (1995) 'Exocytotic Ca^{2+} channels in mammalian central neurons.', *Trends in neurosciences*. England, 18(2), pp. 89–98.

Egunlusi, A. O. (2014) 'Novel tricycloundecane derivatives as potential N -methyl- D - aspartate receptor and calcium channel inhibitors for neuroprotection'.

Elgh, E. *et al.* (2009) 'Cognitive function in early Parkinson's disease: a population-based study', *European Journal of Neurology*. John Wiley & Sons, Ltd (10.1111), 16(12), pp. 1278–1284. doi: 10.1111/j.1468-1331.2009.02707.x.

Faggiani, E. *et al.* (2018) 'Serotonergic neurons mediate the anxiolytic effect of l-DOPA: Neuronal correlates in the amygdala', *Neurobiology of Disease*, 110, pp. 20–28. doi: https://doi.org/10.1016/j.nbd.2017.11.001.

Feuvre, R. Le, Brough, D. and Rothwell, N. (2002) 'Extracellular ATP and P2X7 receptors in neurodegeneration', 447, pp. 261–269.

Finazzi, D. and Arosio, P. (2014) 'Biology of ferritin in mammals: an update on iron storage, oxidative damage and neurodegeneration', *Archives of Toxicology*, 88(10), pp. 1787–1802. doi: 10.1007/s00204-014-1329-0.

Fulvio Celsi, Paola Pizzo, Marisa Brini, Sara Leo, Carmen Fotino, Paolo Pinton, and R. R. (2009) 'Mitochondria, calcium and cell death: A deadly triad in neurodegeneration', 1787(5), pp. 335–344. doi: 10.1016/j.bbabio.2009.02.021.Mitochondria.

Geldenhuys, W.J., Malan, S.F., Murugesan, T., Van der Schyf, C.J., Bloomquist, J.R. (2004) 'potential therapeutic agents in Parkinson ' s disease', 12, pp. 1799–1806. doi: 10.1016/j.bmc.2003.12.045.

Geldenhuys, W. J., Youdim, M.B.H., Carroll, R.T. & Van der Schyf, C.J. (2011) 'The emergence of designed multiple ligands for neurodegenerative disorders', *Progress in Neurobiology*, 94(4), pp. 347–359. doi: https://doi.org/10.1016/j.pneurobio.2011.04.010.

Giacoppo, S. Galuppo, M., Montaut, S., Iori, R., Rollin, P., Bramanti, P. (2015) 'An overview on neuroprotective effects of isothiocyanates for the treatment of neurodegenerative diseases.', *Fitoterapia*. Netherlands, 106, pp. 12–21. doi: 10.1016/j.fitote.2015.08.001.

Gilgun-Sherki, Y., Melamed, E. and Offen, D. (2001) 'Oxidative stress induced-neurodegenerative diseases: the need for antioxidants that penetrate the blood brain barrier', *Neuropharmacology*, 40(8), pp. 959–975. doi: https://doi.org/10.1016/S0028-3908(01)00019-3.

Gonsette, R. E. (2008) 'Journal of the Neurological Sciences Neurodegeneration in multiple sclerosis : The role of oxidative stress and excitotoxicity', 274, pp. 48–53. doi: 10.1016/j.jns.2008.06.029.

Greene, J. G. and Greenamyre, J. T. (1996) 'Manipulation of Membrane Potential Modulates Malonate-Induced Striatal Excitotoxicity In Vivo', *Journal of Neurochemistry*. John Wiley & Sons, Ltd (10.1111), 66(2), pp. 637–643. doi: 10.1046/j.1471-4159.1996.66020637.x.

Grimm, A. and Eckert, A. (2017) 'Brain aging and neurodegeneration: from a mitochondrial point of view', *Journal of Neurochemistry*, 143(4), pp. 418–431. doi: 10.1111/jnc.14037.

Groen, J. L., de Bie, R.M.A., Foncke, E.M.J., Roos, R.A.C., Leenders, K.L., Tijssen, M.A.J. (2010) 'Late-onset Huntington disease with intermediate CAG repeats: true or false?', *Journal of Neurology, Neurosurgery & Psychiatry*, 81(2), pp. 228 LP – 230. doi: 10.1136/jnnp.2008.170902.

Halliwell, B. (2001) 'Role of Free Radicals in the Neurodegenerative Diseases', *Drugs & Aging*, 18(9), pp. 685–716. doi: 10.2165/00002512-200118090-00004.

Hamley, I. W. (2012) 'The Amyloid Beta Peptide: A Chemist's Perspective. Role in Alzheimer's and Fibrillization', *Chemical Reviews*. American Chemical Society, 112(10), pp. 5147–5192. doi: 10.1021/cr3000994.

Hardy, J. (2006) 'A Hundred Years of Alzheimer's Disease Research', *Neuron*, 52(1), pp. 3–13. doi: https://doi.org/10.1016/j.neuron.2006.09.016.

Hardy, J. and Selkoe, D. J. (2002) 'The amyloid hypothesis of Alzheimer's disease: Progress and problems on the road to therapeutics', *Science*, 297(5580), pp. 353–356. doi: 10.1126/science.1072994.

Haugland, J.G., Gregory, J., Spence, M.T.Z., Johnson, I., Miller, E. (2002) 'Handbook of fluorescent probes and research products', (Figure 2), pp. 1–950.

Hawley, Z. C. E., Campos-Melo, D. and Strong, M. J. (2019) 'MiR-105 and miR-9 regulate the mRNA stability of neuronal intermediate filaments. Implications for the pathogenesis of amyotrophic lateral sclerosis (ALS)', *Brain Research*. Elsevier B.V., 1706(July 2018), pp. 93–100. doi: 10.1016/j.brainres.2018.10.032.

Herrero, M. T. and Morelli, M. (2017) 'Progress in Neurobiology Multiple mechanisms of neurodegeneration and progression', *Progress in Neurobiology*. Elsevier Ltd, 155, p. 1. doi: 10.1016/j.pneurobio.2017.06.001.

Hong, G., Antaris, A. L. and Dai, H. (2017) 'Near-infrared fluorophores for biomedical imaging', *Nature Biomedical Engineering*, 1(1), p. 10. doi: 10.1038/s41551-016-0010.

Ito, M. F., Petroni, J.M., de Lima, D.P., Beatriz, A., Marques, M.R., de Moraes, M.O., Costa-Lotufo, L.V., Montenegro, R.C, Magalhaes, H.I.F, do O Pessoa, C. (2007) 'Synthesis and Biological Evaluation of Rigid Polycyclic Derivatives of the Diels-Alder Adduct Tricyclo[6.2.1.02,7]undeca-4,9-dien-3,6-dione', Molecules. doi: 10.3390/12020271.

Jankovic, J. (2008) 'Parkinson ' s disease : clinical features and diagnosis', (1957), pp. 368–376. doi: 10.1136/jnnp.2007.131045.

Johnson, J. W. and Kotermanski, S. E. (2006) 'Mechanism of action of memantine',

Current Opinion in Pharmacology, 6(1), pp. 61–67. doi: https://doi.org/10.1016/j.coph.2005.09.007.

Joubert, Jacques & Dyk, Sandra & Malan, Sarel. (2008). Fluorescent polycyclic ligands for nitric oxide synthase (NOS) inhibition. Bioorganic & medicinal chemistry. 16. 8952-8. 10.1016/j.bmc.2008.08.049.

Joubert, J. *et al.* (2011) 'Bioorganic & Medicinal Chemistry Synthesis and evaluation of fluorescent heterocyclic aminoadamantanes as multifunctional neuroprotective agents', *Bioorganic & Medicinal Chemistry*. Elsevier Ltd, 19(13), pp. 3935–3944. doi: 10.1016/j.bmc.2011.05.034.

Joubert, J. *et al.* (2011b) 'European Journal of Medicinal Chemistry Synthesis , evaluation and application of polycyclic fl uorescent analogues as N -methyl- D - aspartate receptor and voltage gated calcium channel ligands', *European Journal of Medicinal Chemistry*. Elsevier Masson SAS, 46(10), pp. 5010–5020. doi: 10.1016/j.ejmech.2011.08.008.

Joubert, J., Sharma . R., Onani, M., Malan, S.. (2013) 'Microwave-assisted methods for the synthesis', *Tetrahedron Letters*. Elsevier Ltd, 54(50), pp. 6923–6927. doi: 10.1016/j.tetlet.2013.10.047.

Kepe, V., Barrio, J.R., Huang, S., Ercoli, L., Siddarth, P., Shoghi-jadid, K., Cole, G.M., Satyamurthy, N., Cummings, J.L., Small, G.W., Phelps, M.E. (2006) 'Serotonin 1A receptors in the living brain of Alzheimer ' s disease patients', pp. 1–6.

Knowles, T. P. J., Vendruscolo, M. and Dobson, C. M. (2014) 'The amyloid state and its association with protein misfolding diseases', *Nature Reviews Molecular Cell Biology*. Nature Publishing Group, a division of Macmillan Publishers Limited. All Rights Reserved., 15, p. 384. Available at: https://doi.org/10.1038/nrm3810.

Korczyn, A. D. (2016) 'Parkinson's and Alzheimer's diseases: Focus on mild cognitive impairment', *Parkinsonism and Related Disorders*. Elsevier Ltd, 22, pp. S159–S161. doi: 10.1016/j.parkreldis.2015.09.053.

Krantic, S., Mechawar, N., Reix, S. & Quirion, R. (2005) 'Molecular basis of programmed cell death involved in neurodegeneration', *Trends in Neurosciences*, 28(12), pp. 670–676. doi: https://doi.org/10.1016/j.tins.2005.09.011.

Landrigan, P. J., Sonawane, B., Butler, R.N., Trasande, L., Callan, R. & Droller, D. (2005) 'Early Environmental Origins of Neurodegenerative Disease in Later Life', 1230(9), pp. 2003–2006. doi: 10.1289/ehp.7571.

lanke ML, V. A. (2009) *Biology of the NMDA Receptor*.

Lardenoije, R., Iatrou, A., Kenis, G., Kompotis, K., Steinbusch, H.W.M., Mastroeni, D., Coleman, P., Lemere, C.A., Hof, P.R., Hove, D.L.A., Van Den Rutten, B.P.F. (2015) 'Progress in Neurobiology The epigenetics of aging and neurodegeneration', *Progress in Neurobiology*. Elsevier Ltd, 131, pp. 21–64. doi: 10.1016/j.pneurobio.2015.05.002.

Leal, P.C., Bispo, J.M.M., Lins, L.C.R.F., Souza, M.F., Gois, A.M., Moore, C., Marchioro, M. (2019) 'Cognitive and anxiety-like impairments accompanied by

serotonergic ultrastructural and immunohistochemical alterations in early stages of parkinsonism', *Brain Research Bulletin*. Elsevier, 146(October 2018), pp. 213–223. doi: 10.1016/j.brainresbull.2019.01.009.

Lewis, S. J. G., Dove, A., Robbins, T.W., Barker, R.A., Owen, A.M. (2003) 'Cognitive Impairments in Early Parkinson ' s Disease Are Accompanied by Reductions in Activity in Frontostriatal Neural Circuitry', 23(15), pp. 6351–6356.

Li, Y. & Han, T. (2016) 'A theranostic agent for in vivo near-infrared imaging of β-amyloid species and inhibition of β-amyloid aggregation', *Biomaterials*, 94, pp. 84–92. doi: https://doi.org/10.1016/j.biomaterials.2016.03.047.

Lipton, S. A. (2007) 'Pathologically-Activated Therapeutics for Neuroprotection: Mechanism of NMDA Receptor Block by Memantine and S-Nitrosylation', *Current Drug Targets*, pp. 621–632. doi: http://dx.doi.org/10.2174/138945007780618472.

Logroscino, G. *et al.* (2005) 'a population based study', pp. 1094–1098. doi: 10.1136/jnnp.2004.039180.

Lü, J.M., Lin, P.H., Yao, Q., Chen, C. (2010) 'Chemical and molecular mechanisms of antioxidants: Experimental approaches and model systems', *Journal of Cellular and Molecular Medicine*, 14(4), pp. 840–860. doi: 10.1111/j.1582-4934.2009.00897.x.

Madrid, P.B., Liou, A.P., Derisi, J.L., Guy, R.K. (2006) 'Incorporation of an Intramolecular Hydrogen-Bonding Motif in the Side Chain of 4-Aminoquinolines Enhances Activity against Drug-Resistant P . falciparum', pp. 4535–4543. doi: 10.1021/jm0600951.

Marchand, A.P., Arney, B.E., Dave, P. R., Satyanarayana, N., Watson, W.H., Nagl, A. (1988) 'Transannular cyclizations in the pentacyclo[5.4.0.02,6.03,10.05,9] undecane-8,11-dione system. A reinvestigation', *The Journal of Organic Chemistry*. American Chemical Society, 53(11), pp. 2644–2647. doi: 10.1021/jo00246a053.

Marchetti, C. & Usai, C. (1996) 'High affinity block by nimodipine of the internal calcium elevation in chronically depolarised rat cerebellar granule neuron.', *Neuroscience letters*, 207(2), pp. 77–80.

Marner, L., Frokjaer, V.G., Kalbitzer, J., Lehel, S., Madsen, K., Baaré, W.F.C. (2012) 'Loss of serotonin 2A receptors exceeds loss of serotonergic projections in early Alzheimer's disease: a combined [11C]DASB and [18F]altanserin-PET study', *Neurobiology of Aging*, 33(3), pp. 479–487. doi: https://doi.org/10.1016/j.neurobiolaging.2010.03.023.

Martin, L. J., Al-Abdulla, N., Brambrink, A., Kirsch, J., Sieber, F. & Portera-Cailliau, C. (1998) 'Neurodegeneration in Excitotoxicity, Global Cerebral Ischemia, and Target Deprivation: A Perspective on the Contributions of Apoptosis and Necrosis', *Brain Research Bulletin*, 46(4), pp. 281–309. doi: https://doi.org/10.1016/S0361-9230(98)00024-0.

Mastroeni, D., Grover, A., Delvaux, E., Whiteside, C., Coleman, P.D., Rogers, J. (2010) 'Epigenetic changes in Alzheimer's disease: Decrements in DNA methylation', *Neurobiology of Aging*. Elsevier Inc., 31(12), pp. 2025–2037. doi:

10.1016/j.neurobiolaging.2008.12.005.

Mayeux, R. (2003) ‘Epidemiology of neurodegeneration’, pp. 81–104. doi: 10.1146/annurev.neuro.26.043002.094919.

McKhann, G., Drachman, D., Folstein, M., Katzman, R., Price, D., Stadlan, E.M. (1984) ‘Clinical diagnosis of Alzheimer’s disease: report of the NINCDS-ADRDA Work Group under the auspices of Department of Health and Human Services Task Force on Alzheimer’s Disease.’, *Neurology*. United States, 34(7), pp. 939–944. doi: 10.1212/wnl.34.7.939.

Nimmrich, V., Grimm, C., Draguhn, A., Barghorn, S., Lehmann, A., Schoemaker, H. (2008) ‘Amyloid beta oligomers (A beta(1-42) globulomer) suppress spontaneous synaptic activity by inhibition of P/Q-type calcium currents.’, *The Journal of neuroscience : the official journal of the Society for Neuroscience*. United States, 28(4), pp. 788–797. doi: 10.1523/JNEUROSCI.4771-07.2008.

Nimse, S. B. and Pal, D. (2015) ‘Free radicals, natural antioxidants, and their reaction mechanisms’, *RSC Advances*. The Royal Society of Chemistry, 5(35), pp. 27986–28006. doi: 10.1039/C4RA13315C.

Nordlund, A. and Oliveberg, M. (2006) ‘Folding of Cu ¯Zn superoxide dismutase suggests structural hotspots for gain of neurotoxic function in ALS : Parallels to precursors in amyloid disease’.

Ohno, Y., Shimizu, S. and Tokudome, K. (2013) ‘Recent Advances in 5-Hydroxytryptamine (5-HT) Receptor Research : How Many Pathophysiological Roles Does 5-HT Play via Its Multiple Receptor Subtypes ? Pathophysiological Roles of Serotonergic System in Regulating Extrapyramidal Motor Functions’, 36(9), pp. 1396–1400.

Oliver, D.W., Dekker, T.G., Snyckers, F.O., Fourie, T.G. (1991) ‘Synthesis and biological activity of D3-trishomocubyl-4-amines.’, Journal of medicinal chemistry. United States, 34(2), pp. 851–854.

Oliver, D. W., Dekker, T. G. and Snyckers, F. O. (1991) ‘Pentacyclo[5.4.0.02,6.03,10.05,9]undecylamines. Synthesis and pharmacology’, *European Journal of Medicinal Chemistry*, 26(4), pp. 375–379. doi: https://doi.org/10.1016/0223-5234(91)90097-7.

Onajole, O. K., Coovadia, Y., Kruger, H. G., Maguire, G. E. M., Pillay, M., Govender, T. (2012) ‘European Journal of Medicinal Chemistry Novel polycyclic “ cage ” -1 , 2-diamines as potential anti-tuberculosis agents’, *European Journal of Medicinal Chemistry*. Elsevier Masson SAS, 54, pp. 1–9. doi: 10.1016/j.ejmech.2012.03.041.

Ouchi, Y., Yoshikawa, E., Futatsubashi, M., Yagi, S., Ueki, T., Nakamura, K. (2009) ‘Altered Brain Serotonin Transporter and Associated Glucose Metabolism in Alzheimer Disease’, 50(8), pp. 1260–1267. doi: 10.2967/jnumed.109.063008.

Den Oudsten, B. L., Van Heck, G. L. and De Vries, J. (2007) ‘Quality of life and related concepts in Parkinson’s disease: A systematic review’, *Movement Disorders*. John Wiley & Sons, Ltd, 22(11), pp. 1528–1537. doi: 10.1002/mds.21567.

Palmer, A. M. *et al.* (1988) 'Possible neurotransmitter basis of behavioral changes in alzheimer's disease', *Annals of Neurology*. John Wiley & Sons, Ltd, 23(6), pp. 616–620. doi: 10.1002/ana.410230616.

Pavese, N. *et al.* (2011) 'Progression of monoaminergic dysfunction in Parkinson's disease: A longitudinal 18F-dopa PET study', *NeuroImage*, 56(3), pp. 1463–1468. doi: https://doi.org/10.1016/j.neuroimage.2011.03.012.

Politis, M. and Loane, C. (2011) 'Serotonergic Dysfunction in Parkinson ' s Disease and Its Relevance to Disability', pp. 1726–1734. doi: 10.1100/2011/172893.

Prediger, R.D.S., Matheus, F.C., Schwarzbold, M.L., Lima, M.M.S., Vital, M.A.B.F (2012) 'Anxiety in Parkinson's disease: A critical review of experimental and clinical studies', *Neuropharmacology*, 62(1), pp. 115–124. doi: https://doi.org/10.1016/j.neuropharm.2011.08.039.

Prince, M., Comas-Herrera, A., Knapp, M., Guerchet, M., Karagiannidou, M. (2016) 'World Alzheimer Report 2016 Improving healthcare for people living with dementia. Coverage, Quality and costs now and in the future', pp. 1–140. Available at: https://www.alz.co.uk/research/world-report-2016.

Raffray, M. and Gerald M., C. (1997) 'Apoptosis and necrosis in toxicology: A continuum or distinct modes of cell death?', *Pharmacology & Therapeutics*, 75(3), pp. 153–177. doi: https://doi.org/10.1016/S0163-7258(97)00037-5.

Rajasekhar, K., Narayanaswamy, N., Murugan, N.A., Viccaro, K. (2017) 'Biosensors and Bioelectronics A β plaque-selective NIR fl uorescence probe to di ff erentiate Alzheimer ' s disease from tauopathies', 98(April), pp. 54–61. doi: 10.1016/j.bios.2017.06.030.

Ramsden, M., Henderson, Z. and Pearson, H. A. (2002) 'Modulation of Ca2+ channel currents in primary cultures of rat cortical neurones by amyloid beta protein (1-40) is dependent on solubility status', *Brain research*. School of Biomedical Sciences, University of Leeds, Leeds LS2 9JT, UK., 956(2), pp. 254–261. doi: 10.1016/s0006-8993(02)03547-3.

Roe, M. W. (1990) 'Assessment of Fura-2 for measurements of cytosolic free calcium', *Cell calcium.* [London] : Harcourt, p. 63. doi: 10.1016/0143-4160(90)90060-8.

Ryff, IlhaBediou, B. *et al.* (2008) 'Impaired Social Cognition in Mild Alzheimer Disease', pp. 130–140.

Sattler, R. and Tymianski, M. (2000) 'Sattler R, Tymianski MMolecular mechanisms of calcium-dependent excitotoxicity. J Mol Med 78:3-13', *Journal of molecular medicine (Berlin, Germany)*, 78, pp. 3–13. doi: 10.1007/s001090000077.

Schweichel, J.-U. and Merker, H.-J. (1973) 'The morphology of various types of cell death in prenatal tissues', *Teratology*. John Wiley & Sons, Ltd, 7(3), pp. 253–266. doi: 10.1002/tera.1420070306.

Selkoe, D. J. (2012) 'Disease prevention', 337(September), pp. 1488–1493.

Sen, I. *et al.* (2005) 'Cerebrospinal fluid from amyotrophic lateral sclerosis patients

preferentially elevates intracellular calcium and toxicity in motor neurons via AMPA / kainate receptor', 235, pp. 45–54. doi: 10.1016/j.jns.2005.03.049.

Sipe, J. D. and Cohen, A. S. (2000) 'Review: history of the amyloid fibril.', *Journal of structural biology*. United States, 130(2–3), pp. 88–98. doi: 10.1006/jsbi.2000.4221.

Smith, G.S., Barrett, F.S., Hui, J., Nassery, N., Savonenko, A., Sodums, D.J., Marano, C.M., Munro, C.A., Brandt, J., Kraut, M.A., Zhou, Y., Wong, D. F., Workman, C.I. (2017) 'Neurobiology of Disease Molecular imaging of serotonin degeneration in mild cognitive impairment', *Neurobiology of Disease*. Elsevier Inc., 105, pp. 33–41. doi: 10.1016/j.nbd.2017.05.007.

Soh, S.-E., Morris, M. E. and McGinley, J. L. (2011) 'Determinants of health-related quality of life in Parkinson's disease: A systematic review', *Parkinsonism & Related Disorders*, 17(1), pp. 1–9. doi: https://doi.org/10.1016/j.parkreldis.2010.08.012.

Soto, C. (2003) 'Unfolding the role of protein misfolding in neurodegenerative diseases', *Nature Reviews Neuroscience*, 4(1), pp. 49–60. doi: 10.1038/nrn1007.

Specht, E. A., Braselmann, E. and Palmer, A. E. (2017) 'A Critical and Comparative Review of Fluorescent Tools for Live-Cell Imaging', *Annual Review of Physiology*, 79(1), pp. 93–117. doi: 10.1146/annurev-physiol-022516-034055.

Spires-Jones, T. L. and Hyman, B. T. (2014) 'The Intersection of Amyloid Beta and Tau at Synapses in Alzheimer's Disease', *Neuron*, 82(4), pp. 756–771. doi: https://doi.org/10.1016/j.neuron.2014.05.004.

Starkstein, S.E., Sabe, L., Petracca, G., Chemerinski, E., Kuzis, G., Merello, M., Leiguarda, R. (1996) 'Neuropsychological and psychiatric differences between Alzheimer's disease and Parkinson's disease with dementia.', *Journal of Neurology, Neurosurgery & Psychiatry*, 61(4), pp. 381 LP – 387. Available at: http://jnnp.bmj.com/content/61/4/381.abstract.

Stout, A.K., Raphael, H.M., Kanterewicz, B.I., Klann, E., Reynolds, I.J. (1998) 'Glutamate-induced neuron death requires mitochondrial calcium uptake', *Nature Neuroscience*, 1(5), pp. 366–373. doi: 10.1038/1577.

Sturza, A., Leisegang, M.S., Babelova, A., Schröder, K., Benkhoff, S., Loot, A.E., Fleming, I., Schulz, R., Muntean, D.M., Brandes, R.P. (2013) 'Monoamine Oxidases Are Mediators of Endothelial Dysfunction in the Mouse Aorta', pp. 140–146. doi: 10.1161/HYPERTENSIONAHA.113.01314.

Tarrants, M.L., Denarié, M.F., Castelli-Haley, J., Millard, J., Zhang, D. (2010) 'Drug therapies for Parkinson's disease: A database analysis of patient compliance and persistence', *The American Journal of Geriatric Pharmacotherapy*, 8(4), pp. 374–383. doi: https://doi.org/10.1016/j.amjopharm.2010.08.001.

Teponnou, G. A. K. (2017) 'Tacrine , trolox and tryptoline as lead compounds for the design and synthesis of multi-target drugs for Alzheimer ' s disease therapy . by'.

Tokuchi, R., Hishikawa, N., Sato, K., Hatanaka, N., Fukui, Y., Takemoto, M., Ohta, Y., Yamashita, T., Abe, K. (2016) 'Differences between the behavioral and psychological symptoms of Alzheimer's disease and Parkinson's disease', *Journal of*

the Neurological Sciences. Elsevier B.V., 369, pp. 278–282. doi: 10.1016/j.jns.2016.08.053.

Troeung, L., Egan, S. J. and Gasson, N. (2013) 'A Meta-Analysis of Randomised Placebo-Controlled Treatment Trials for Depression and Anxiety in Parkinson's Disease', *PLOS ONE*. Public Library of Science, 8(11), p. e79510. Available at: https://doi.org/10.1371/journal.pone.0079510.

Tsien, R.W., Lipscombe, D., Madison, D.V., Bley, K.R., Fox, A.P. (1988) 'Multiple types of neuronal calcium channels and their selective modulation.', *Trends in neurosciences*. England, 11(10), pp. 431–438. doi: 10.1016/0166-2236(88)90194-4.

Tymianski, M. and Tator, C. H. (1996) 'Normal and Abnormal Calcium Homeostasis in Neurons: A Basis for the Pathophysiology of Traumatic and Ischemic Central Nervous System Injury', *Neurosurgery*, 38(6), pp. 1176–1195. doi: 10.1097/00006123-199606000-00028.

Ueda, K., Shinohara, S., Yagami, T., Asakura, K., Kawasaki, K.. (1997) 'Amyloid beta protein potentiates Ca2+ influx through L-type voltage-sensitive Ca2+ channels: a possible involvement of free radicals.', *Journal of neurochemistry*. England, 68(1), pp. 265–271. doi: 10.1046/j.1471-4159.1997.68010265.x.

Uttara, B., Singh, A.V., Zamboni, P., Mahajan, R.T. (2009) 'Oxidative Stress and Neurodegenerative Diseases : A Review of Upstream and Downstream Antioxidant Therapeutic Options', pp. 65–74.

van de Berg, W. D. J. et al. (2012) 'Patterns of alpha-synuclein pathology in incidental cases and clinical subtypes of Parkinson's disease', Parkinsonism & Related Disorders, 18, pp. S28–S30. doi: https://doi.org/10.1016/S1353-8020(11)70011-6.

Van der Schyf, C. J. (1989) 'The polycyclic calcium antagonist, NGP1-01, has an oxa rather than an aza bird-cage structure: Evidence from n.m.r. spectroscopy and the X-ray crystal structure', South African journal of chemistry = Suid-Afrikaanse tydskrif vir chemie. Pretoria : Foundation for Education Science and Technology, pp. 46–48.

Van der Schyf, C. J., Squier, G. J. and Coetzee, W. A. (1986) 'Characterization of NGP 1-01, an aromatic polycyclic amine, as a calcium antagonist', Pharmacological Research Communications, 18(5), pp. 407–417. doi: https://doi.org/10.1016/0031-6989(86)90162-1.

Van der Schyf, C. J. and Youdim, M. B. H. (2009) 'Multifunctional drugs as neurotherapeutics', Neurotherapeutics, 6(1), pp. 1–3. doi: 10.1016/j.nurt.2008.11.001.

Veldman, B.A.J., Wijn, A.M., Knoers, N., Praamstra, P., Horstink, M.W.I.M. (1998) 'Genetic and environmental risk factors in Parkinson's disease', Clinical Neurology and Neurosurgery, 100(1), pp. 15–26 doi: https://doi.org/10.1016/S0303-8467(98)00009-2.

Wakabayashi, K., Tanji, K., Mori, F., Takahashi, H. (2007) 'The Lewy body in Parkinson's disease: Molecules implicated in the formation and degradation of α-synuclein aggregates', Neuropathology, 27(5), pp. 494–506. doi: 10.1111/j.1440-

1789.2007.00803.x.

Waldmeier, P. C. (2003) 'Prospects for antiapoptotic drug therapy of neurodegenerative diseases', *Progress in Neuro-Psychopharmacology and Biological Psychiatry*, 27(2), pp. 303–321. doi: https://doi.org/10.1016/S0278-5846(03)00025-3.

Wang, R. and Zhang, F. (2014) 'NIR luminescent nanomaterials for biomedical imaging', *Journal of Materials Chemistry B*. The Royal Society of Chemistry, 2(17), pp. 2422–2443. doi: 10.1039/C3TB21447H.

Weintraub, D., Xie, S., Karlawish, J., Siderowf, A. (2007) 'Differences in depression symptoms in patients with Alzheimer's and Parkinson's diseases: evidence from the 15-item Geriatric Depression Scale (GDS-15)', International Journal of Geriatric Psychiatry. John Wiley & Sons, Ltd., 22(10), pp. 1025–1030. doi: 10.1002/gps.1785.

Wenk, G. L. (2007) 'Chapter 16 - Neurodegenerative diseases and memory: A treatment approach', in Kesner, R. P. and Martinez, J. L. B. T.-N. of L. and M. (Second E. (eds). Burlington: Academic Press, pp. 519–539. doi: https://doi.org/10.1016/B978-012372540-0/50017-0.

Werner, P. and Korczyn, A. D. (2008) 'Mild cognitive impairment: Conceptual, assessment, ethical, and social issues', *Clinical Interventions in Aging*. Dove Press, Volume 3(3), pp. 413–420. doi: 10.2147/CIA.S1825.

Wood, H. (2012) 'Proteomic tools identify dementia biomarkers in PD', *Nature Reviews Neurology*, 8(4), p. 180. doi: 10.1038/nrneurol.2012.34.

World Health Organization (2006) 'Neurological disorders: a public health approach', *Neurological disorders: public health challenges.*, pp. 41–176. doi: 10.1001/archneurol.2007.19.

Zhang, X. *et al.* (2015) 'A near-infrared fl uorescent probe for rapid detection of hydrogen peroxide in living cells', *Tetrahedron*. Elsevier Ltd, 71(29), pp. 4842–4845. doi: 10.1016/j.tet.2015.05.025.

Zhang, X., Zhang, L., Liu, Y., Bao, B., Zang, Y., Li, J., Lu, W. (2015) 'A near-infrared fl uorescent probe for rapid detection of hydrogen peroxide in living cells', Tetrahedron. Elsevier Ltd, 71(29), pp. 4842–4845.. doi: 10.1039/C3CS60430F.

Zindo, F.T., Barber, Q.R., Joubert, J., Bergh, J.J., Petzer, J.P., Malan, S.F. (2014) 'European Journal of Medicinal Chemistry Polycyclic propargylamine and acetylene derivatives as multifunctional neuroprotective agents', 80, pp. 122–134.

Appendix 1

SPECTRAL DATA:

INFRARED, MASS AND

NUCLEAR MAGNETIC RESONANCE

SPECTRA

Pentacyclo[5.4.0.0^{2,6}.0^{3,10}.0^{5,9}]undecane-8,11-dione

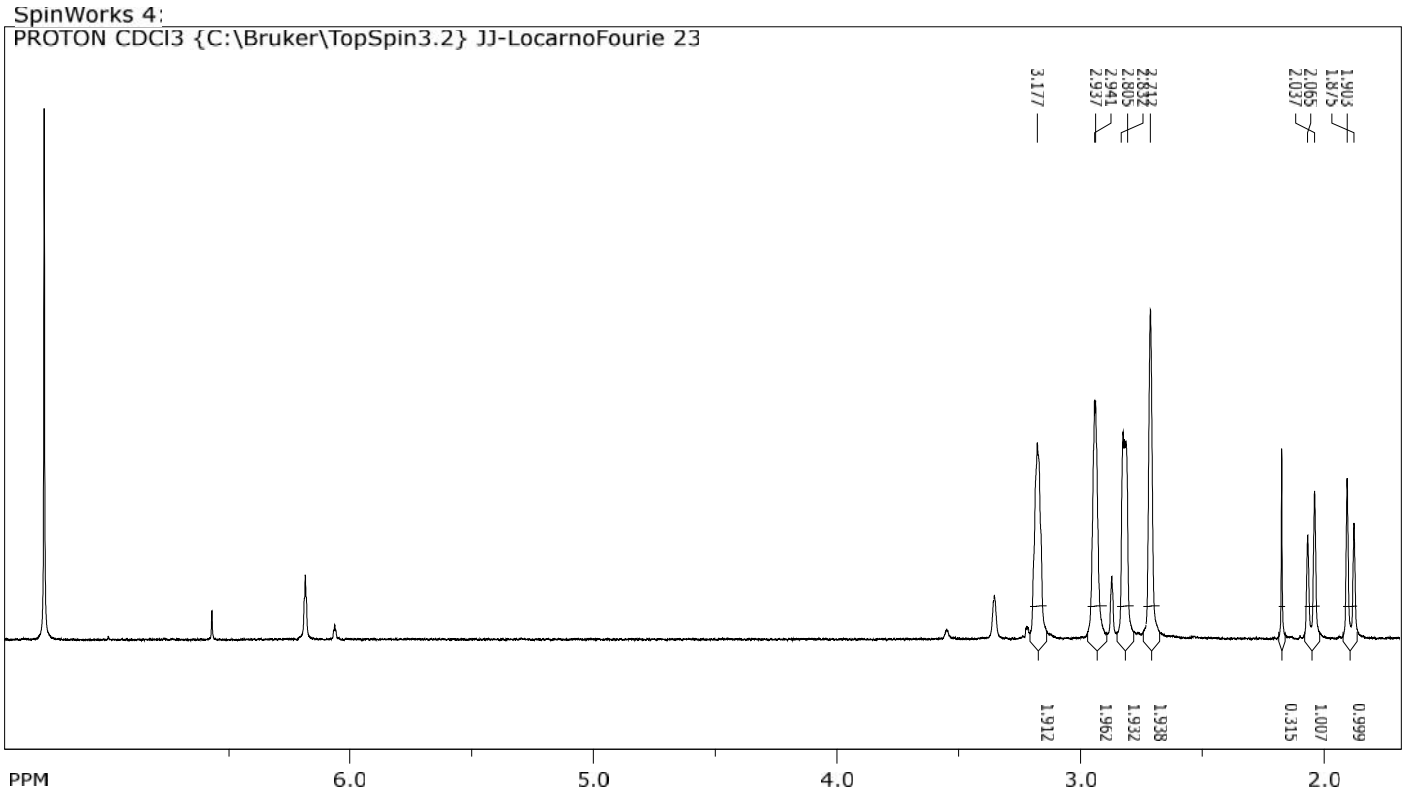

Spectrum 1: ^{1}H-NMR of Pentacyclo[5.4.0.0^{2,6}.0^{3,10}.0^{5,9}]undecane-8,11-dione

Compound 1

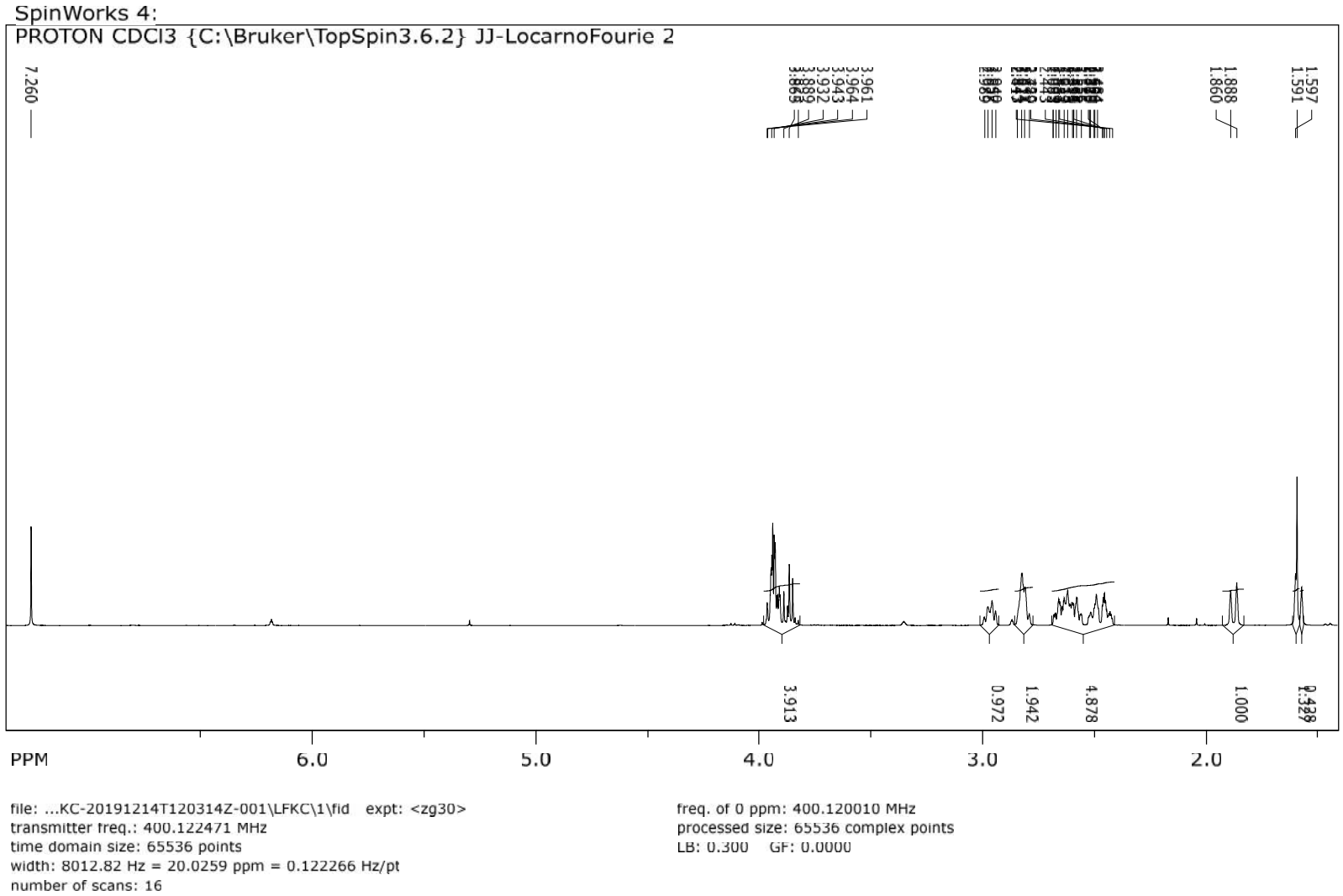

Spectrum 2: 1H-NMR of Spiro[1,3-dioxolane-2,8'-pentacyclo[5.4.0.02,6.0^{3,10}.0^{5,9}]undecan]-11'-one

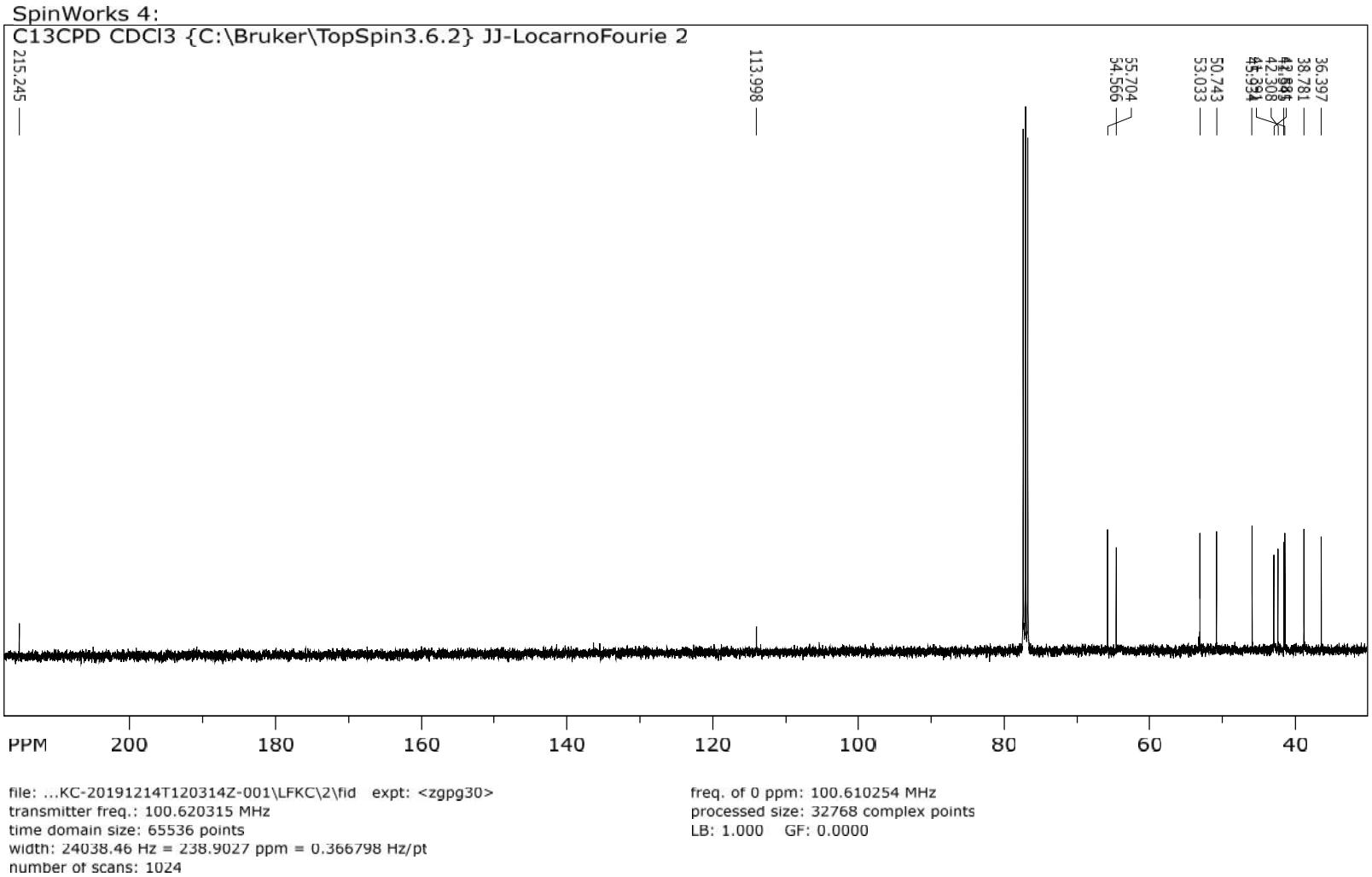

Spectrum 3: ^{13}C-NMR of Spiro[1,3-dioxolane-2,8'-pentacyclo[5.4.0.02,6.0^{3,10}.0^{5,9}]undecan]-11'-one

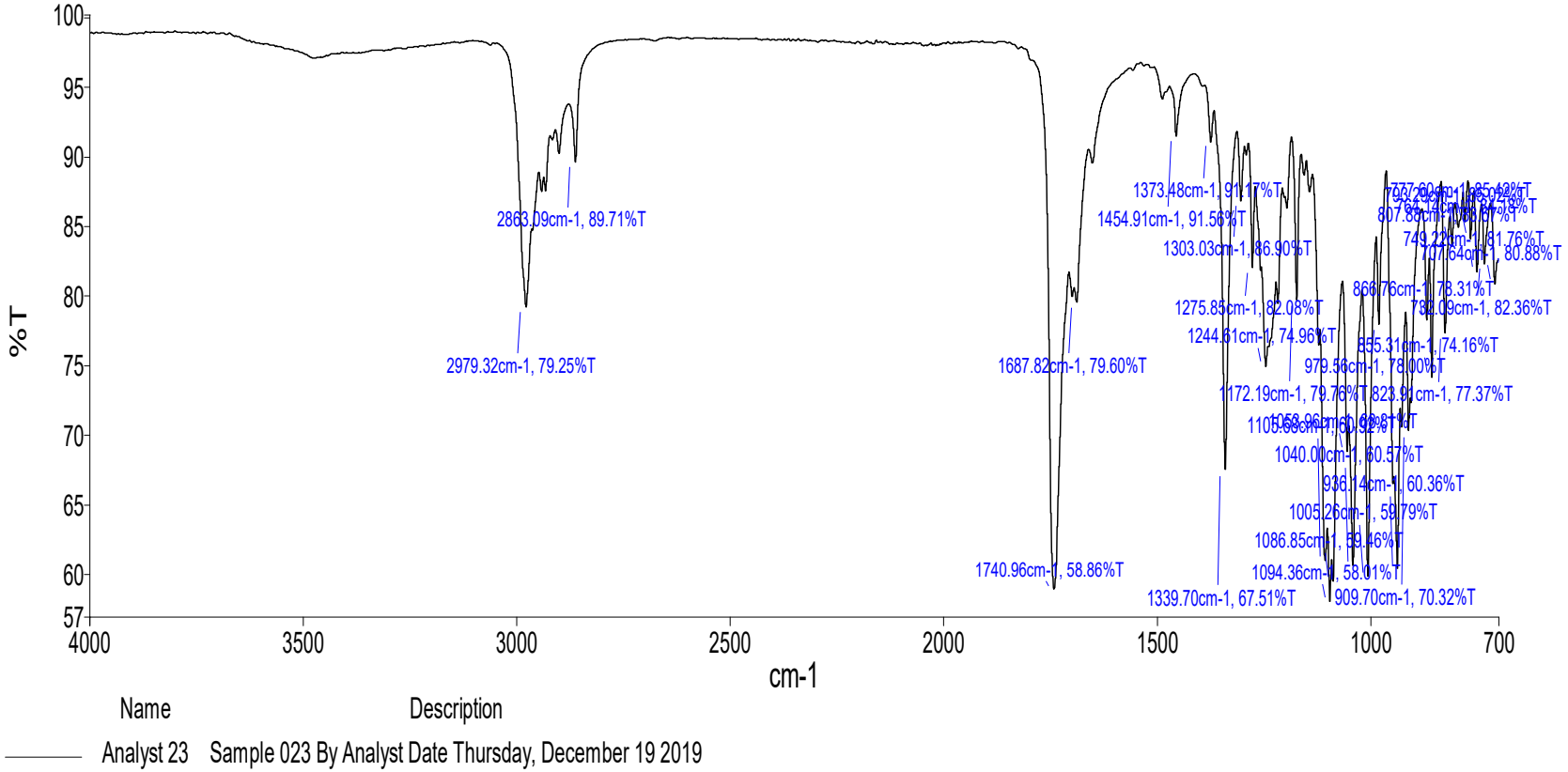

Spectrum 4: Infrared of Spiro[1,3-dioxolane-2,8'-pentacyclo[5.4.0.02,6.0^{3,10}.0^{5,9}]undecan]-11'-one

Compound 2

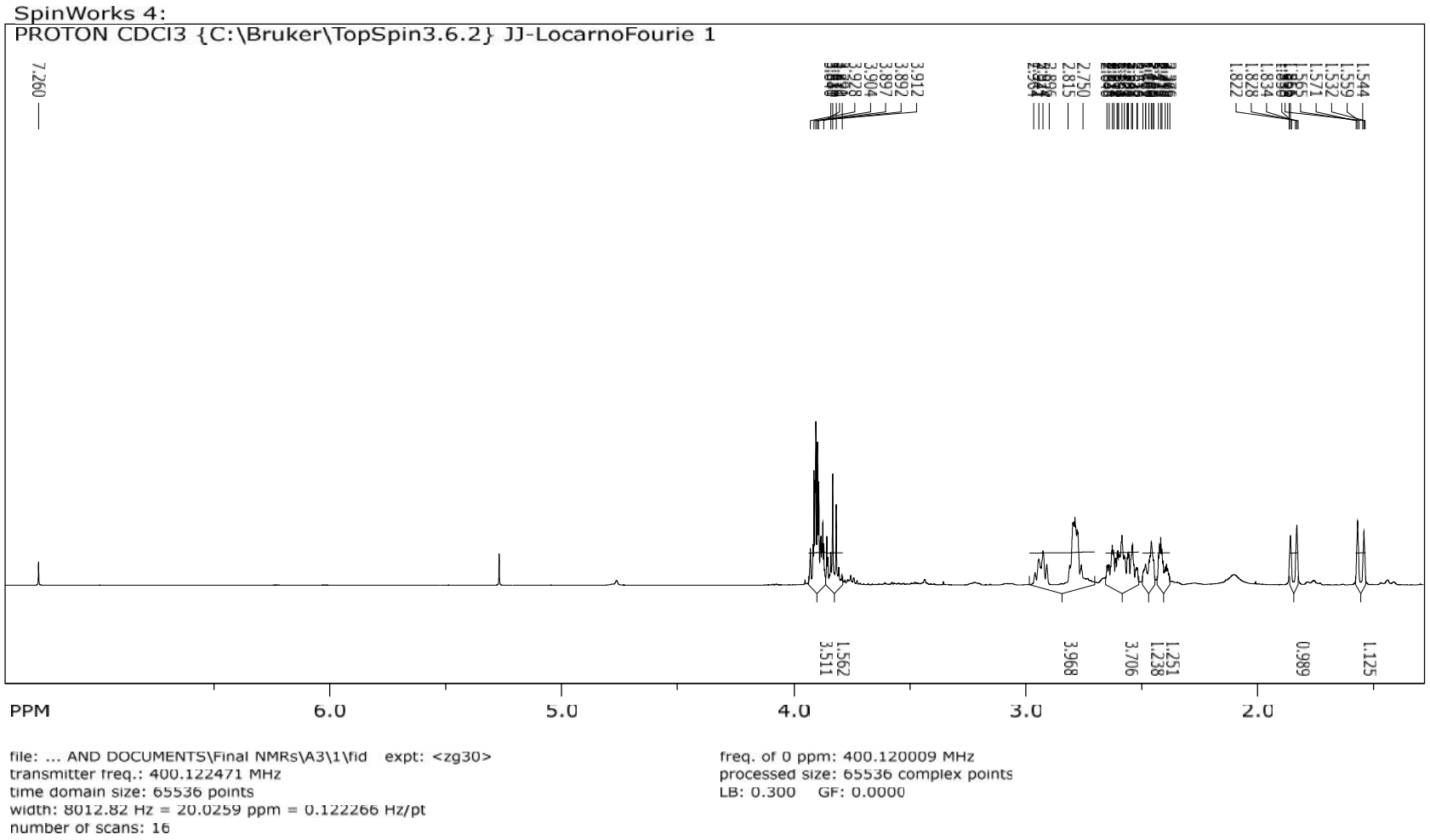

Spectrum 5: ^{1}H-NMR of N^{1}-{spiro[1,3-dioxolane-2,8'-pentacyclo[5.4.0.0^{2,6}.0^{3,10}.0^{5,9}]undecan]-11'-ylidene}ethane-1,2-diamine

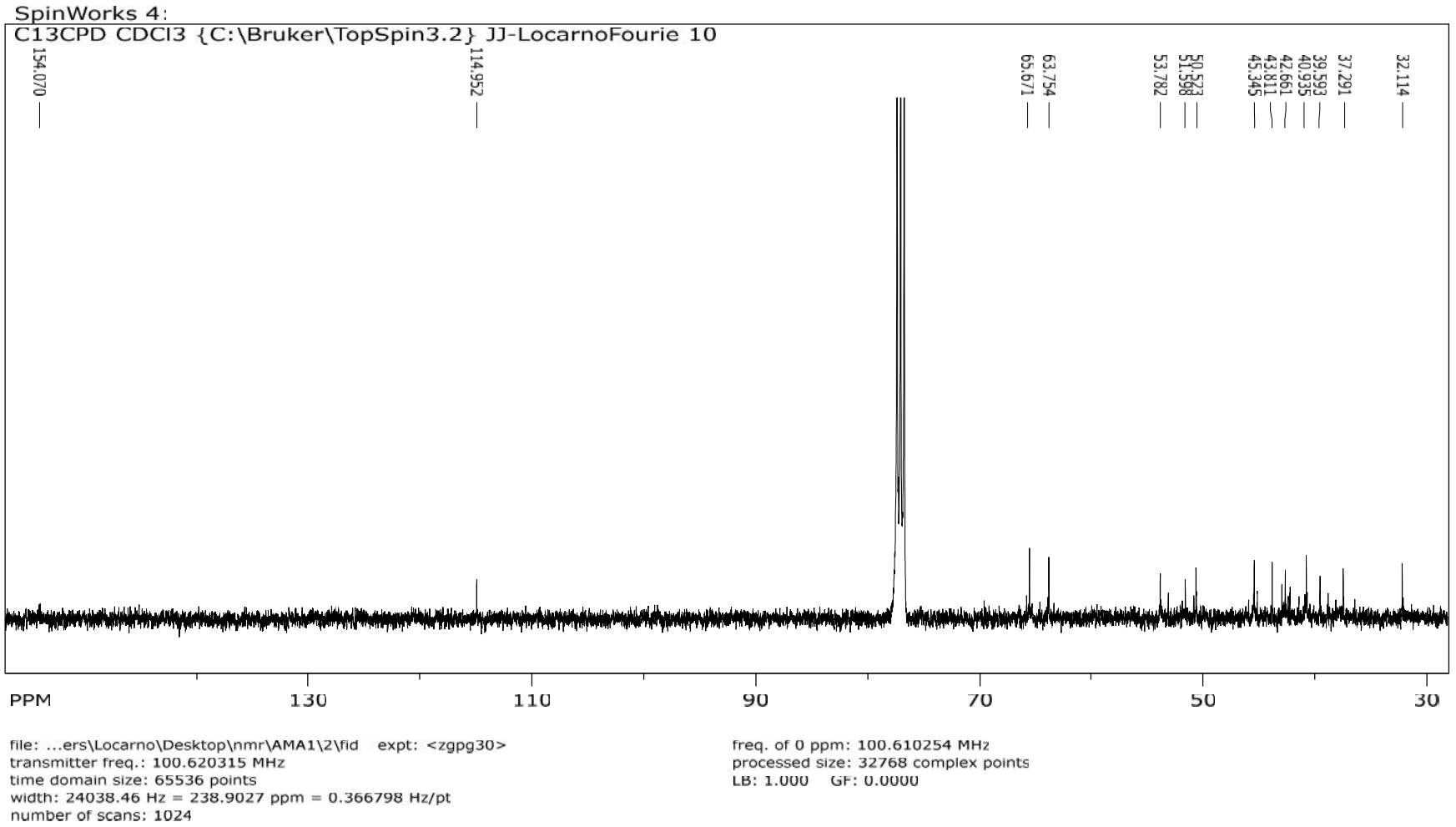

Spectrum 6: ^{13}C-NMR of N^{1}-{spiro[1,3-dioxolane-2,8'-pentacyclo[5.4.0.0^{2,6}.0^{3,10}.0^{5,9}]undecan]-11'-ylidene}ethane-1,2-diamine

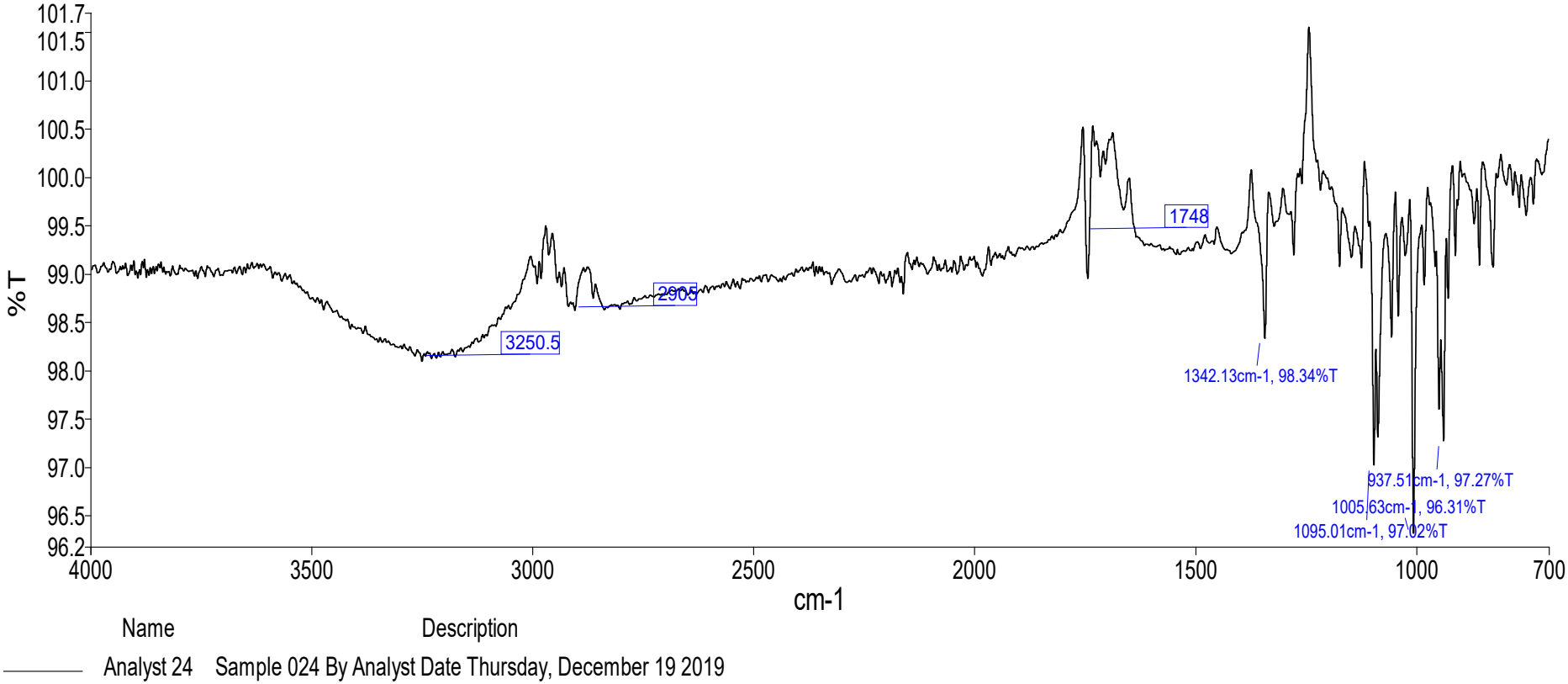

Spectrum 7: Infrared of N^1-{spiro[1,3-dioxolane-2,8'-pentacyclo[5.4.0.0^{2,6}.0^{3,10}.0^{5,9}]undecan]-11'-ylidene}ethane-1,2-diamine

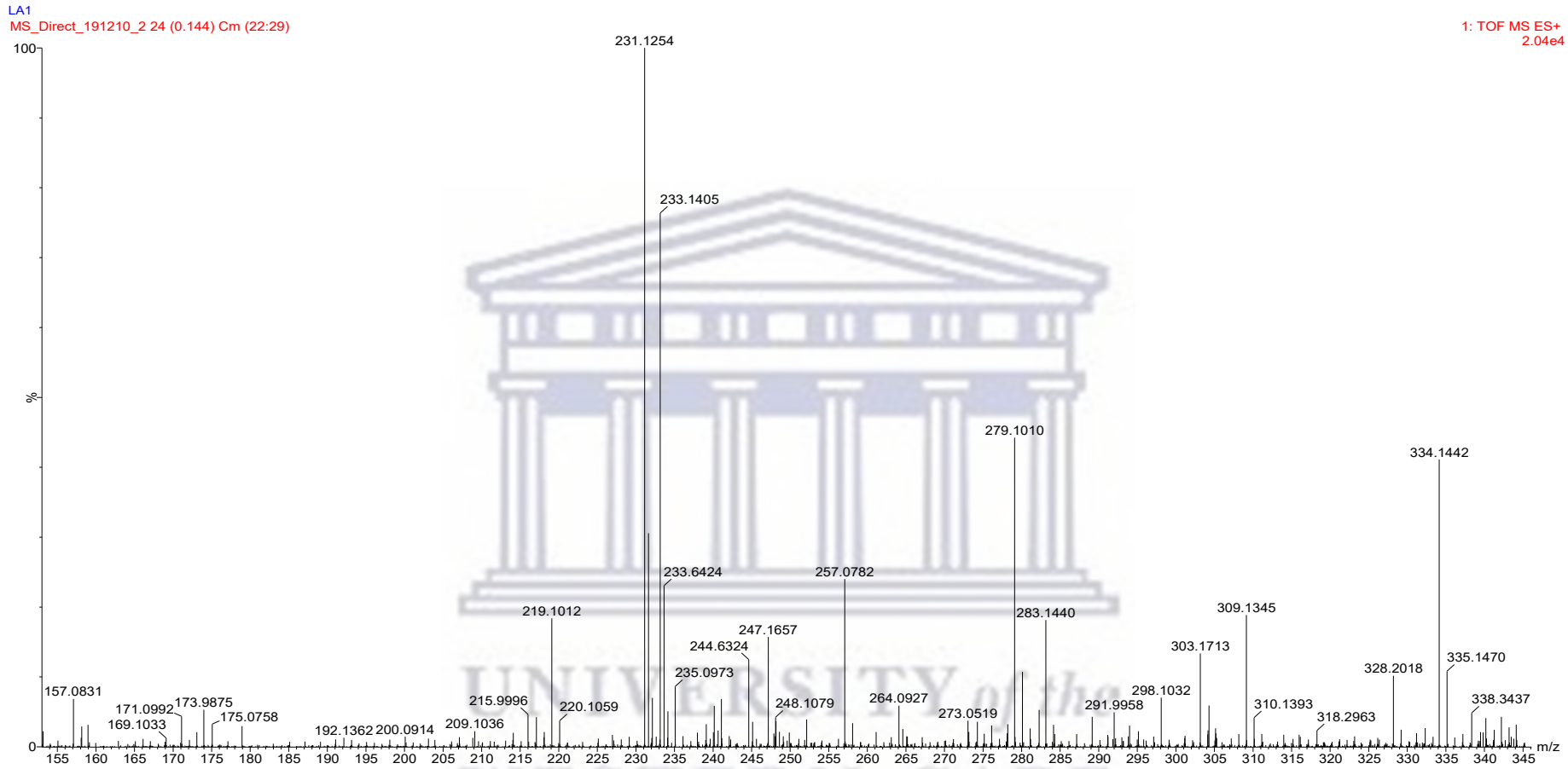

Spectrum 8: MS of N^1-{spiro[1,3-dioxolane-2,8'-pentacyclo[5.4.0.0^{2,6}.0^{3,10}.0^{5,9}]undecan]-11'-ylidene}ethane-1,2-diamine

Compound 3

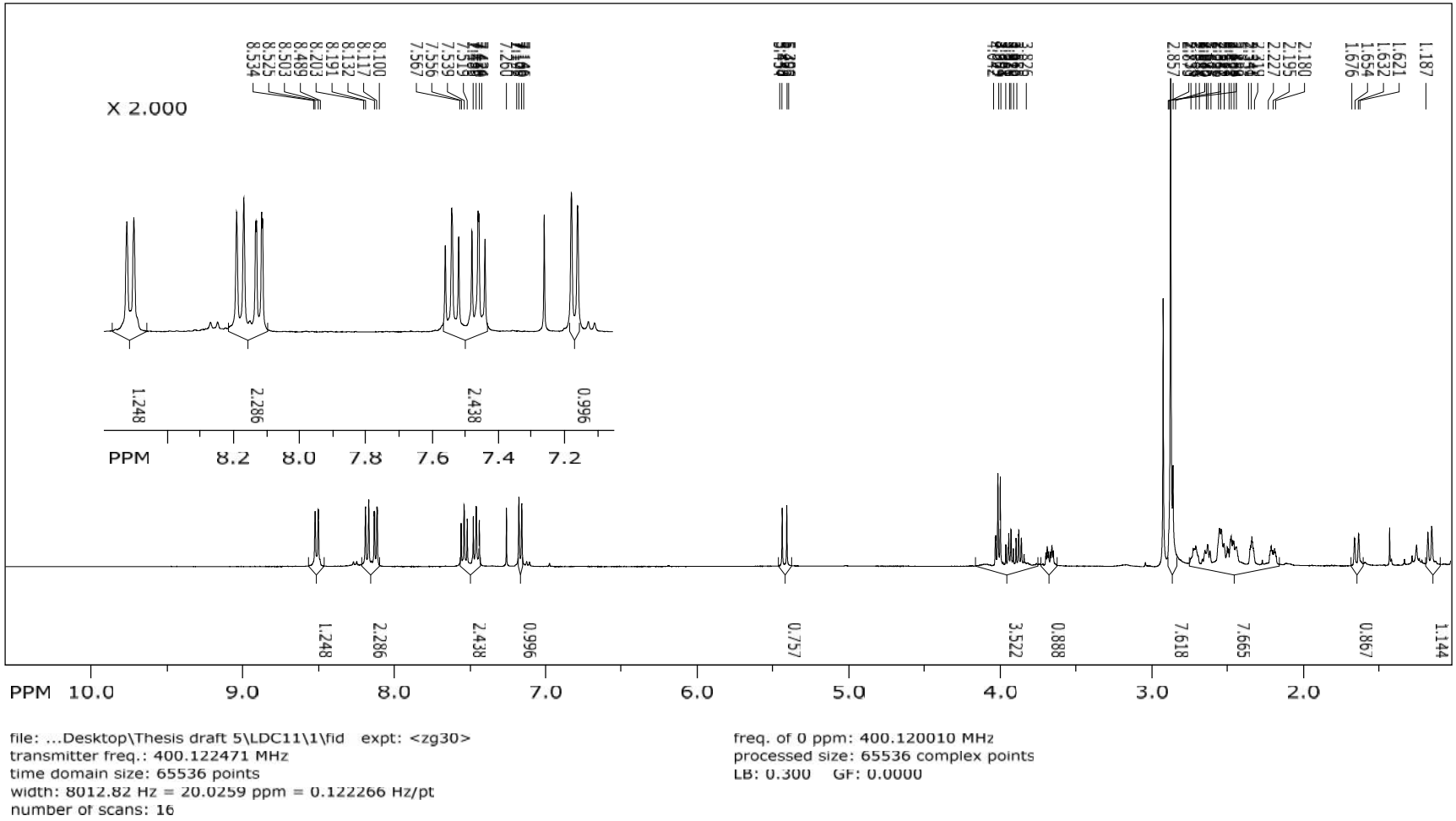

Spectrum 9: ^{1}H-NMR of 5-(dimethylamino)-N-[2-({spiro[1,3-dioxolane-2,8'-pentacyclo[5.4.0.0^{2,6}.0^{3,10}.0^{5,9}]undecan]-11'-ylidene}amino)ethyl]naphthalene-1-sulfonamide

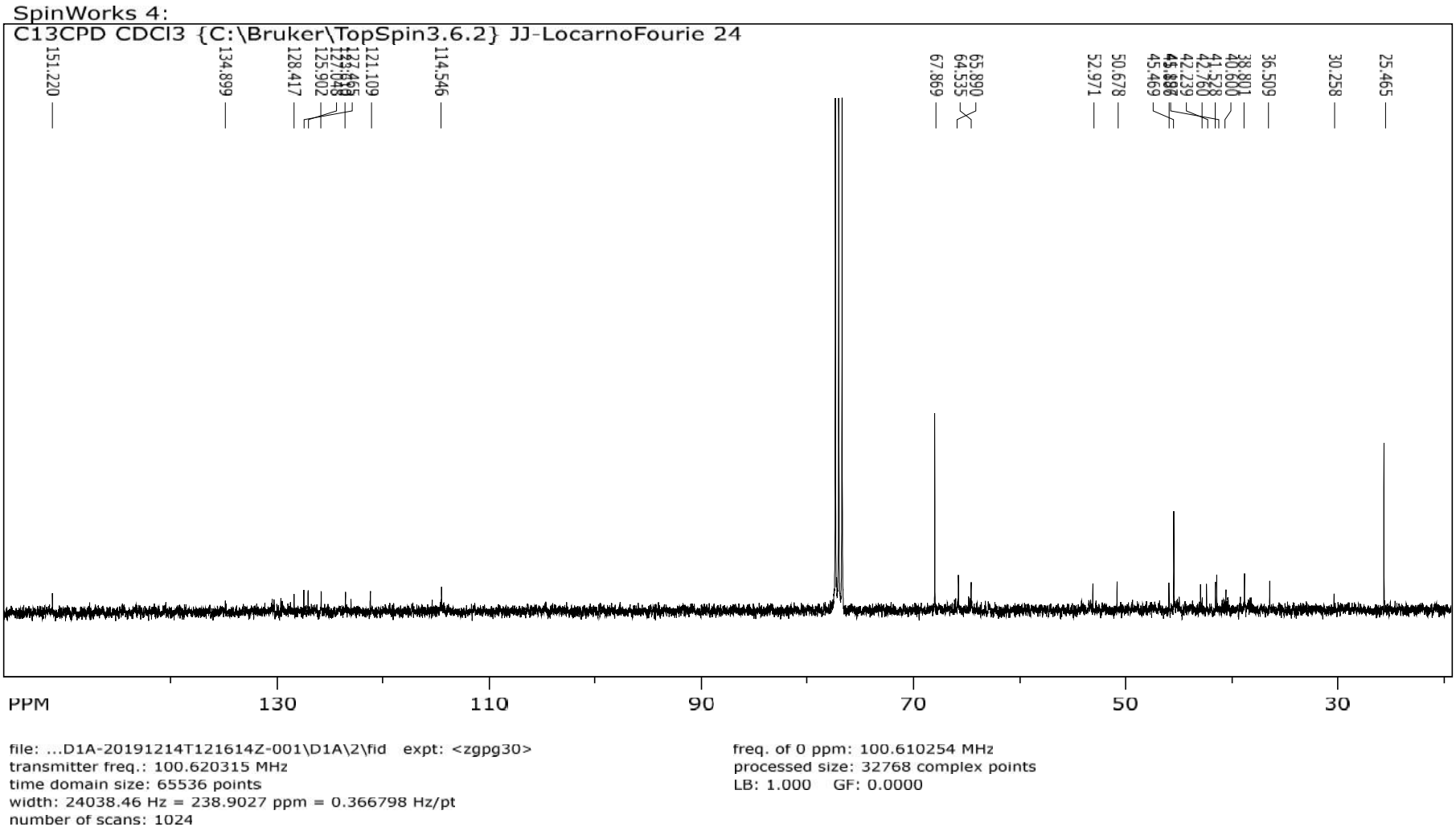

Spectrum 10: ^{13}C-NMR of 5-(dimethylamino)-N-[2-({spiro[1,3-dioxolane-2,8'-pentacyclo[5.4.0.0^{2,6}.0^{3,10}.0^{5,9}]undecan]-11'-ylidene}amino)ethyl]naphthalene-1-sulfonamide

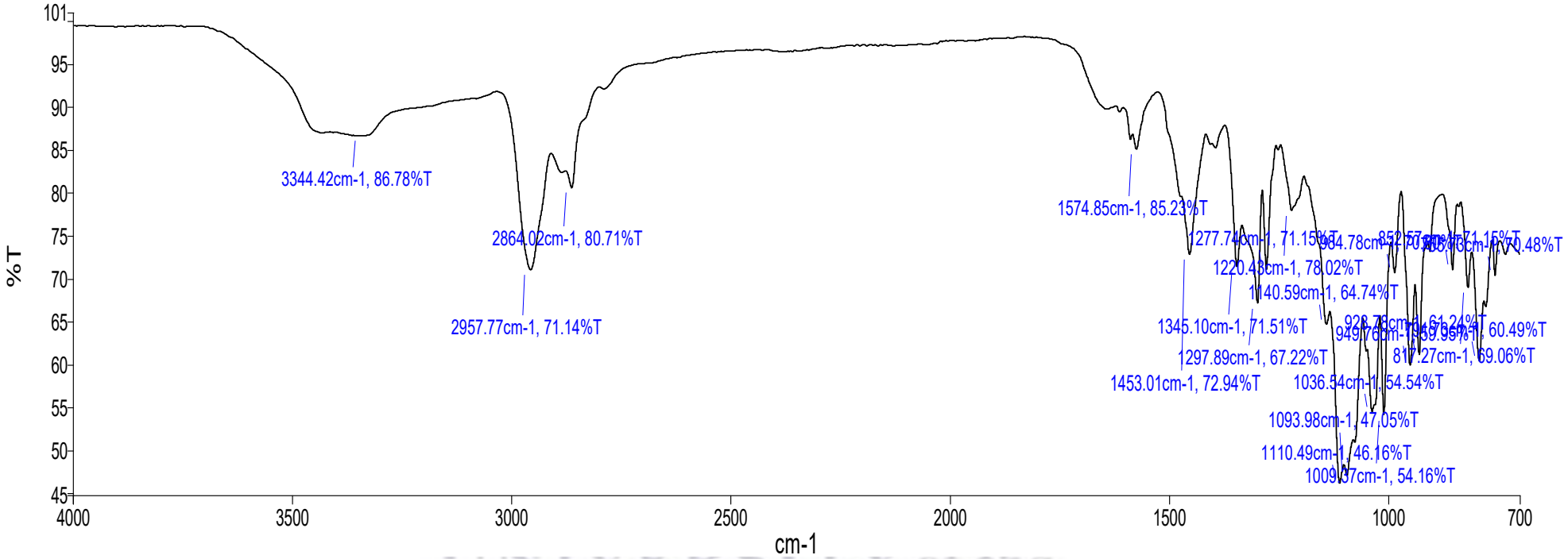

Spectrum 11: Infrared of 5-(dimethylamino)-N-[2-({spiro[1,3-dioxolane-2,8'-pentacyclo[5.4.0.0^{2,6}.0^{3,10}.0^{5,9}]undecan]-11'-ylidene}amino)ethyl]naphthalene-1-sulfonamide

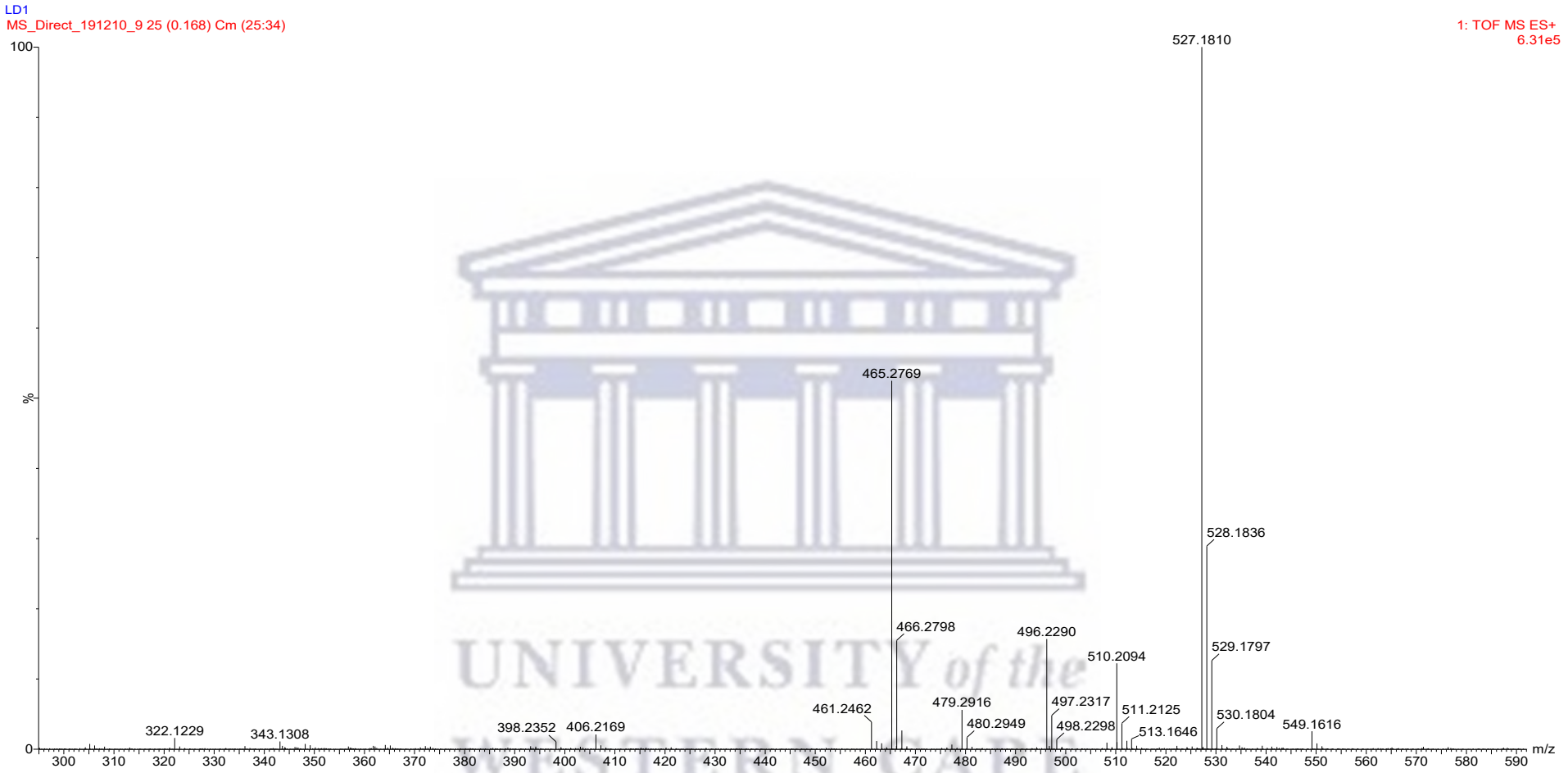

Spectrum 12: MS of 5-(dimethylamino)-N-[2-({spiro[1,3-dioxolane-2,8'-pentacyclo[5.4.0.0^{2,6}.0^{3,10}.0^{5,9}]undecan]-11'-ylidene}amino)ethyl]naphthalene-1-sulfonamide

Compound 4

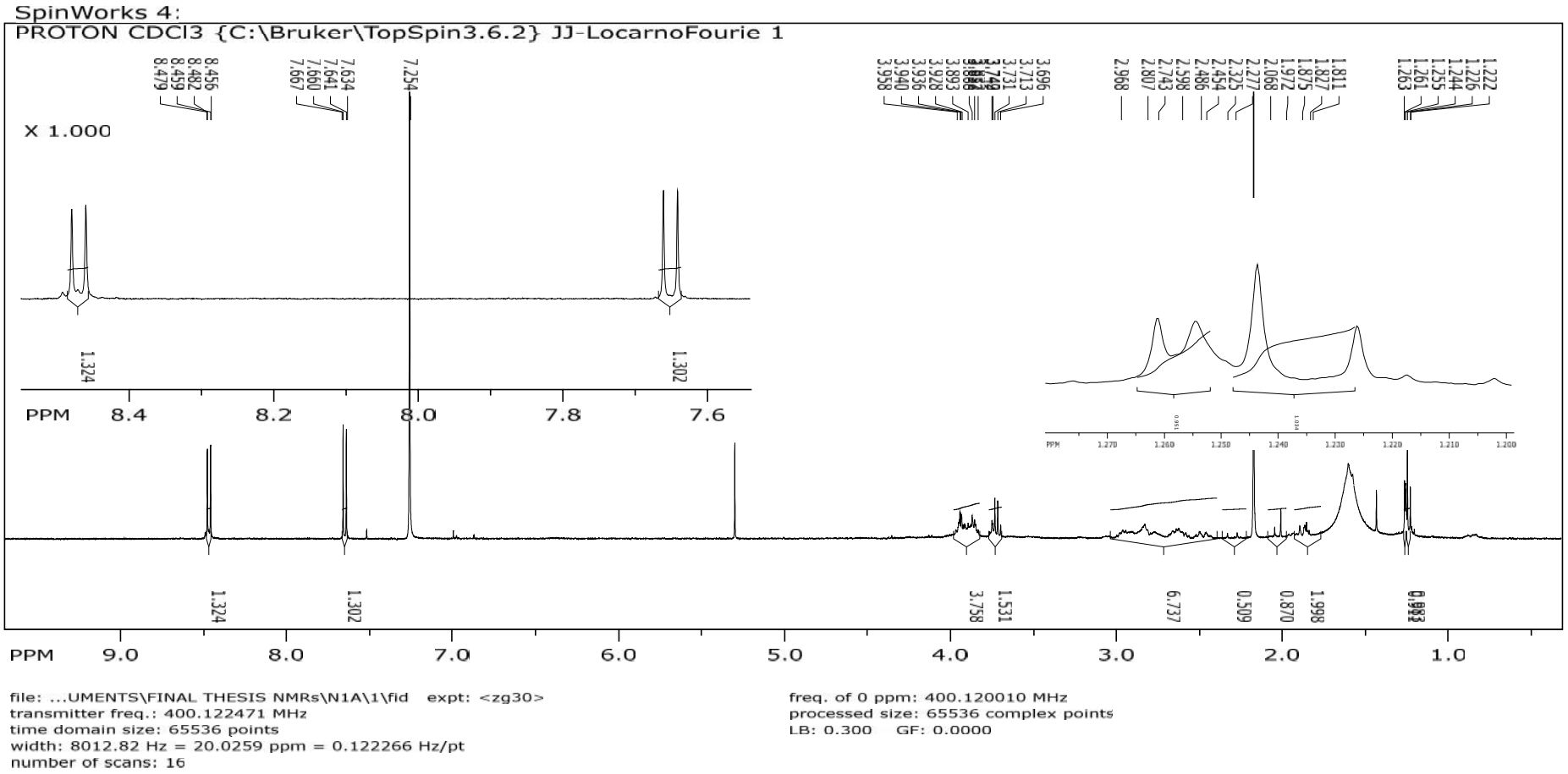

Spectrum 13: ^{1}H-NMR of N^{1}-(7-nitro-2,1,3-benzoxadiazol-4-yl)-N^{2}-{spiro[1,3-dioxolane-2,8'-pentacyclo[5.4.0.0^{2,6}.0^{3,10}.0^{5,9}]undecan]-11'-yl}ethane-1,2-diamine

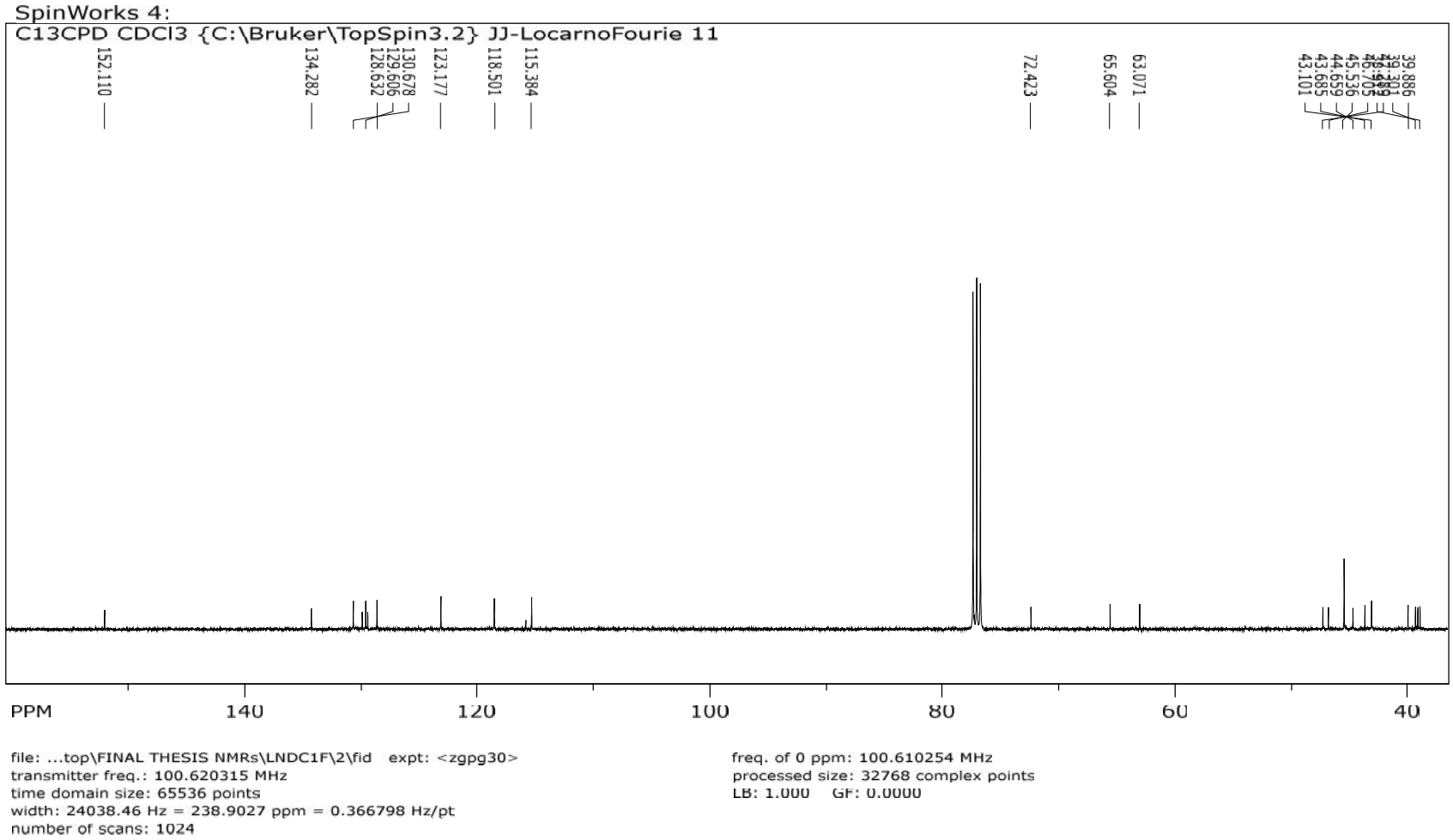

Spectrum 14: ^{13}C-NMR of N^{1}-(7-nitro-2,1,3-benzoxadiazol-4-yl)-N^{2}-{spiro[1,3-dioxolane-2,8'-pentacyclo[5.4.0.0^{2,6}.0^{3,10}.0^{5,9}]undecan]-11'-yl}ethane-1,2-diamine

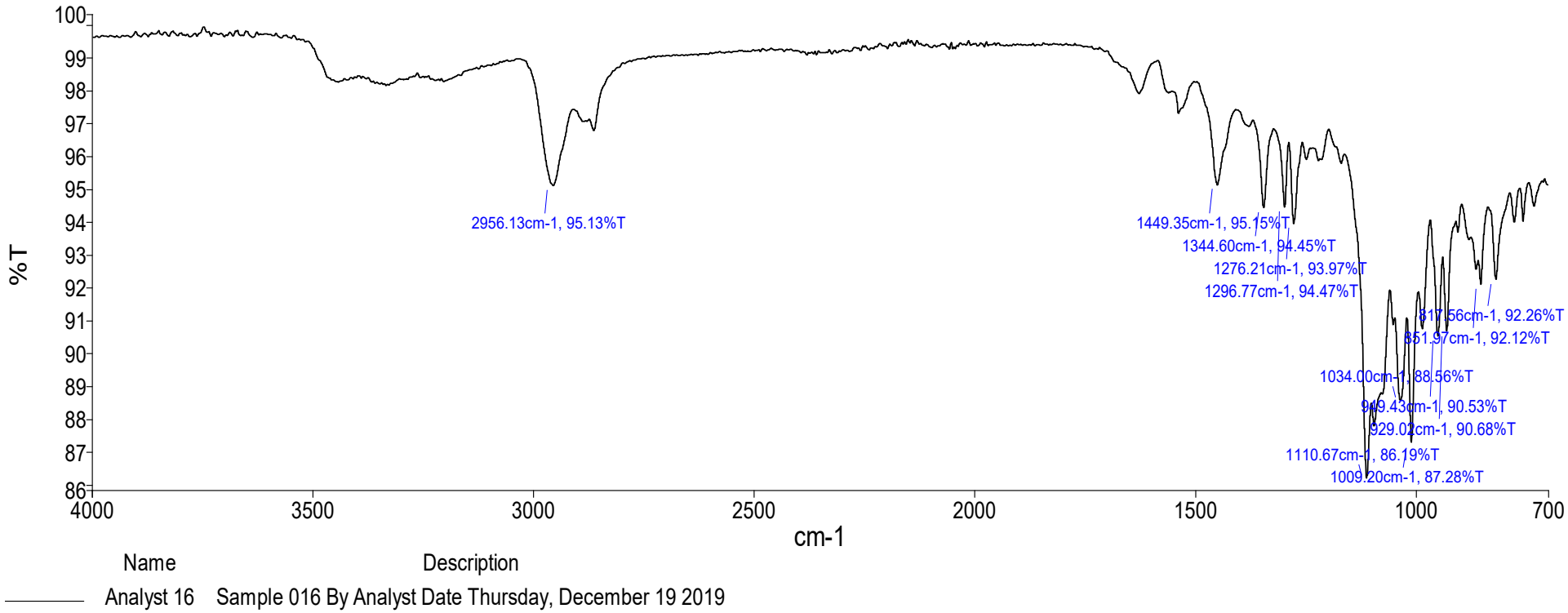

Spectrum 15: Infrared of N^1-(7-nitro-2,1,3-benzoxadiazol-4-yl)-N^2-{spiro[1,3-dioxolane-2,8'-pentacyclo[5.4.0.0^{2,6}.0^{3,10}.0^{5,9}]undecan]-11'-yl}ethane-1,2-diamine

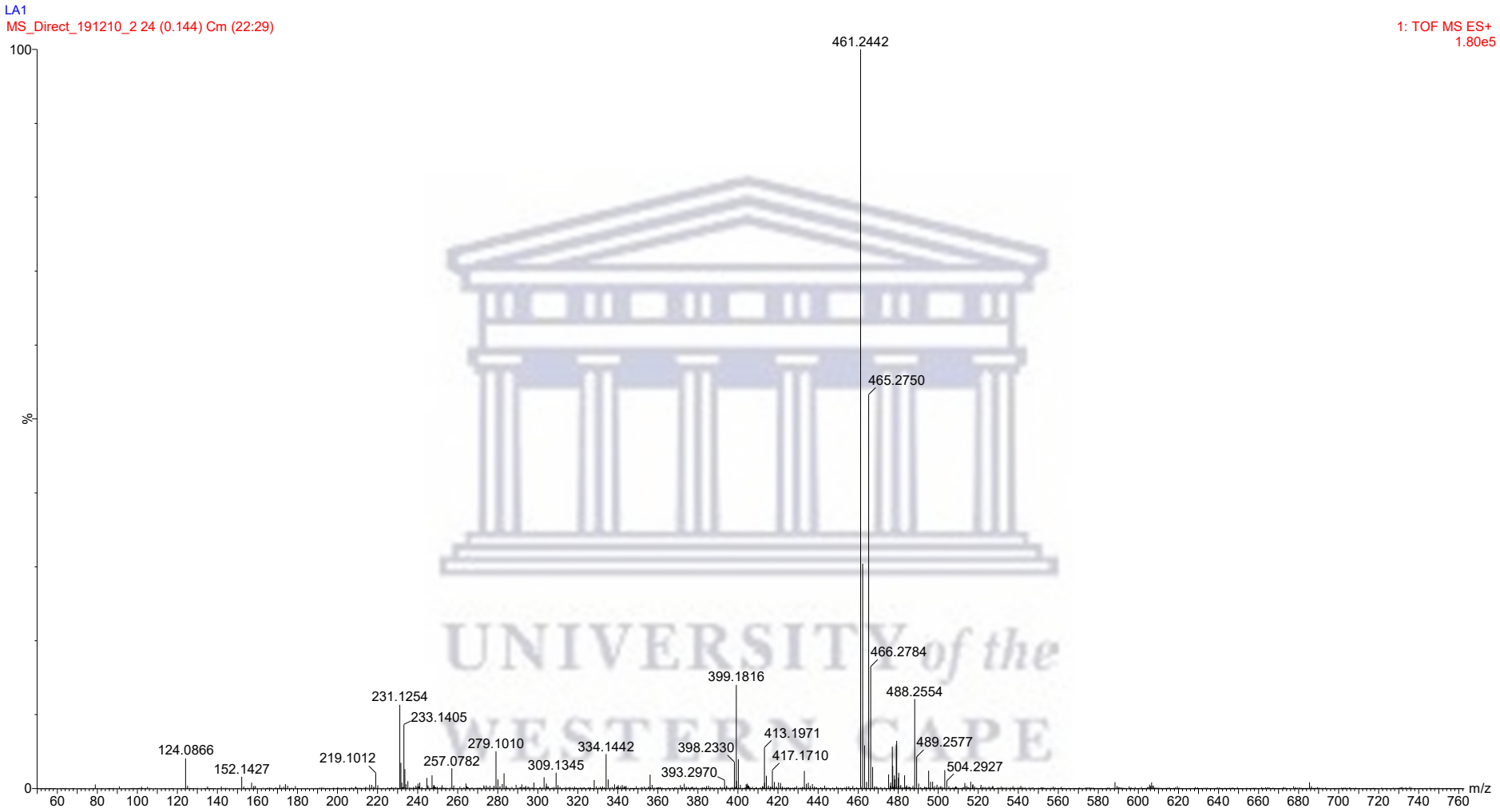

Spectrum 16: MS of N^1-(7-nitro-2,1,3-benzoxadiazol-4-yl)-N^2-{spiro[1,3-dioxolane-2,8'-pentacyclo[5.4.0.0^{2,6}.0^{3,10}.0^{5,9}]undecan]-11'-yl}ethane-1,2-diamine

2-(2-methyl-4H-chromen-4-ylidene)propanedinitrile

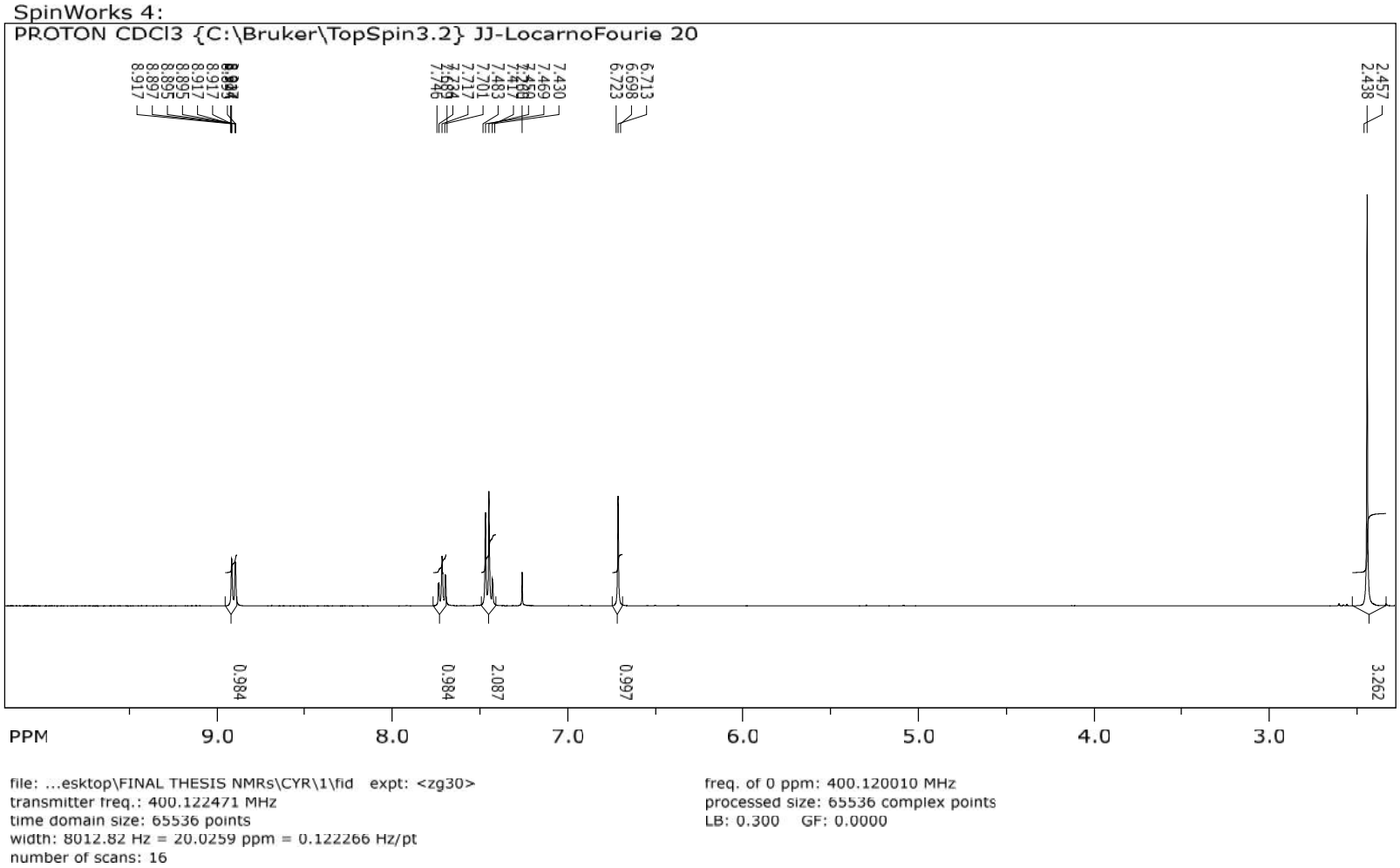

Spectrum 17: ^{1}H-NMR of 2-(2-methyl-4H-chromen-4-ylidene)propanedinitrile

Compound 5

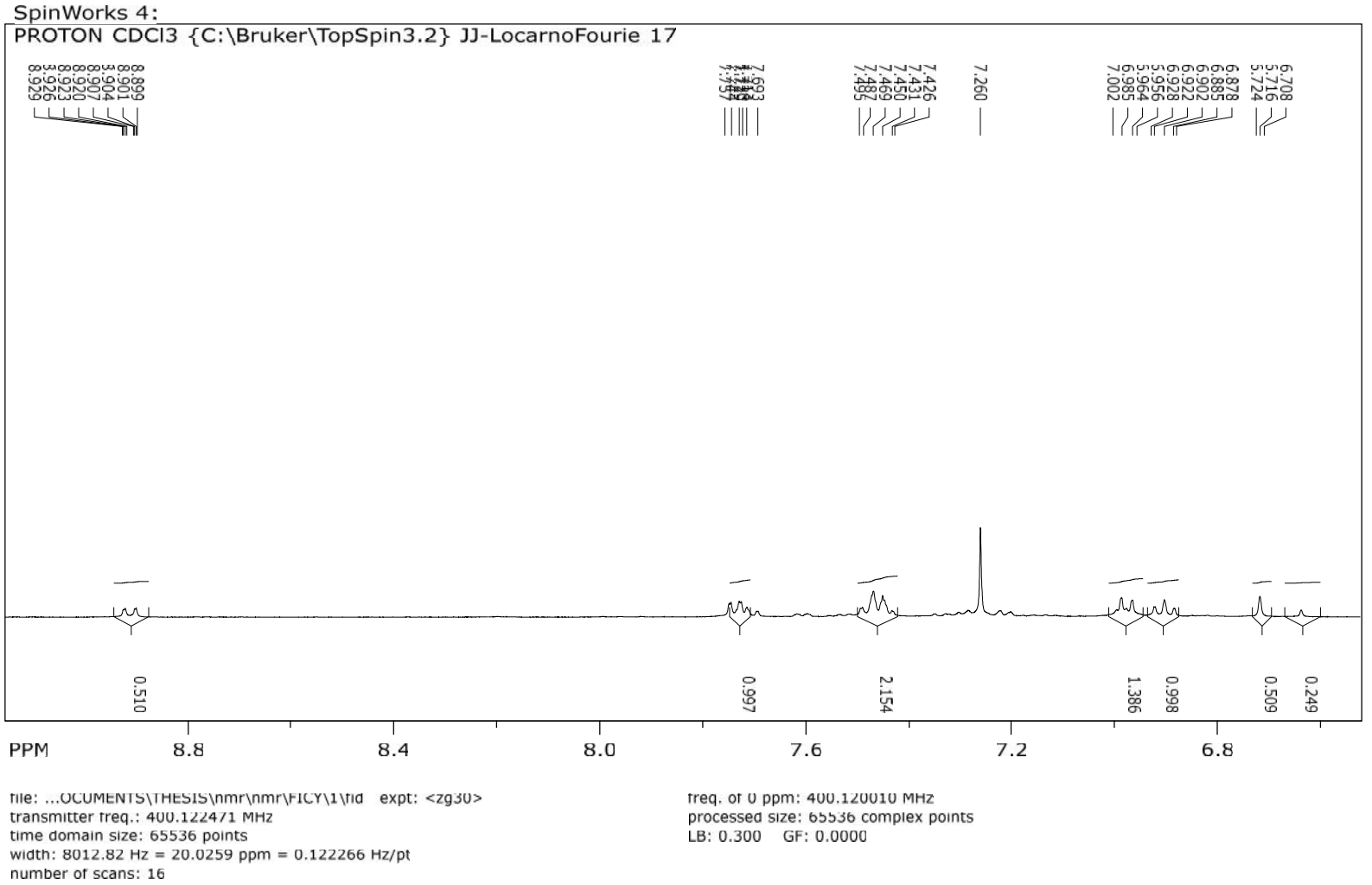

Spectrum 18: ^{1}H-NMR of 2-{2-[(1E)-2-aminoethenyl]-4H-chromen-4 ylidene}propanedinitrile

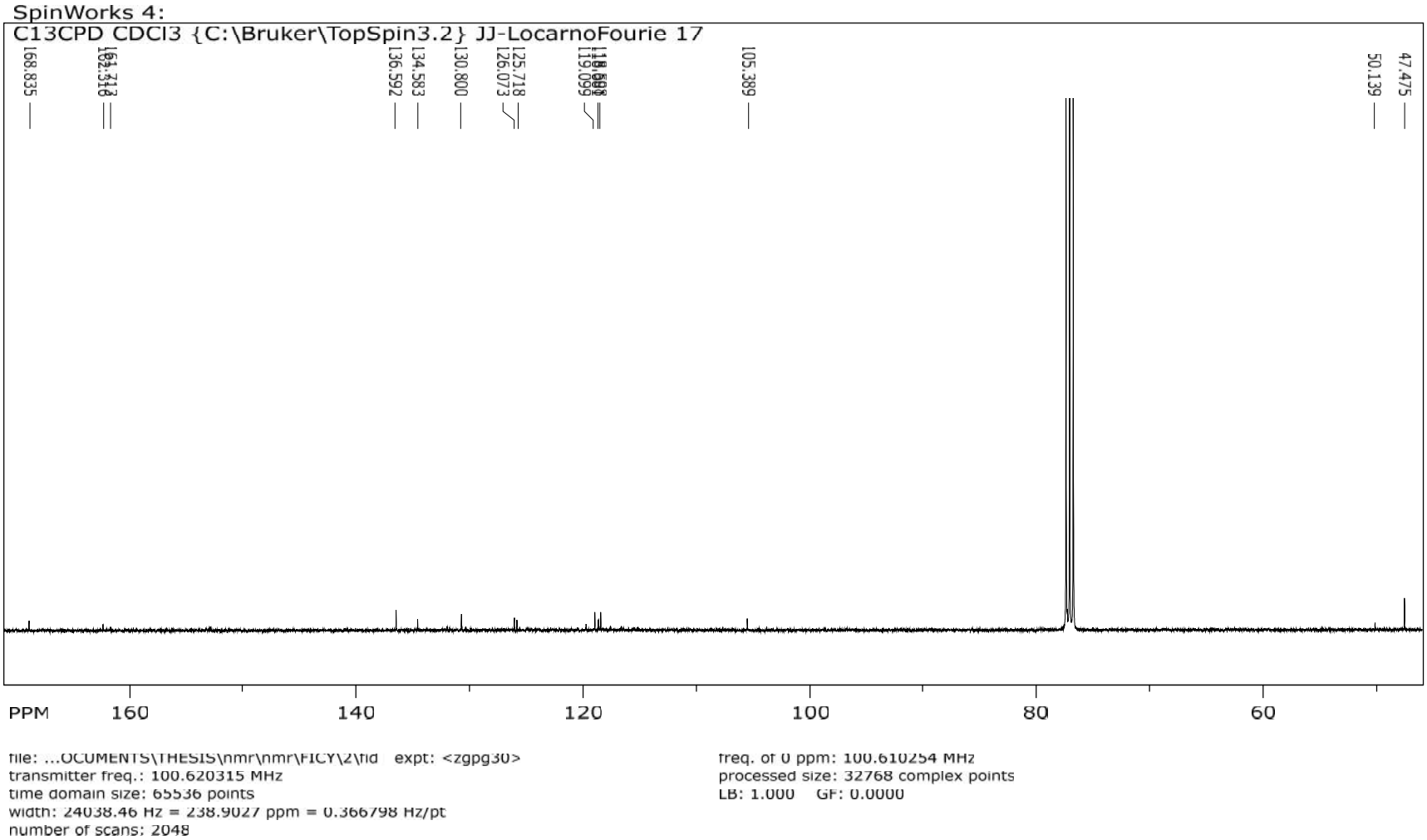

Spectrum 19: ^{13}C-NMR of 2-{2-[(1E)-2-aminoethenyl]-4H-chromen-4-ylidene}propanedinitrile

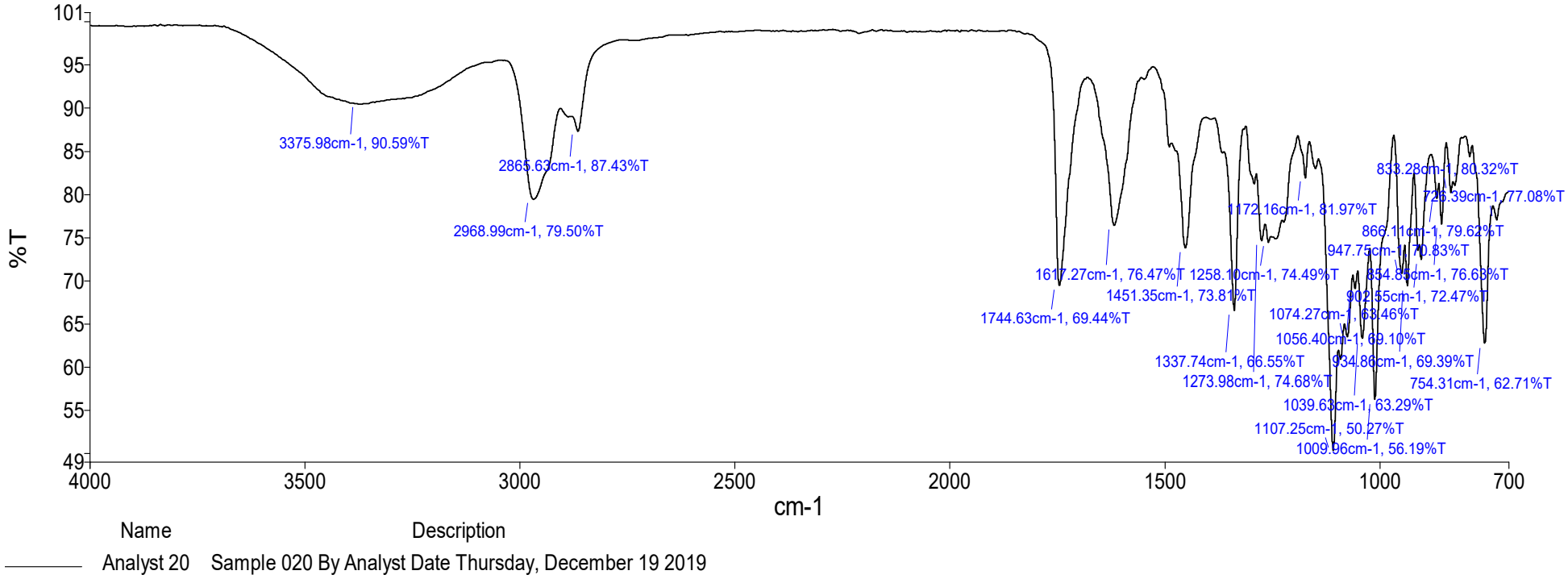

Spectrum 20: Infrared Spectrum of 2-{2-[(1E)-2-aminoethenyl]-4H-chromen-4-ylidene}propanedinitrile

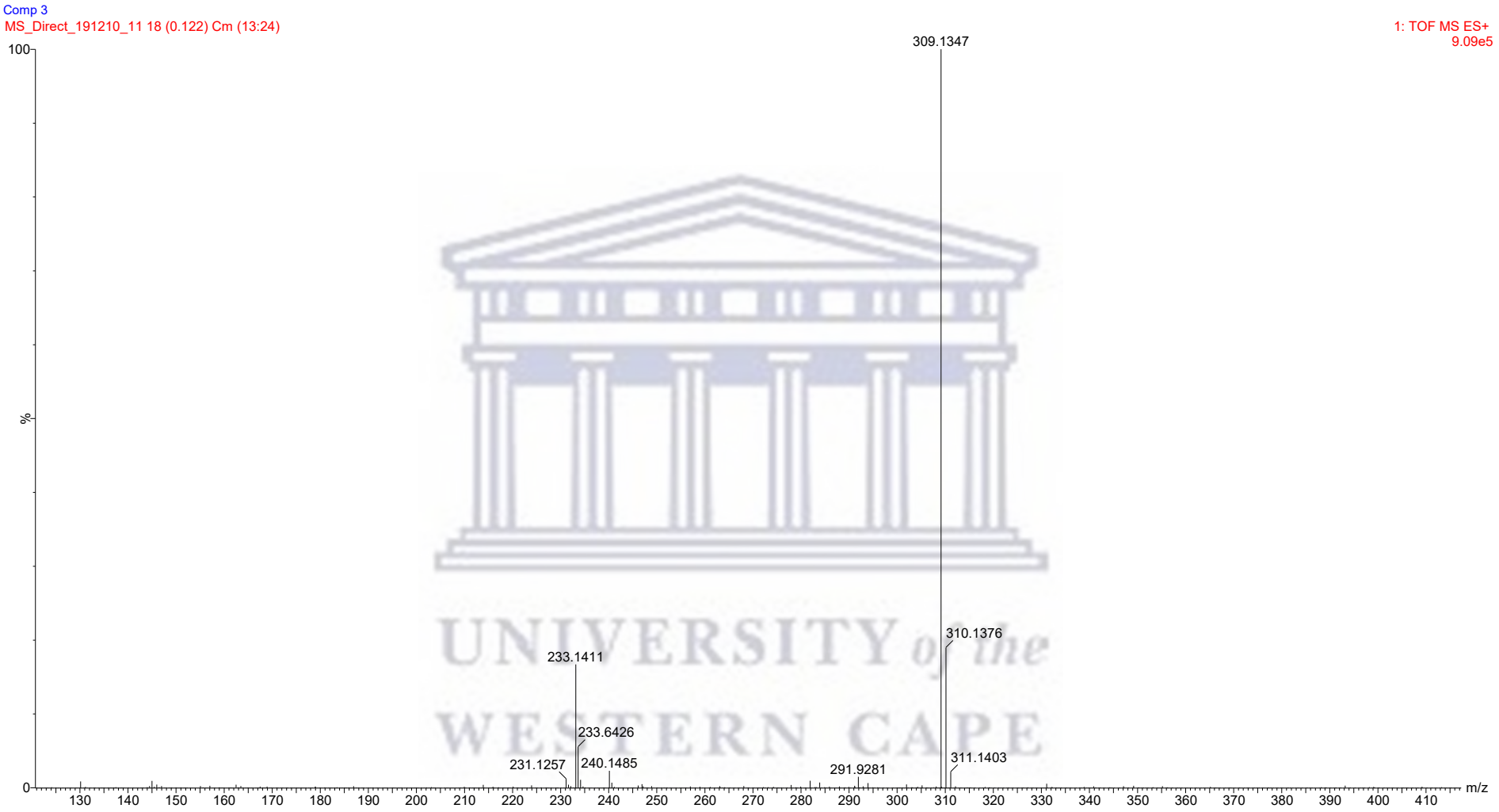

Spectrum 21: MS of 2-{2-[(1E)-2-aminoethenyl]-4H-chromen-4-ylidene}propanedinitrile

Compound 7

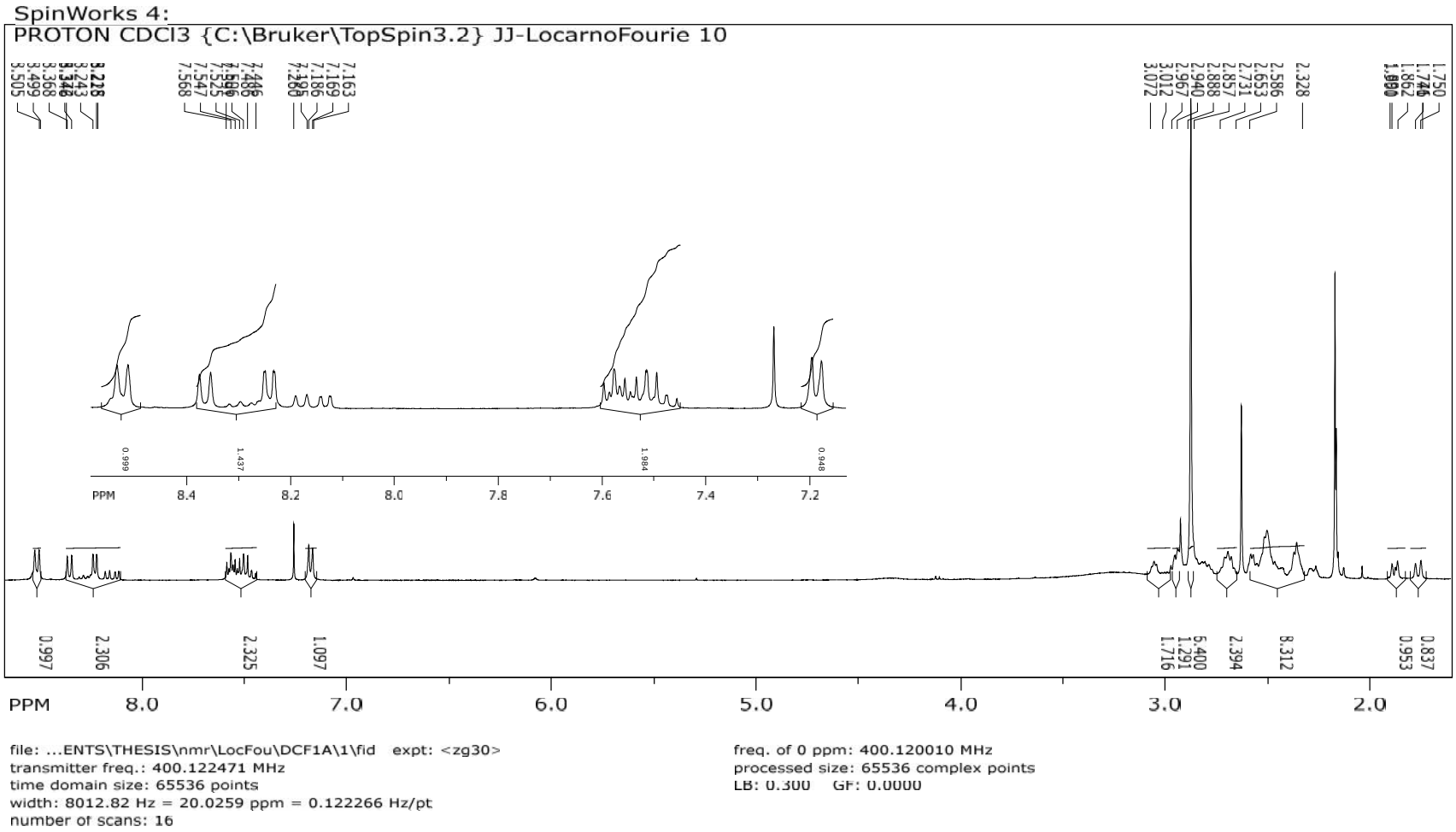

Spectrum 22: ^{1}H-NMR of 5-(3-{[5-(propan-2-yl)naphthalen-1-yl]sulfonyl}propyl)-5-azahexacyclo[5.4.1.0^{2,6}.0^{3,10}.0^{4,8}.0^{9,12}]dodecan-4-ol

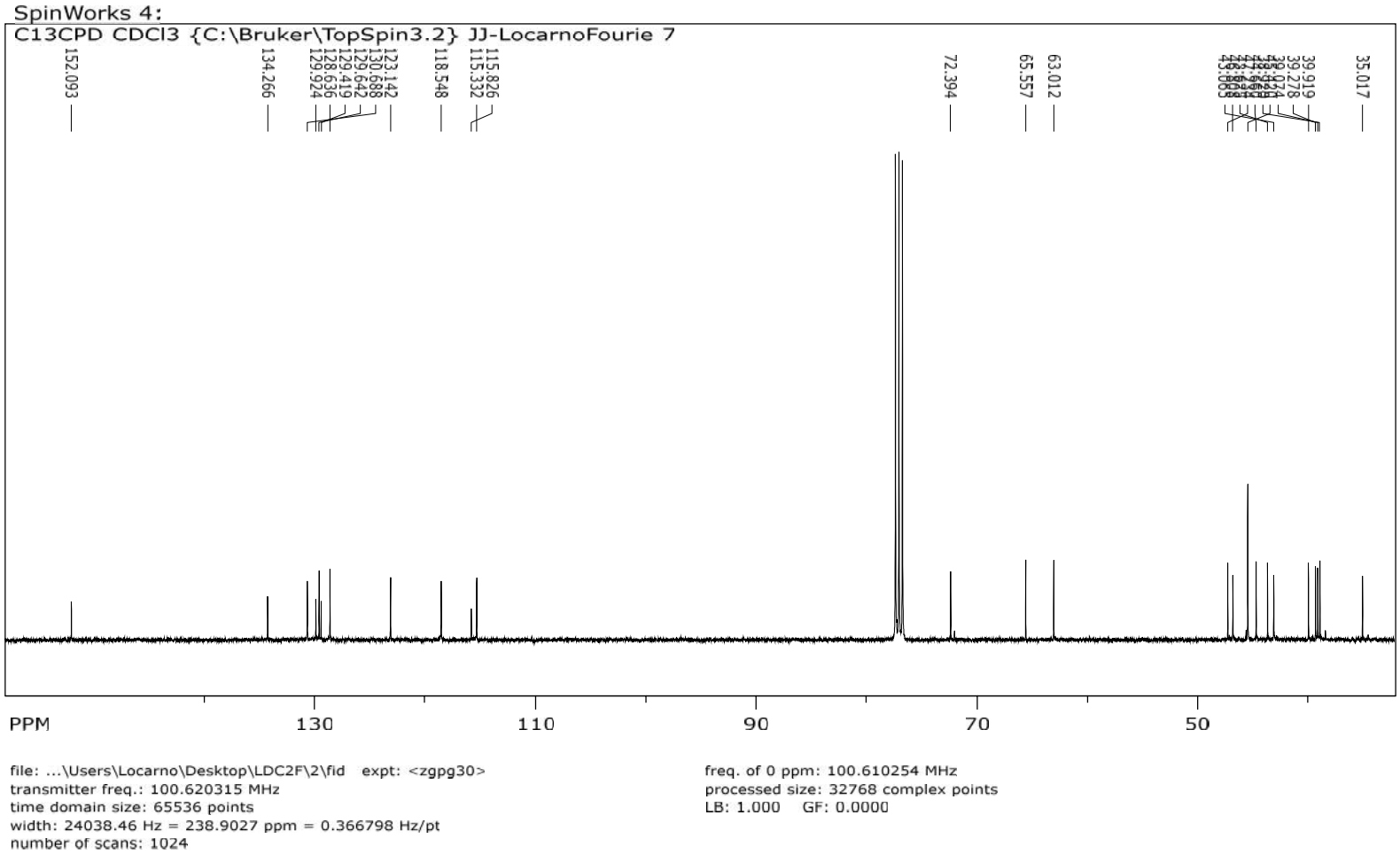

Spectrum 23: ^{13}C-NMR of 5-(3-{[5-(propan-2-yl)naphthalen-1-yl]sulfonyl}propyl)-5-azahexacyclo[5.4.1.0^{2,6}.0^{3,10}.0^{4,8}.0^{9,12}]dodecan-4-ol

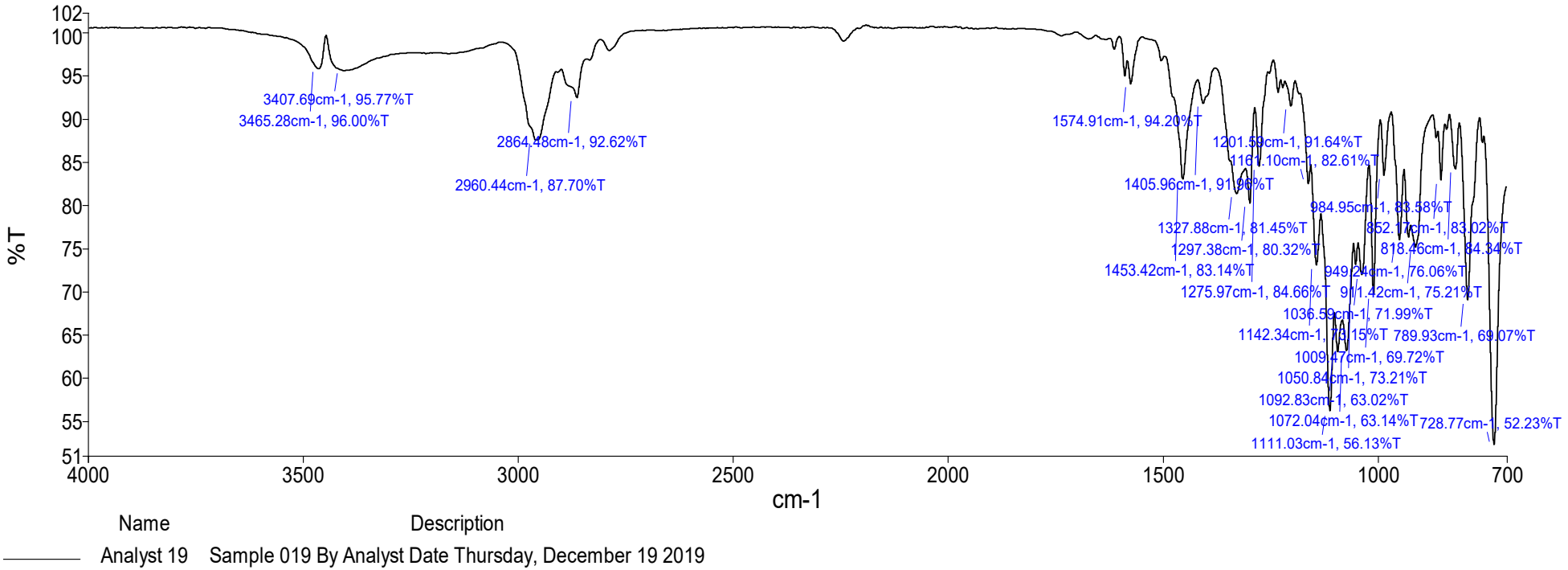

Spectrum 24: Infrared of 5-(3-{[5-(propan-2-yl)naphthalen-1-yl]sulfonyl}propyl)-5-azahexacyclo[5.4.1.$0^{2,6}$.$0^{3,10}$.$0^{4,8}$.$0^{9,12}$]dodecan-4-ol

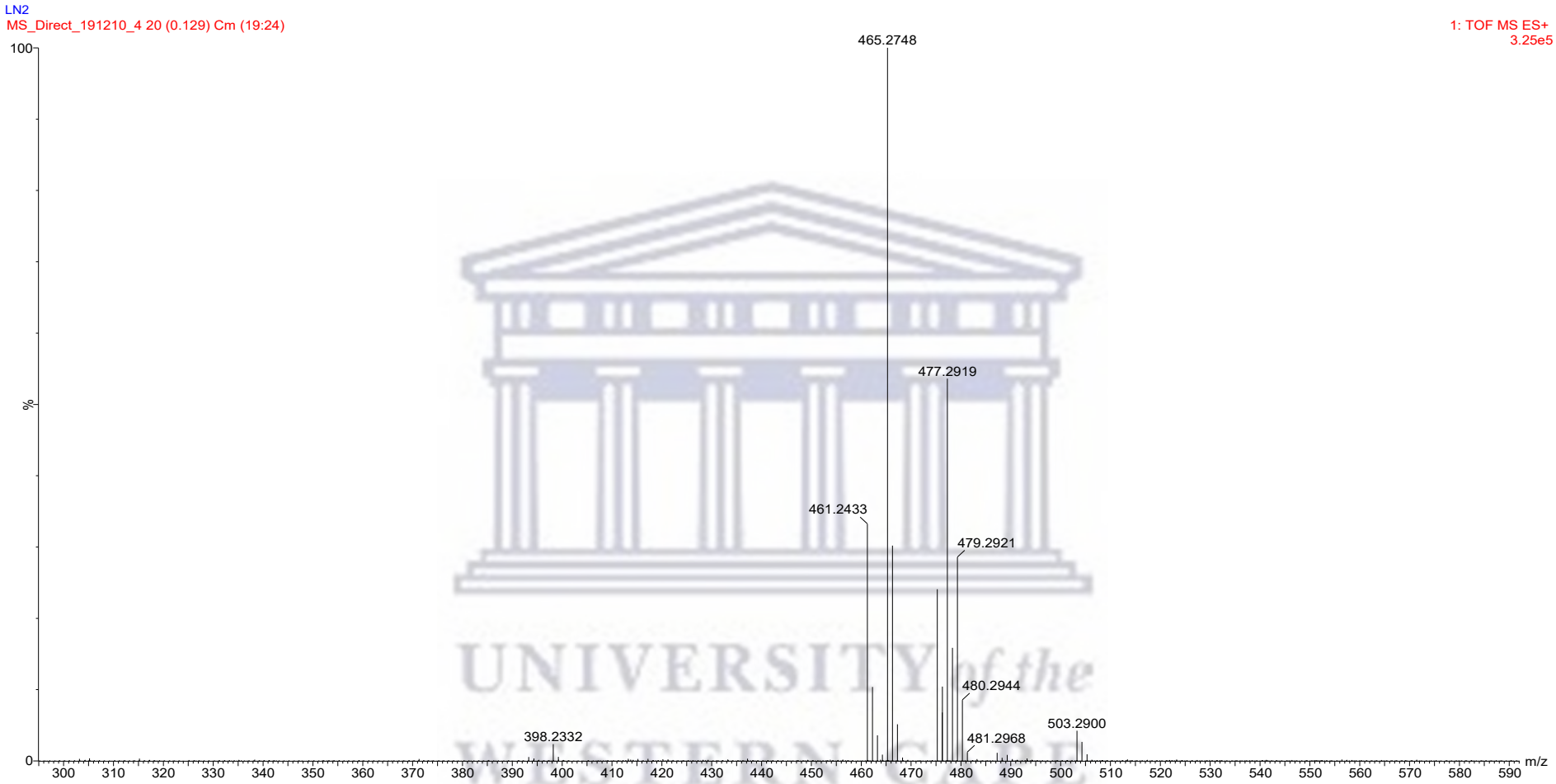

Spectrum 25: MS of 5-(3-{[5-(propan-2-yl)naphthalen-1-yl]sulfonyl}propyl)-5-azahexacyclo[5.4.1.$0^{2,6}$.$0^{3,10}$.$0^{4,8}$.$0^{9,12}$]dodecan-4-ol